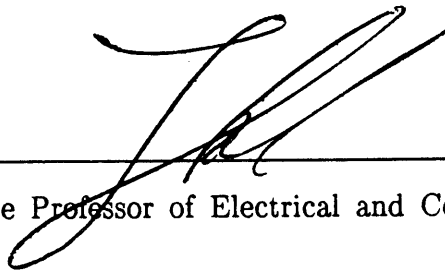# DEVELOPMENT OF A DECOMPOSITION APPROACH
FOR TESTING LARGE ANALOG CIRCUITS

Dissertation Presented to

the Faculty of the College of Engineering and Technology

Ohio University

In Partial Fulfillment

of the Requirements for the Degree

Doctor of Philosophy

by

Hong Dai

June, 1989

This dissertation has been approved for

the Department of Electrical and Computer Engineering

and

the College of Engineering and Technology

_____

Associate Professor of Electrical and Computer Engineering

_____

Dean of the College of Engineering and Technology

ACKNOWLEDGEMENTS

I am greatly indebted to my advisor and instructor, Dr. Janusz A. Starzyk, for his continuous guidance, encouragement and support, without which the completion of this dissertation would not have been possible. I am thankful for being his student, for the challenging problems, ideals and directions he set in the course of developing my research program.

I wish to thank also the other members of my dissertation committee: Dr's Mehmet Celenk, M. Ebrahim Mokari, Donald O. Norris and Roger D. Radciliff. I am also grateful to Ms. Terry Thielen for carefully reviewing the dissertation.

My thanks are due to all the scientists at the Metrology group of the Electrosystems Division, National Institute of Standards and Technology, especially to T. Michael Souders and Gerard Stenbakken for stimulating suggestions and helpful discussions, and to Don Flach and Peter Hetrick for their help with the time domain testing. I would like to express my sincere appreciation to Mohamed El–Gamal, the doctoral student at Ohio University, for valuable comments and assistance with the software development.

Thanks also go to Ohio University for its financial support that made my graduate studies possible.

And finally, I wish to thank my husband, Jiyao Liu, for his love, patient understanding, encouragement and assistance. During all this time he somehow managed to take care of everything at home.

TABLE OF CONTENTS

LIST OF FIGURES

LIST OF TABLES

Notation

The following notation is used in this dissertation:

N — network

S — subnetwork

t — time

ω — frequency

j — discrete time indices

n — number of nodes

m — external node indices

i — internal node indices

$\mathbf{p}^*$ — vector of actual parameters

$\mathbf{p}^0$ — vector of nominal or designed parameters

$\mathbf{p}$ — vector of computed or updated parameters

$\Delta\mathbf{p}$ — parameter deviations $(\mathbf{p}^* - \mathbf{p}^0)$

$\mathbf{d}$ — relative parameter deviations in percent $(\dfrac{\Delta\mathbf{p}}{\mathbf{p}^0}\ 100\%)$

$\mathbf{x}$ — vector of the circuit variables

$\dot{\mathbf{x}}$ — partial derivative of $\mathbf{x}$ w.r.t. time

$\mathbf{x}'$ — transpose of $\mathbf{x}$

$\mathbf{x}_0$ — nominal vector or initial vector

$\mathbf{x}_j$ — vector $\mathbf{x}$ at the jth time instance

$\mathbf{x}^*$ — measured vector

$\bar{\mathbf{x}}$ — computed vector

$\mathbf{x}^a$ — adjoint vector

$\mathbf{X}$ — spectrum of $\mathbf{x}$

$|X|$ — magnitude of X

$\tilde{X}$ — complex conjugate of X

ϕ — vector of test functions

f — circuit function waveforms

F — circuit function spectra

S — sensitivity matrix in frequency domain $(\frac{\partial X}{\partial p})$

s — sensitivity matrix in time domain $(\frac{\partial x}{\partial p})$

s_j — sensitivity matrix at the jth time instance $(\frac{\partial x_j}{\partial p})$

T — test matrix $(\frac{\partial \phi}{\partial p})$

$\mathcal{T}$ — test matrix in time domain

$\mathcal{T}_j$ — test matrix at the jth time instance

M — Jacobian matrix in time domain $(\frac{\partial f}{\partial p})$

$\mathcal{D}$ — diagonal submatrix of M

$\mathcal{C}$ — column submatrix of M

$\mathcal{R}$ — row submatrix of M

$\mathcal{E}$ — external matrix of M

$\mathcal{A}$ — selected matrix

Y — admittance matrix in frequency domain (Jacobian matrix $\frac{\partial V}{\partial p}$)

$\mathcal{Y}$ — admittance matrix in time domain

Y_{ii} — diagonal submatrix of Y

Y_{im} — column submatrix of Y

Y_{mi} — row submatrix of Y

Y_{mm} — external submatrix of Y

v, V — node voltage waveforms, spectra

i, I — node current waveforms, spectra

w, W — input waveforms, spectra

$\mathbf{q}$ — capacitor charges and inductor fluxes

C — capacitance of the capacitor

G — admittance of the conductor

$\mathbf{C}$ — reactive matrix

$\mathbf{G}$ — resistive matrix

$\mathbf{A}$ — incident matrix

$\mathbf{Q}$ — orthogonalized matrix

$\mathbf{R}$ — upper triangle matrix

α — subnetwork indices

k — number of subnetworks

n_p — number of parameters

n_m — number of test nodes

n_e — number of excitation nodes

n_f — number of test frequencies

n_h — number of harmonic frequencies

n_l — number of DC excitation levels

n_s — number of piecewise linear segmentations

n_r — number of piecewise linear regions

n_t — number of time points

tf — testability factor

σ — standard deviation

1. INTRODUCTION

1.1 Statement of Testing Problems

As the demand for electronic circuits and systems in modern technology increases, both their scale and complexity grow rapidly. The phenomenal development of electronic systems would not have been possible without the advances in large scale and very large scale integration (LSI/VLSI) in semiconductor circuit technologies. Large analog or integrated analog and digital circuits are applied to many fields such as medical technology [Stotts 1989], neural networks [Mead 1989, Graf *et al.* 1988, and Hutchinson *et al.* 1988], and space technology. With the growth in significance and pervasiveness of electronic systems, availability, reliability and cost effectiveness become the main characteristics of quality. Therefore, in order to achieve the desired quality, product testing is of the utmost importance.

Testing, generally speaking, means examination of a product, to ensure that it functions and exhibits the properties and capabilities for which it was designed. The main purpose of testing is to *detect* malfunctions and *locate* their cause so that they can be eliminated. The quality of a test system can be evaluated on the basis of its availability, reliability and cost–effectiveness.

For large scale circuits and systems, testing is not only important but also complex, difficult and costly. It is difficult to gain access to different subsystems for functional testing. It is costly to analyze test results since the computations increase with the cube of the system size. Therefore, in order to meet the

needs of modern technology, a reliable and cost–efficient automatic test system for large scale electronic circuits should be developed.

Electronic circuit testing can be broadly classified into digital circuit testing and analog circuit testing. Digital circuit testing has developed quite rapidly in recent years. Excellent research results have contributed substantially to this advancement [Tsui, 1987]. Testing of analog circuits is more difficult than that of digital circuits because of the following reasons:

1. Analog circuits do not have precise accept/reject criteria in terms of clearly defined thresholds.

2. Analog components do not have good fault models like the stuck–at or stuck–open models widely accepted in digital testing.

3. Element tolerances and signal noise increase the difficulty of analog testing.

In an electronic system, digital circuits and analog circuits are interfaced through interacting circuits such as sensors, transducers and other forms of converters (e.g., A/D and D/A converters). These circuits are called mixed–mode (digital/analog) circuits. Testing of mixed–mode circuits has been attracting the interest of researchers in the past few years [Mahoney, 1987].

Testing of analog and mixed–mode circuits is a very important and challenging task. In the following discussion, a brief review of the existing methods for analog testing is given.

1.2 Brief Review of Analog Testing

Testing and fault diagnosis of analog circuits have been an active research topic for more than twenty five years. Some of the earliest publications in this area [Berkowitz 1962, Brown *et al.* 1962, Allen 1963, and Seshu and Waxman 1966] described basic techniques and their limitations as well as difficulties in analog testing. Over the years many researchers have worked to make analog testing more powerful and reliable. They have considered topics such as testability measures, computational requirements, effects of measurement errors and element tolerances. Yet, to this day, many problems remain unsolved and many techniques need better implementation.

Bandler and Salama (1985) gave an excellent review of the techniques and research publications in fault diagnosis for analog circuits. They compared the existing techniques in a systematic and understandable format. Depending on whether circuit simulation takes place before or after the test, analog circuit diagnosis methods can be classified into two main categories: the simulation before test (SBT) methods and the simulation after test (SAT) methods. The former methods consist of two major steps. The first step is to construct a fault dictionary by analyzing the circuit being tested for various faults with given measurement points. The second is to compare the measured responses with the simulated results in this dictionary to locate faults (so called <u>fault dictionary technique</u>). The latter methods try to locate faults directly from measurement data by verifying faulty assumptions (so called <u>fault verification technique</u>) or by calculating parameter values (so called <u>parameter identification technique</u>).

In order to ascertain the effectiveness of an analog test technique, it is necessary to establish a measure of testability. Testability can be measured in different ways depending on the technique being used and the type of circuit being tested. In order to insure the efficiency of the test, an optimum set of measurement points is selected before performing the measurement. Different measurement points are selected depending on the test situation. In the following sections, three techniques are discussed including the testability analysis and test point selection.

1.2.1 Fault Dictionary Technique

The fault dictionary technique is well suited for the diagnosis of <u>hard faults</u> (shorts, opens, catastrophic changes in bias points, *etc.*) [Seshu and Waxman 1966, Schreiber 1979, and Lin and Elcherif 1988]. As mentioned above, this technique is implemented in two steps. The first step is to construct a dictionary which includes the most likely faults. A circuit under test is simulated for the hypothesized faulty cases. Sets of stimuli are designed to produce desired responses in order to detect and isolate the faults. Signatures of the response are stored in the dictionary for use in the second step. An optimum set of stimuli, responses, and signatures is required to store the minimum amount of data and to achieve the desired degree of detection. In the second step, the circuit is excited by the stimuli designed in the first step. The signatures obtained are compared with those stored in the dictionary. The fault, or an ambiguity set that contains the number of possible faults, is identified if the signature matches one of the prestored signatures. Different methods were used to select an optimum set of measurements for the fault dictionary

[Freeman 1979, Hochwald and Bastian 1979, and Varghese *et al.* 1978].

1.2.2 Fault Verification Technique

With a limited number of measurements, not all parameters of the network can be identified. The fault verification technique addresses this problem based on the assumption that a few elements are faulty and the rest of network elements are within design tolerances. A set of faulty elements is assumed first. Then test equations generated on the basis of the assumed faulty elements are checked. If the fault assumption is correct, then the equations are consistent. Otherwise they are not. A number of research results have been developed based on this technique. Wu *et al.* (1982) introduced the self-testing method. Wu (1985), Wu and Wu (1986), and Wey (1987,1988) have discussed design testability and test point selection based on this method. Starzyk and Bandler (1981,1982), Huang *et al.* (1983), Lin, *et al.* (1983) have formulated topological testability conditions for the fault verification technique. Maeda *et al.* (1986) extended these topological conditions to the case of nonlinear systems. Reisig and DeCarlo (1987) expanded this method to analog–digital multiple fault diagnosis. These verification techniques were generalized to handle multi–excitation and multi–frequency tests for piecewise–linear circuits by Starzyk and Dai (1988) and to handle nonlinear circuits by Starzyk and El–Gamal (1988). Nodal and branch decomposition techniques for fault diagnosis and calibration of large networks have been presented by Salama, Starzyk and Bandler (1984) and by Hatzopoulos and Kontoleon (1987). The effect of element tolerances in this technique has been studied by Zou (1988).

1.2.3 Element Identification Technique

The element identification technique is well suited for soft faults (the faults due to the deviations of parameters). Assuming that enough independent measurements are available, all circuit parameters can be identified. The element tolerances are automatically taken into consideration in this technique. The element identification technique is useful in calibration, alignment and fault diagnosis. Most practical electronic circuits are frequency dependent and nonlinear. Consequently, in such networks, a large number of independent measurements can be produced by changing excitation levels and test frequencies. Navid and Willson (1979) have studied the testability of resistive networks based on the rank of the sensitivity matrix. Sen and Saeks (1977,1979) have developed a theory for multi–frequency testing of linear circuits. Visvanathan and Sangiovanni–Vincentelli (1981) and Saeks *et al.* (1981) addressed diagnosability of DC and dynamic nonlinear circuits.

Stenbakken and Souders (1987) developed an efficient algorithm for test point selection and testability measures for the element identification technique. They studied relations between the circuit's testability and measurement errors. In their study, testability is related to the condition number of the test matrix. Test point selection is performed by QR factorization in order to minimize the condition number and increase testability.

1.2.4 Comparisons

Of the three techniques discussed, the element identification technique is the most general and powerful. In the fault dictionary technique, a large number of potential faults should be simulated in order to construct the fault dictionary. However, the amount of computation required to simulate these faults is enormous. This make the faulty dictionary technique suitable for specific circuits but too expensive for general large scale networks. In the fault verification technique, the faults can be located after verifying *all* fault assumptions. For linear circuits, the solution can be obtained by solving linear system equations. But the number of combinations of different fault assumptions increases exponentially as the size of the circuit increases. Therefore, the process of verifying for all assumptions is time consuming.

On the other hand, the element identification method can handle a broad range of test situations (DC testing, frequency domain testing, time domain testing, *etc.*) and test circuits (linear, piecewise linear or nonlinear). Without making any assumptions, faulty elements can be located when the circuit parameters are evaluated. Consequently, the actual element deviations are estimated. The elements can be calibrated to their designed values in order to make the circuit work properly. Based on the estimated parameter values, responses to arbitrary input signals can be predicted. Therefore, the element identification technique is very useful in practical applications such as trimming, alignment, functional testing, fault diagnosis, and calibration.

Normally, the element identification technique is based on the sensitivity

approach, i.e. the sensitivity of the responses with respect to all parameters. The element deviations are found through deviations of the responses and the sensitivity matrix. Testing strategies developed for the sensitivity approach consider many practical aspects including test point selection, element tolerances, measurement errors, *etc.*.

In summary, the element identification technique is general and powerful. Its implementation, based on the sensitivity approach, is very useful in practice, but, unfortunately, cannot handle large scale circuits. The sensitivity matrix is dense which requires an enormous amount of memory space to store and takes a long time to compute when the circuit size is large. Overcoming these deficiencies was the main motivation behind this dissertation.

1.3 Objective and Organization

The objective of this dissertation is to develop a new testing method for large scale circuits based on the element identification technique. This new method must be useful for functional testing and calibration of complex systems as well as identifying element characteristics and verifying macromodels or entire subsystems. It must also be able to diagnose faults and evaluate elements efficiently and reliably, while meeting the requirements of the automatic test system.

In order to realize this objective, two major tasks are defined:
1) develop a decomposition approach for testing large scale circuits and
2) establish testing strategies related to calibration, functional testing and fault

diagnosis.

The first task is realized by decomposing the interconnected system into a number of small subnetworks. To achieve this decomposition without breaking interconnections, voltage measurements are taken at the partition points and new test equations are formulated at these nodes. In this way the effects of the measurement errors are reduced to a local area, and computations are performed in each subcircuit. Subcircuit analysis is facilitated since the boundary conditions are determined by the measurement voltages. Thus, the speed and accuracy of the diagnosis process are improved.

In order to realize the second goal, we must account for all practical aspects of testing. Therefore, we consider finite accuracy of the computer simulation as well as effects of measurement errors on the validity of the results obtained. The best set of test points (DC excitation levels, test frequencies, and type of input signals applied) is selected in order to achieve adequate test coverage with minimum cost. In addition, an accurate response prediction and an effective method to eliminate ambiguity groups are proposed.

Figure 1.3.1 shows classification of testing techniques with special emphasis on two approaches presented in this dissertation — sensitivity approach and decomposition approach.

```
┌─────────────────────────┐
│   Electronic  Circuit   │
│        Testing          │
└─────────────────────────┘
            │
     ┌──────┴───────┐
     ▼              ▼
┌──────────┐   ┌──────────────┐
│ Digital  │   │ Analog       │
│ Circuit  │   │ Circuit      │
│ Testing  │   │ Testing      │
└──────────┘   └──────────────┘
                     │
        ┌────────────┼────────────┐
        ▼            ▼            ▼
┌──────────────┐ ┌──────────────┐ ┌──────────────┐
│ Fault        │ │ Element      │ │ Fault        │
│ Dictionary   │ │ Identification│ │ Verification │
│ Technique    │ │ Technique    │ │ Technique    │
└──────────────┘ └──────────────┘ └──────────────┘
                     │
          ┌──────────┴──────────┐
          ▼                     ▼
   ┌──────────────┐      ┌──────────────┐
   │ Sensitivity  │      │ Decomposition│
   │ Approach     │      │ Approach     │
   └──────────────┘      └──────────────┘
```
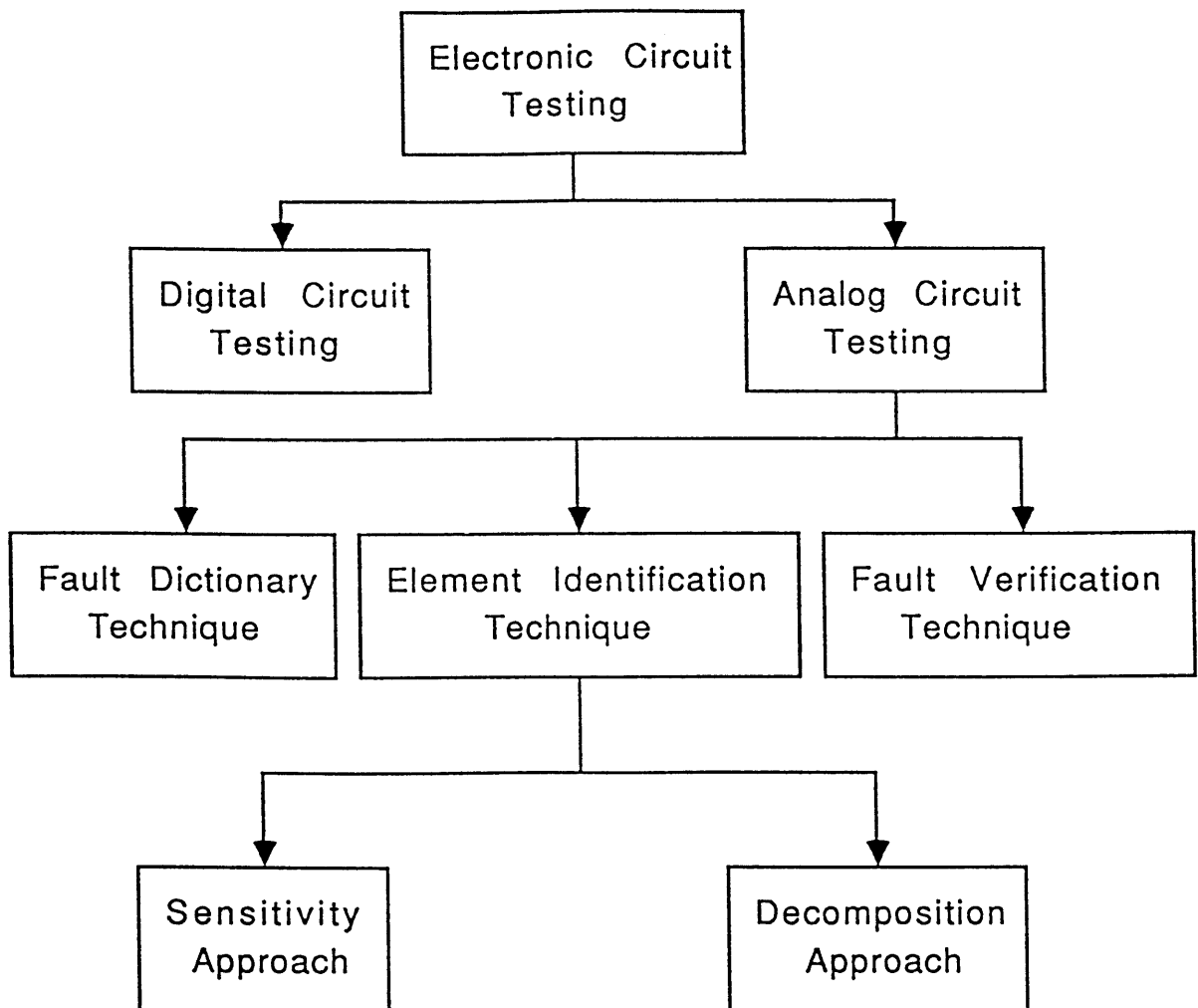
Fig. 1.3.1 Classification of electronic circuit testing.

Remaining of this dissertation is organized as follows: In Chapter 2, general test methods and the test procedure for element identification techniques are given. In Chapter 3, the sensitivity approach is discussed. The response simulation and sensitivity matrix are derived in DC, time and frequency domains respectively. The research for this approach stems from the need to implement the sensitivity based methods in a practical testing situation and to include them as software tools in circuit simulators. The discussion in Chapter 3 serves also as an introduction to the decomposition approach. In Chapter 4, the decomposition approach for large scale circuits is developed. Test equations are formed based on Kirchhoff's current law (KCL) equations at the partition nodes. In a similar way, the internal voltage simulation and the test matrix are derived in DC, time and frequency domains. The test matrix obtained by the decomposition approach is a bordered block diagonal (BBD) matrix thereby allowing sparse matrix and parallel processing techniques to be used to speed up computation in circuit simulation and fault diagnosis. In Chapter 5, test strategies for practical considerations, including test point selection, response prediction, and the effects of ambiguity groups, measurement errors, and time skews are covered. In Chapter 6, computer simulation and experimental results are given. The results obtained by the sensitivity approach and decomposition approach are compared. Chapter 7 presents the conclusion which includes discussion and suggestions for future work.

2. GENERAL APPROACH

When a new circuit is built, the responses of the circuit to one or several specific input signals must be measured to determine whether it works or not. This is called <u>functional testing</u>. If the responses are out of the range of design specifications, the circuit can be adjusted by calibrating its parameter values. This is referred to as <u>calibration</u>. In order to perform trimming, alignment and calibration, the actual parameter deviations must be estimated. The purpose of element identification and fault diagnosis is to find the actual parameter deviations from the measurements.

In general, fault diagnosis is more difficult than analysis. Equations for determining element values from measurement data such as input and output voltages are nonlinear, even for a linear circuit. One numerical approach to element identification is to linearize these equations. A solution of the linearized equations can be obtained by the Newton—Raphson iteration process. This approach is called <u>the first order approximation method</u>. Testing techniques based on the first order approximation method are both general and powerful. Techniques developed in this dissertation belong to this category. In the following sections, classification of the test methods is defined. A test procedure for the proposed method is described in a general way and the corresponding iterative process is given.

2.1 Test Methods

Test methods can be classified according to the following factors: test subjects — circuits under test, test environments and test functions.

2.1.1 Test Subjects

Circuits under test can be linear or nonlinear. Linear circuits contain linear RCL elements, operational amplifiers, controlled sources, nullators, norators, and switches. Nonlinear circuits contain the components which have nonlinear characteristics such as nonlinear resistors and capacitors, diodes, BJT transistors, and MOS transistors.

2.1.2 Test Environments

Depending upon the type of circuit being tested and the test equipment used, a test can be performed in DC domain, frequency domain or time domain:

DC domain:

excitations:	DC voltage/current sources,
measurements:	DC voltage, DC current, transfer function.

Frequency domain:

excitations:	sinusoidal − single frequency, multifrequency, or arbitrary periodic function,
measurements:	magnitude/phase of voltages at test frequencies, or harmonic frequencies.

Time domain:

excitations:	step function, impulse function, arbitrary waveforms,
measurements:	step response, impulse response arbitrary time domain response.

2.1.3 Test Functions

Test equations are derived from test functions using the information obtained from the tested circuit (such as circuit topology, parameter values and element models, etc.) and measurements. In general, test functions can be represented as a system of nonlinear functions in variable p as.

$$\phi = \phi (p) \qquad (2.1.1)$$

where p is a vector of parameter values. We denote the actual parameters values by p^* and the nominal or designed parameter values by p^0. The purpose of fault diagnosis is to find the deviations of actual parameters from design parameters as $\Delta p^* = p^* - p^0$. Once the actual parameter values are known, the faulty components can be identified and can be calibrated to the designed parameter values. Test functions are defined in such a way that for $p = p^*$,

$$\phi(p^*) = 0 , \qquad (2.1.2)$$

To solve (2.1.2), we expand the system functions in the Taylor series about p^0:

$$\phi(p^*) \cong \phi(p^0) + \frac{\partial \phi}{\partial p}\bigg|_{p=p^0} (p^* - p^0) + \cdots \qquad (2.1.3)$$

In the case of the actual parameters p^* being close to their nominal values p^0, higher order terms in (2.1.3) may be ignored and the system can be written in a linearized form:

$$\phi(p^*) \cong \phi(p^0) + T \Delta p , \qquad (2.1.4)$$

where T is the Jacobian matrix

$$T = \frac{\partial \phi}{\partial p} , \qquad (2.1.5)$$

and Δp are unknown deviations

$$\Delta p = p^* - p^0. \tag{2.1.6}$$

Substituting (2.1.2) into (2.1.4), we have

$$T \, \Delta p = - \phi(p^0) \, . \tag{2.1.7}$$

The element deviations Δp can be obtained by solving (2.1.7). If Δp is large, the iterative process can be applied in which case we replace p^0 by a variable p. Solvability of (2.1.7) depends on the condition number of the coefficient matrix T in (2.1.5). We give the following definitions:

Test function: $\phi(p)$,

Test matrix T: $\dfrac{\partial \, \phi}{\partial \, p}$,

Test equation: $T \, \Delta p = - \phi(p)$.

The test function can be defined in different ways. Depending upon different test functions, the test matrix has different properties. Consequently, the test equation is solved using different techniques.

Normally, output voltages are defined as test functions. Since in such approach the test matrix is equivalent to the sensitivity matrix, we call it the sensitivity approach. The advantage of this approach is that test points can be selected directly by performing the QR factorization [Leon 1980] on the sensitivity matrix [Stenbakken and Souders 1987]. The disadvantage is that the sensitivity matrix is dense, therefore it needs a large memory capacity to store and a significant amount of computational effort to analyze.

To overcome the problems of the sensitivity approach, we define the node current function at the measurement nodes as the test function. The resulting test matrix has bordered block diagonal structure so the decomposition technique can be applied. We call this method <u>decomposition approach</u>. The advantage of this approach is that the effect of faults is limited to local subcircuits, and the memory requirement and computational effort is much less than in the sensitivity approach. The disadvantage is that voltage measurements must be performed at partitioned nodes, and that the test point selection is not as intuitive as that in the sensitivity approach.

The classification factors of test methods discussed in this section are illustrated in Fig. 2.1.1
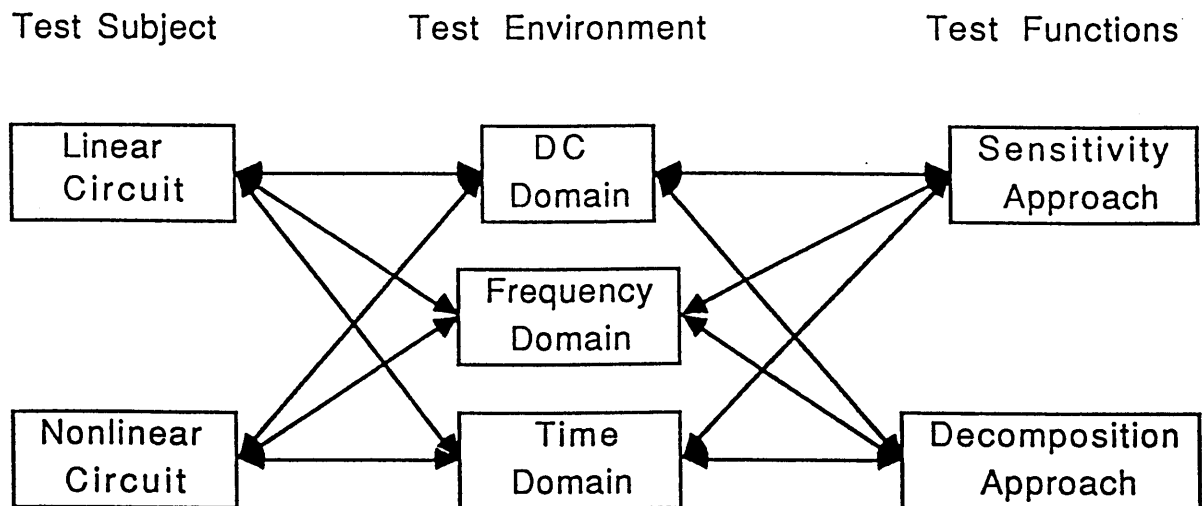
Fig. 2.1.1 Classification factors of the element identification methods.

2.2 Test Procedure

Test procedure developed in this dissertation is implemented in three stages: pre—test, real—test and post—test. In the pre—test stage, the following tasks are performed:

(1) The physical circuit is modeled. Modeling is the process by which electrical properties of a device or a group of interconnected devices are represented through mathematical equations, circuit representations or tables. Complex devices and large scale systems are characterized by macromodels which reflect their terminal behavior. There are several different modeling techniques and device element models [Meiner and Spina 1980, Antognetti and Massobrio 1988, and Milnes 1980].

(2) The response to one or more specific input signals is simulated based on the circuit model. The DC response, time domain response or frequency domain response are simulated depending on the type of test environment. This step can be implemented with the help of circuit simulators such as SPICE [Nagel 1976], SABER [Goering 1986], *etc.*.

(3) The test matrix is formulated depending on the type of test function. In the sensitivity approach, the test matrix is equivalent to the sensitivity matrix. In the decomposition approach, the test matrix is derived based on the Kirchhoff current law equations. Up until now, sensitivity analysis has not been available in the public domain circuit simulators. This dissertation has developed the software for sensitivity calculation in the

frequency domain and the time domain.

(4)   Test selection and test analysis are performed. One possible approach is to run the QR factorization on the test matrix.

Pre—test computations are performed either at the design stage or before performing the real test. The computational effort at this stage is quite large but can be computed off—line. Only one sample circuit is used to prepare the information needed to test other circuits of the same design. This information is useful to both design and test engineers. Design engineers may propose the accessible nodes. Test engineers know which measurements should be taken in order to achieve a reliable and cost effective test.

During testing, reference input signals are applied to the circuit using input signals (DC levels, signal frequencies and waveforms) selected in the pre—test stage. Either a network or spectrum analyzer or waveform recorder is used to measure the output response(s) at the previously selected test points (test nodes, test frequencies, harmonics, and sampling time point).

In the post—test stage, the measurement data and the test matrix are used to estimate the actual circuit parameters. Accurate predictions of the circuit's response to other arbitrary inputs can be made by performing response simulations using the updated parameters.

The post—test computation should be performed on—line. It requires an algorithm to calculate the parameter deviations quickly, so that the circuit

components can be adjusted to their designed values by the automatic calibration system once the measurements have been made. Computation is accomplished for each tested circuit. This test procedure is summarized in Fig. 2.2.1.

2.3 Iterative Process

If the actual circuit parameters are substantially different from the nominal values on which the test matrix is based, then the iteration process is needed. Using superscript k to indicate the kth iteration sequence, the iterative procedure will be as follows:

1. calculate Δp^k from

$$T^k(p^k) \ \Delta p^k = -\phi(p^k) \tag{2.3.1}$$

2. update element values

$$p^{k+1} = p^k + w^k \ \Delta p^k \tag{2.3.2}$$

where w^k is the weight factor $(0 < w^k < 1)$. Usually w^k is selected such that

$$|| \ \phi(p^{k+1}) \ || \ \leq \ || \ \phi(p^k)|| \tag{2.3.3}$$

3. check the condition

$$||\phi(p^{k+1})|| \ \leq \ \epsilon_1 \ \text{ and } \ \Delta p^k \leq \epsilon_2 \tag{2.3.4}$$

where ϵ_1 and ϵ_2 are the preset bounds.

4. stop if the conditions (2.3.4) are satisfied, otherwise

set k=k+1 and go back to step 1.

Since the starting point p^0 for the iterative process is close to the actual solution point p^*, this iterative process converges for all practical situations.
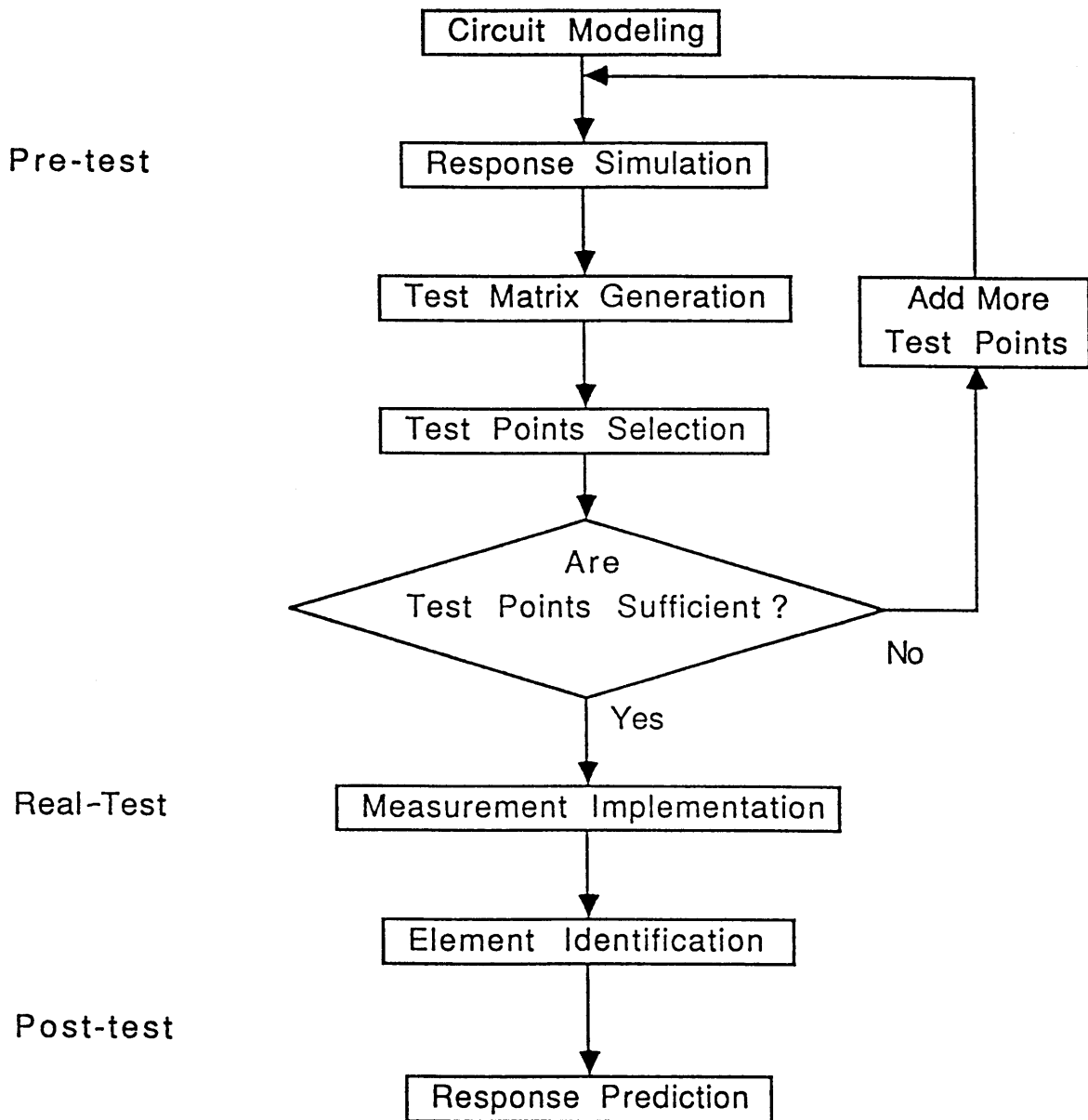
Fig. 2.2.1 General test procedure

3. SENSITIVITY APPROACH

This chapter presents the sensitivity approach for fault diagnosis and calibration. Sensitivity s is a derivative of a response x(p) with respect to any parameter p; i.e., $s = \partial x / \partial p$. Sensitivities help us to understand how variations of parameters influence the response. In Section 3.1 we derive test equations based on responses x and their sensitivities. Sensitivity computation is the key element for this approach. DC sensitivity, time domain sensitivity, and frequency domain sensitivity are derived. Although sensitivity computations have been described and used in many research papers [Navid and Willson 1979, Saeks *et al.* 1981 and Visvanathan and Sangiovanni–Vincentelli 1981, 1984, Flecha and DeCarlo, 1984], we present them in this chapter in order to use a uniform notation for different test environments, and as a reference for the decomposition approach developed in Chapter 4.

3.1 Test Equations and Sensitivity Matrix

Test functions can be defined as the differences between measured responses x^* and nominal responses x(p) as

$$\phi(p) = x(p) - x^* , \tag{3.1.1}$$

where x(p) can be simulated based on the circuit model with element values **p**.

A test matrix corresponding to the test function (3.1.1) consists of derivatives of responses x w.r.t. parameters **p**. Since the test matrix is equivalent to the sensitivity matrix, it can be denoted by s and given by

$$s = \frac{\partial \phi}{\partial p} = \frac{\partial x(p)}{\partial p} \qquad (3.1.2)$$

The test equation is obtained by substituting (3.1.1) into (2.1.7)

$$s \, \Delta p = \Delta x \qquad (3.1.3)$$

where $\Delta x = x^* - x(p)$. It can be seen from (3.1.3) that in order to obtain Δp, the sensitivity matrix s should be computed first. Sensitivities can be calculated either by the finite difference method or the adjoint technique. The finite difference method is easily implemented, requiring only repeated simulation of the circuit response with parameter values perturbed from the nominal. However, unacceptable errors may occur, and the computational cost is prohibitive in most cases. The adjoint technique is a popular numerical method for computing sensitivities [Director and Rohrer, 1969]. Once the system response is obtained, the sensitivity can be determined by solving a system of linear equations.

After each element and device in a circuit is modeled, a system of circuit equations is determined using both the element model equations and topological constraints. The topological constraints reflect KCL and KVL. The circuit equations are, in general, a system of algebraic–differential equations of the form

$$f(\dot{x}, \, x, \, p, \, t, \, w) = 0 \, , \qquad (3.1.4)$$

where

x is the vector of voltages, currents, capacitor charges, and inductor fluxes spanning the solution space of the circuit,

$\dot{x}$ is the vector of partial derivatives with respect to t ($\dot{x} = \partial x / \partial t$),

p   is the vector of circuit parameters,

w   is the vector of input functions.

The solution of (3.1.4) and the sensitivity matrix $\partial x/\partial p$ can be determined for different cases such as DC, time domain and frequency domain.

3.2 DC Sensitivity

Usually, the DC solution is determined for the equilibrium case, that is, for the case when $\dot{x}$ is zero. Energy storage in the circuit is ignored (capacitors are replaced by open circuits and inductors are replaced by short circuits). With excitation fixed and with no time–varying circuit elements, the circuit equations are not dependent on time. Without loss of generality, t can be set to 0, and hence (3.1.4) can be modified to

$$f\ (0,\ x_0,\ p,\ 0,\ w)\ =\ 0 \qquad\qquad (3.2.1)$$

or simply

$$f(x_0,\ p,\ w)\ =\ 0\ . \qquad\qquad (3.2.2)$$

If the circuit contains a nonlinear element, then the DC solution is obtained by an iterative sequence of a linearization algorithm.   The Newton–Raphson algorithm is the common method of linearization. Beginning with an initial "guess" for the solution, all nonlinear equations are linearized about this initial operating point. The system equations for the linear equivalent circuit can be solved using linear methods. The circuit solution is then used as the next "guess", and the process is repeated. The iteration stops when successive solutions agree within a specified tolerance. The linearized equation is

$$\frac{\partial \, f}{\partial \, x_0} \Delta x_0 = - \, f \, . \tag{3.2.3}$$

Iterations in (3.2.3) provide x_0. At the convergence, the Jacobian matrix is available in its factored form.

Differentiating (3.2.1) with respect to p, yields

$$\frac{\partial \, f}{\partial \, x_0} \frac{\partial \, x_0}{\partial \, p} + \frac{\partial \, f}{\partial \, p} = 0 \, . \tag{3.2.4}$$

The DC sensitivities can be found by solving the following equation:

$$\frac{\partial \, f}{\partial \, x_0} \frac{\partial \, x_0}{\partial \, p} = - \frac{\partial \, f}{\partial \, p} \, . \tag{3.2.5}$$

Let us denote

$$s_0 = \frac{\partial \, x_0}{\partial \, p} \, , \tag{3.2.6}$$

Then (3.2.5) becomes

$$\frac{\partial \, f}{\partial \, x_0} s_0 = - \frac{\partial \, f}{\partial \, p} \, . \tag{3.2.7}$$

The DC solutions x_0 and their sensitivities s_0 can be used as the initial values in time domain analysis, or the operating point values in the frequency domain analysis.

3.3 Time Domain Sensitivity

Time domain analysis determines the response of a circuit to specified time domain inputs. The sensitivity of the response w.r.t. to a parameter can be calculated when the response is determined. The initial time instant can be arbitrarily defined as time zero. The initial conditions (response and sensitivity at the initial time instant) are determined by previous DC operating point solutions x_0 and DC sensitivities s_0.

The time interval $(0, \tau)$ is divided into the discrete time instants $(0, t_1, t_2, ..., \tau)$. At each time instant, the solution of (3.1.4) is determined by a nonlinear equation solver first. Then the sensitivities of (3.1.4) w.r.t. all parameters can be obtained simultaneously with the solution vector by solving linear equations. The time interval between successive time instants is controlled by a computer program to insure an accurate solution. After that, computed data is interpolated at the time instants at which measurements will be taken.

First we derive the sensitivity matrix based on the general formulation. Then the modified nodal equation formulation is given as an example to illustrate the procedure.

3.3.1 General Formulation

The sensitivity calculation is implemented in two steps: 1) network analysis, in which the system solution is found, and 2) sensitivity analysis, in which the system sensitivity is obtained.

A. Network Analysis

At a certain time instant t_j, (3.1.4) becomes a nonlinear algebraic equation

$$f(\dot{x}_j, x_j, p) = 0 . \tag{3.3.1}$$

Using the *backward differentiation formula* (BDF) [Gear 1971], $\dot{x}$ can be represented by

$$\dot{x}_j = \sum_{\ell=0}^{k_j} \frac{1}{h_j} \alpha_{\ell j} x_{j-\ell}, \tag{3.3.2}$$

where

$$h_j = t_j - t_{j-1} ,$$

In order to solve (3.3.1) by the modified Newton–Raphson method or other techniques [see, for example, Ortega and Rheinboldt, 1970], the Jacobian matrix is evaluated by

$$\mathbf{M}_j = \frac{d f}{d x_j} = \frac{\partial f}{\partial \dot{x}_j} \frac{\partial \dot{x}_j}{\partial x_j} + \frac{\partial f}{\partial x_j} . \tag{3.3.3}$$

Using (3.3.2), we can get

$$\frac{\partial \dot{x}_j}{\partial x_j} = \frac{\alpha_{0j}}{h_j} .1 . \tag{3.3.4}$$

Let us denote

$$a_\ell = \frac{\alpha_{\ell j}}{h_j} , \tag{3.3.5}$$

and the Jacobian matrix (3.3.3) becomes

$$M_j = \frac{\partial f}{\partial \dot{x}_j} a_0 + \frac{\partial f}{\partial x_j} \quad . \tag{3.3.6}$$

The nonlinear iterations are solved using Newton–Raphson method

$$M_j \, \Delta x_j = - \, f_j \quad . \tag{3.3.7}$$

B. Sensitivity Analysis

Sensitivities of the solution x_j of the original system (3.3.1) w.r.t. parameters p can be obtained by differentiating both sides of (3.3.1)

$$\frac{\partial f}{\partial \dot{x}_j} \frac{\partial \dot{x}_j}{\partial p} + \frac{\partial f}{\partial x_j} \frac{\partial x_j}{\partial p} + \frac{\partial f}{\partial p} = 0 \quad . \tag{3.3.8}$$

Let us denote

$$s_j = \frac{\partial x_j}{\partial p} \quad , \tag{3.3.9}$$

then (3.3.8) becomes

$$\frac{\partial f}{\partial \dot{x}_j} \dot{s}_j + \frac{\partial f}{\partial x_j} s_j = - \frac{\partial f}{\partial p} \quad . \tag{3.3.10}$$

Using BDF, we can write $\dot{s}_j$ as

$$\dot{s}_j = a_0 \, s_j + \sum_{\ell=1}^{k_j} a_\ell \, s_{j-\ell} \quad . \tag{3.3.11}$$

Substituting (3.3.11) into (3.3.10), we get

$$\left[\frac{\partial f}{\partial \dot{x}_j} a_0 + \frac{\partial f}{\partial x_j} \right] s_j = - \frac{\partial f}{\partial p} - \frac{\partial f}{\partial \dot{x}_j} \sum_{\ell=1}^{k_j} a_\ell \, s_{j-\ell} \quad . \tag{3.3.12}$$

The system of linear equations (3.3.12) has the following form:

$$\mathbf{M}_j \, \mathbf{s}_j = - \, \mathbf{B}_j \, , \tag{3.3.13}$$

where

$$\mathbf{M}_j = \frac{\partial f}{\partial \dot{x}_j} a_0 + \frac{\partial f}{\partial x_j} \, , \tag{3.3.14}$$

and

$$\mathbf{B}_j = \frac{\partial f}{\partial p} + \frac{\partial f}{\partial \dot{x}_j} \sum_{\ell=1}^{k} a_\ell \, \mathbf{s}_{j-\ell} \, . \tag{3.3.15}$$

Remarks:

1.   The coefficient matrix (3.3.14) is the same as the Jacobian matrix (3.3.6) of the original system calculated at the solution point. When the iterations (3.3.7) at time instant t_j converge, the matrix $\mathbf{M}_j$ is available in a factored form.

2.   Equation (3.3.13) is linear. Sensitivities can be obtained by solving linear equations with the coefficient matrix known in the factored form.

3.   Matrices $\dfrac{\partial f}{\partial \dot{x}_j}$, $\dfrac{\partial f}{\partial x_j}$ and $\dfrac{\partial f}{\partial p}$ are functions of $\dot{x}$, x and p. At each time instant, these matrices can be evaluated using the solutions x, derivative $\dot{x}$ obtained from BDF (3.3.2), and the nominal parameter values p_0.

3.3.2. Sensitivity Formulation Based on the Modified Nodal Equations

The modified nodal equation generally has the following form:

$$f(x,p,t) = \mathcal{Y}(p)\, x + y(x) - w = 0 \ . \tag{3.3.16}$$

Here $\mathcal{Y}$ consists of linear elements and y consists of nonlinear elements, and the vector x has the form

$$x = \begin{bmatrix} v \\ q \end{bmatrix} , \tag{3.3.17}$$

where the vector v consists of the nodal voltages and currents through inductors, independent and controlled voltage sources, and current–controlled voltage sources. The vector q consists of capacitor charges and inductor fluxes.

If charges/fluxes of linear capacitors/inductors are expressed as functions of the branch voltages/currents, then q contains only charges/fluxes of nonlinear reactive elements. Equation (3.3.16) can be written as

$$f(x,p,t) = C\,\dot{x} + G\,x + y(x) - w = 0 \ , \tag{3.3.18}$$

where C is the linear reactive matrix and G is the linear resistive matrix.

A. General Case

In most cases, the charge of a capacitive branch q can be explicitly expressed by the voltage v across that branch

$$q = q(v) \ .$$

A transformation of q into v is allowed so that the unknown vector is v rather than larger vector x. The modified nodal equations can be rewritten in the

following form:

$$f(\dot{v},v,p,t) = G\ v + C\ \dot{v} + A\ g(v,p) + A\ \dot{q}(v,p) - w = 0, \qquad (3.3.19)$$

where

A is the incidence matrix,

g(v,p) is a vector of currents through nonlinear resistive elements,

q(v,p) is a vector of currents through nonlinear reactive elements.

For simplicity, let C_{eq} denote $\partial f/\partial \dot{x}$, G_{eq} denote $\partial f/\partial x$ and u_{eq} denote $\partial f/\partial p$. Derivatives of the system function f needed in (3.3.8) can be evaluated as follows:

$$G_{eq} = \frac{\partial\ f}{\partial\ v} = G + A\ \frac{\partial\ g}{\partial\ v} + A\ \frac{\partial\ \dot{q}}{\partial\ v}, \qquad (3.3.20)$$

$$C_{eq} = \frac{\partial\ f}{\partial\ \dot{v}} = C + A\ \frac{\partial\ \dot{q}}{\partial\ \dot{v}} = C + A\ \frac{\partial\ q}{\partial\ v}, \qquad (3.3.21)$$

$$u_{eq} = \frac{\partial\ f}{\partial\ p} = \frac{\partial\ G}{\partial\ p}\ v + \frac{\partial\ C}{\partial\ p}\ \dot{v} + A\ \frac{\partial\ g}{\partial\ p} + A\ \frac{\partial\ \dot{q}}{\partial\ p}, \qquad (3.3.22)$$

where

$$\frac{\partial\ \dot{q}}{\partial\ v} = \frac{\partial}{\partial v}\ \frac{\partial\ q}{\partial\ v}\ \frac{d\ v}{d\ t} = \frac{\partial^2 q}{\partial v^2}\ \dot{v}, \qquad (3.3.23)$$

and

$$\frac{\partial\ \dot{q}}{\partial\ p} = \frac{\partial}{\partial p}\ \frac{\partial\ q}{\partial\ v}\ \frac{d\ v}{d\ t} = \frac{\partial^2\ q}{\partial p\ \partial v}\ \dot{v}. \qquad (3.3.24)$$

Since the branch equations are described by analytic functions of their

arguments, the above derivatives can be obtained directly. The equation (3.3.10) can be written as

$$C_{eq} \, \dot{s}_j + G_{eq} \, s_j = - \, u_{eq} \, . \qquad (3.3.25)$$

In similar way (3.3.12) can be simplified as

$$(C_{eq} \, a_0 + G_{eq} \,) \, s_j = - \, u_{eq} - C_{eq} \, \sum_{\ell=1}^{k_j} a_\ell \, s_{j-\ell} \, . \qquad (3.3.26)$$

B. DC Case

In a DC case, $t = 0$ and $\dot{v} = 0$. The DC equations are obtained from (3.3.19) as

$$f \, (v_0, p) = G \, v_0 + A \, g(v_0, p) - w_0 = 0 \, , \qquad (3.3.27)$$

$$q = q(v_0, p) \, .$$

Differentiating both sides of (3.3.27) w.r.t. p yields

$$(G + A \, \frac{\partial \, g}{\partial \, v_0}) \, \frac{\partial \, v_0}{\partial \, p} = - \, (\frac{\partial \, G}{\partial \, p} \, v_0 + A \, \frac{\partial \, g}{\partial \, p}) \quad . \qquad (3.3.28)$$

Let

$$u_{geq} = \frac{\partial \, f}{\partial \, p} = \frac{\partial \, G}{\partial \, p} \, v + A \, \frac{\partial \, g}{\partial \, p} \, . \qquad (3.3.29)$$

The DC sensitivities can be obtained from

$$G_{eq} \, s_0 = - \, u_{geq} \, . \qquad (3.3.30)$$

Note that (3.3.30) is the nodal formulation of the DC sensitivity equation (3.2.7).

C. Linear Case

In the case of a linear network, both $g(v,p)$ and $q(v,p)$ are equal to zero. The linear equations are obtained from (3.3.19) as

$$f(\dot{v}, \ v, \ p, \ t) \ = \ C \ \dot{v} \ + \ G \ v \ - \ w(t) \ = \ 0 \ . \tag{3.3.31}$$

Let

$$u \ = \ \frac{\partial \ f}{\partial \ p} \ = \ \frac{\partial \ G}{\partial \ p} \ v \ + \ \frac{\partial \ C}{\partial \ p} \ \dot{v} \ , \tag{3.3.32}$$

then the system sensitivity equation is simplified to

$$C \ \dot{s}_j \ + \ G \ s_j \ = \ - \ u \ . \tag{3.3.33}$$

After applying BDF, sensitivities can be obtained by solving

$$(C \ a_0 \ + \ G \ ) \ s_j \ = \ - \ u \ - \ C \ \sum_{\ell=1}^{k_j} \ a_\ell \ s_{j-\ell} \ . \tag{3.3.34}$$

3.3.3. Procedure to Generate the Sensitivity Matrix in Time Domain

The sensitivity matrix can be obtained using the following procedure:

1. Evaluate the linear resistive matrix G and the reactive matrix C. These two matrices do not depend on time or the solution vector.

2. Select the initial values v_0 and s_0 obtained at the DC analysis.

3. Predict v_j using the forward differentiation formula [Gear 1971]

4. Calculate $\dot{v}_j$ using the backward differentiation formula.

5. Evaluate derivatives for nonlinear branches and form C_{eq}, G_{eq} and u_{eq}. Calculate the Jacobian matrix M_j and the function vector f_j .

6. Apply the Newton–Raphson algorithm.

7. Solve the linear system (3.3.26) to obtain the sensitivity vector s_j.

8. Repeat 3–7 for each time instance within $(0-\tau)$, the sensitivity matrix will have the form

$$s = [s_1', s_2',...,s_T']' ,\qquad (3.3.35)$$

where ' stands for the matrix transpose operation.

This procedure is summarized in Fig. 3.3.1.

Remarks:

1. Newton–Raphson's method requires that the Jacobian be constructed and factored at each iteration. If the changes in the Jacobian from iteration to iteration are sufficiently small, then the old Jacobian closely approximates the new one. Therefore, the factored Jacobian from one iteration can be used for several subsequent iterations.

2. If the system response can be obtained from a general circuit simulation program, Steps 3, 5 and 6 are omitted. The sensitivity calculation can be added to this simulation program.

```
                    ┌─────────┐
                    │  t=0    │
                    └────┬────┘
                         ▼
          ┌──────────────────────────────────┐
          │ Evaluate Linear Matrices C & G   │
          │ Find DC Solution and Sensitivity │
          └──────────────┬───────────────────┘
                         ▼
                    ┌─────────┐
                    │ t=t+h   │
                    └────┬────┘
                         ▼
              ┌──────────────────────┐
              │ Numerical Integration│
              └──────────┬───────────┘
                         ▼
          ┌──────────────────────────────────┐
          │ Evaluate Nonlinear Matrices      │
          │ Ceq and Geq                      │
          └──────────────┬───────────────────┘
                         ▼
          ┌──────────────────────────────────┐
          │ Equation Formulation and Solution│
          └──────────────┬───────────────────┘
                         ▼
                    Converged? ──No
                         │
                        Yes
                         ▼
          ┌──────────────────────────────────┐
          │ Store Time Instant Solution Vj   │
          └──────────────┬───────────────────┘
                         ▼
          ┌──────────────────────────────────┐
          │ Calculate Sensitivity Sj by      │
          │ Solving Linear Equation          │
          └──────────────┬───────────────────┘
                         ▼
          ┌──────────────────────────────────┐
          │ Store Sensitivity S              │
          └──────────────┬───────────────────┘
                         ▼
                   Last Time Instant? ──No
                         │
                        Yes
                         ▼
          ┌──────────────────────────────────┐
          │ Generate Output and Sensitivity Matrix │
          └──────────────────────────────────┘
```
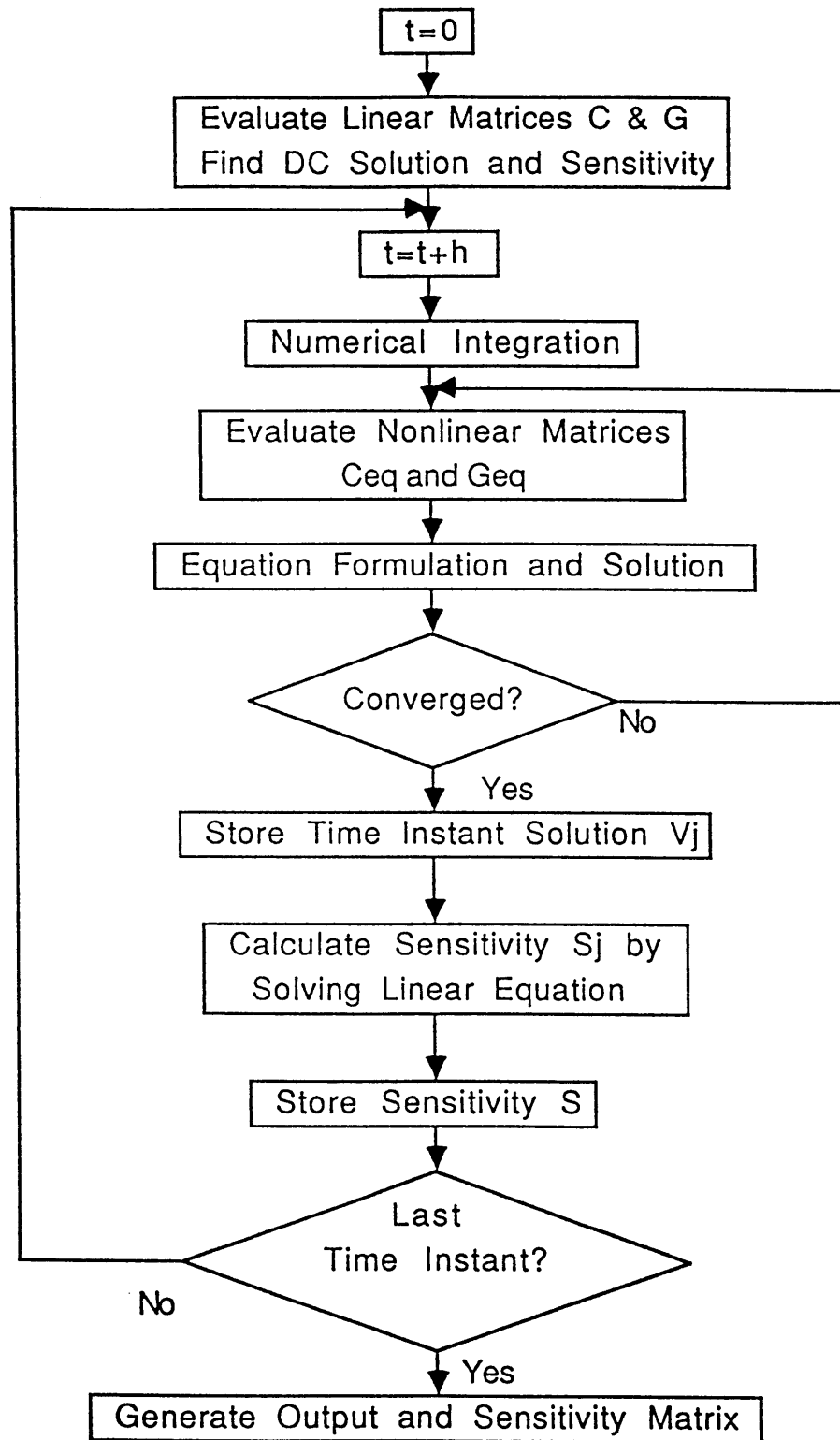
Fig. 3.3.1 Flowchart of sensitivity computation in time domain.

Example

A small nonlinear circuit (Fig. 3.3.2) is chosen to illustrate sensitivity evaluation using the derived formulas. There are two nonlinear elements in this circuit: a nonlinear capacitor C_n and a diode D.

The characteristic equation of the nonlinear capacitor is

$$q = C_n v^2 , \qquad \text{i.e.} \quad i_{C_n} = \dot{q} = 2 C_n v \dot{v},$$

and the corresponding derivatives are

$$\frac{\partial q}{\partial v} = 2C_n v , \qquad \frac{\partial^2 q}{\partial v^2} = 2C_n , \qquad \frac{\partial^2 q}{\partial C_n \partial v} = 2v .$$

The characteristic equation of the diode can be described by

$$i_D = I_s(e^{Kv} - 1) ,$$

where K is a constant, and the corresponding derivatives are

$$\frac{\partial i_D}{\partial v} = KI_s e^{Kv} , \qquad \text{and} \qquad \frac{\partial i_D}{\partial I_s} = e^{Kv} - 1 .$$

The nodal equations are

Node 1 $f_1 = i_{C_n} + G\,(v_1 - v_2) - J_s \qquad = 0 ,$

Node 2 $f_2 = -\,G\,(v_1 - v_2) + i_C + i_D \qquad = 0 .$
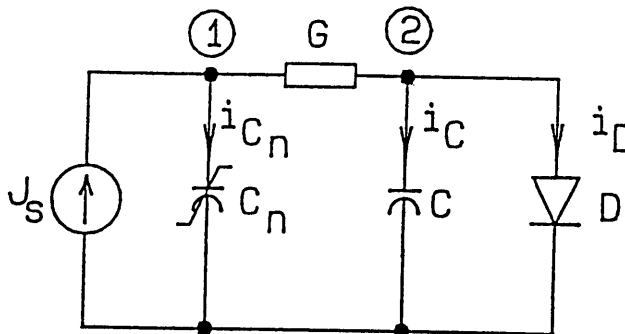
Fig. 3.3.2   A nonlinear circuit.

From (3.3.20) and (3.3.21) we have

$$G_{eq} = \frac{\partial \, f}{\partial \, v} = G + A \, \frac{\partial g}{\partial v} + A \, \frac{\partial \dot{q}}{\partial v} = \begin{bmatrix} G + \frac{\partial^2 q}{\partial v_1^2} \, \dot{v}_1 & -G \\ & \\ -G & G + \frac{\partial i_D}{\partial v_2} \end{bmatrix},$$

$$C_{eq} = \frac{\partial \, f}{\partial \, \dot{v}} = C + A \, \frac{\partial q}{\partial v} = \begin{bmatrix} \frac{\partial q}{\partial v_1} & 0 \\ & \\ 0 & C \end{bmatrix}.$$

The Jacobian matrix is

$$M = C_{eq} \, a_0 + G_{eq} = \begin{bmatrix} G + \frac{\partial^2 q}{\partial v_1^2} \, \dot{v}_1 + \frac{\partial q}{\partial v_1} a_0 & -G \\ & \\ -G & G + \frac{\partial i_D}{\partial v_2} + a_0 C \end{bmatrix}$$

$$= \begin{bmatrix} G + 2C_n \dot{v}_1 + 2\, C_n v_1 a_0 & -G \\ & \\ -\, G & G + \frac{\partial i_D}{\partial v_2} + a_0 C \end{bmatrix},$$

and on the basis of (3.3.22) we have

$$u_{eq} = \frac{\partial \, f}{\partial \, p} = \frac{\partial G}{\partial p} \, v + \frac{\partial C}{\partial p} \, \dot{v} + A \, \frac{\partial g}{\partial p} + A \, \frac{\partial \dot{q}}{\partial p}$$

$$= \begin{bmatrix} G & C & I_s & C_n \\ v_1 - v_2 & 0 & 0 & \frac{\partial^2 q}{\partial C_n \partial v_1} \dot{v}_1 \\ & & & \\ v_2 - v_1 & \dot{v}_2 & \frac{\partial i_D}{\partial I_s} & 0 \end{bmatrix} = \begin{bmatrix} G & C & I_s & C_n \\ v_1 - v_2 & 0 & 0 & 2v_n \dot{v}_1 \\ & & & \\ v_2 - v_1 & \dot{v}_2 & e^{Kv_2} - 1 & 0 \end{bmatrix}.$$

The sensitivity matrix can now be calculated by solving (3.3.26).

3.4 Frequency Domain Sensitivity

A time domain signal x is called a <u>waveform.</u> A frequency domain signal X is called a <u>spectrum.</u> All waveforms are assumed to be of real value, whereas all spectra are assumed to be of complex value. A periodic waveform x with a period T_0 can be written as a Fourier series [Bracewell, 1978]

$$x(t) = \sum_{k=-\infty}^{\infty} X(k) \, e^{jk\omega_0 t}, \qquad \text{where } \omega_0 = \frac{2\pi}{T_0}, \qquad (3.4.1)$$

$$X(k) = \frac{1}{T_0} \int_0^{T_0} x(t) \, e^{-jk\omega_0 t} \, dt \, .$$

The kth harmonic of $x(t)$ is the frequency $k\omega_0$ and $X(k)$ is its Fourier coefficient or phasor. $X=\{..., X(-1), X(0), X(1), ...\}$ is called the <u>frequency domain representation</u> or the spectrum of x.

In frequency domain testing, the spectrum X of response can be measured. For testing purposes, we should find the sensitivity of spectrum X w.r.t. circuit parameter p , $\dfrac{\partial X}{\partial p}$. The deviations Δp can be found by solving the system of linear test equations

$$\frac{\partial X}{\partial p} \, \Delta p = \Delta X \, , \qquad (3.4.2)$$

where $\Delta X = X^* - X(p^0)$, X^* is the spectrum of the measured response, and $X(p^0)$ is the calculated spectrum of the nominal circuit.

In the following discussion, we consider sensitivity calculation in two different cases. First, the circuit is linearized when a small sinusoidal signal or a linear combination of several small sinusoidal signals are applied. In this case, spectrum X can be obtained from the phasor method and the sensitivity calculation can be implemented directly in the frequency domain representation. In the second case, a periodic arbitrary signal is applied to the nonlinear circuit. In this case the simulation of steady-state response and sensitivity calculation becomes complicated. Subsection 3.4.1 presents a method to calculate the AC sensitivity and Subsection 3.4.2 presents methods of sensitivity analysis for a nonlinear circuit excited by periodic functions.

3.4.1 Linearized Circuit (AC) Sensitivity

AC analysis determines the small-signal solution of the circuit in sinusoidal steady state. Since the circuit is in sinusoidal steady state, the system of differential algebraic equations (3.1.4) is transformed into a system of algebraic equations in frequency domain using the phasor method

$$\mathbf{F}\ (\mathbf{X},\ \omega,\ \mathbf{p},\ \mathbf{x}_0,\ \mathbf{W}) = \mathbf{0}\ , \tag{3.4.3}$$

where

$\mathbf{X}$ is the complex (amplitude) vector analogous to the real vector $\mathbf{x}$,

$\mathbf{W}$ is the complex (amplitude) vector analogous to the real vector $\mathbf{w}$,

ω is the input frequency in radians/second,

$\mathbf{x}_0$ is the vector of the DC quiescent conditions, and

$\mathbf{p}$ is the parameter vector.

A. General Linearized Circuit

For small–signal analysis, nonlinear elements are modeled by equivalent linearized models. The parameter values of the linearized model are determined by a DC operating point analysis x_0. For simplicity, the modified nodal analysis formulation is considered for AC circuit equation

$$Y[p, v_0(p)] \ V(p) = W \ , \tag{3.4.4}$$

where V is the complex vector of node voltages analogous to v,

W is the excitation vector analogous to w, and

Y is the admittance matrix dependent on the DC solution v_0.

The AC response V can be obtained from (3.4.4). In order to obtain sensitivities we differentiate (3.4.4) w.r.t. parameters p and use the chain rule. This yields

$$Y \frac{\partial V}{\partial p} = - [\frac{\partial Y}{\partial p} + \frac{\partial Y}{\partial v_0} \frac{\partial v_0}{\partial p}] V + \frac{\partial W}{\partial p} \ . \tag{3.4.5}$$

For a particular frequency ω, we can denote the sensitivity matrix $\dfrac{\partial V}{\partial p}$ by S_ω and rewrite (3.4.5) as

$$Y S_\omega = - [\frac{\partial Y}{\partial p} + \frac{\partial Y}{\partial v_0} s_0] V + \frac{\partial W}{\partial p} \ . \tag{3.4.6}$$

where the DC sensitivity s_0 can be obtained from (3.2.7) or (3.3.30). A circuit

usually has separate DC and AC sources. Power supplies, for example, are DC sources with zero AC values whereas input AC sources often have zero DC values. When the circuit has AC sources only ($v_0=0$ and $s_0=0$), (3.4.6) can be simplified

$$Y S_\omega = - \frac{\partial Y}{\partial p} V + \frac{\partial W}{\partial p} . \qquad (3.4.7)$$

If the excitations do not depend on the parameters, then $\dfrac{\partial W}{\partial p} = 0$. Thus (3.4.7) becomes

$$Y S_\omega = - \frac{\partial Y}{\partial p} V . \qquad (3.4.8)$$

The sensitivity matrix can be explicitly evaluated from

$$S_\omega = - Y^{-1} \frac{\partial Y}{\partial p} V . \qquad (3.4.9)$$

To avoid the matrix inversion, the adjoint technique is used. This results in

$$S_\omega = - V^a \frac{\partial Y}{\partial p} V , \qquad (3.4.10)$$

where V^a is the adjoint matrix [J. Vlach, 1983].

Remarks:

1. $Y(\omega) = G + j \omega C$. Since G and C are independent of frequency ω, they can be precomputed based on the DC solution. Comparing the matrix $Y(\omega)$ with the coefficient matrix of (3.3.26), we find that these two matrices have an identical structure with a_0 in (3.3.26) substituted by $j\omega$.

2. When solution V is known, the sensitivity can be simply obtained by the adjoint technique.

3. Suppose that p is the element incident to the nodes i and j in the network

N. Let v_{qr} be the voltage at node q (q=1,2,...,n) when an excitation is applied at node r. Since $\dfrac{\partial Y}{\partial p}$ has four or less nonzero elements, individual sensitivities in (3.4.10) can be obtained from

$$\frac{\partial v_{qr}}{\partial p} = (v_{qi}^{a} - v_{qj}^{a}) (v_{ir} - v_{jr}) . \qquad (3.4.11)$$

Generally, when an element p appears in the coefficient matrix Y on the intersection of rows i,j and columns k,l, then

$$\frac{\partial v_{qr}}{\partial p} = (v_{qi}^{a} - v_{qj}^{a}) (v_{kr} - v_{lr}) . \qquad (3.4.12)$$

B. Piecewise Linear Circuit

In a piecewise linear circuit, a nonlinear element can be approximated by several linear segments as shown in Fig. 3.4.1.
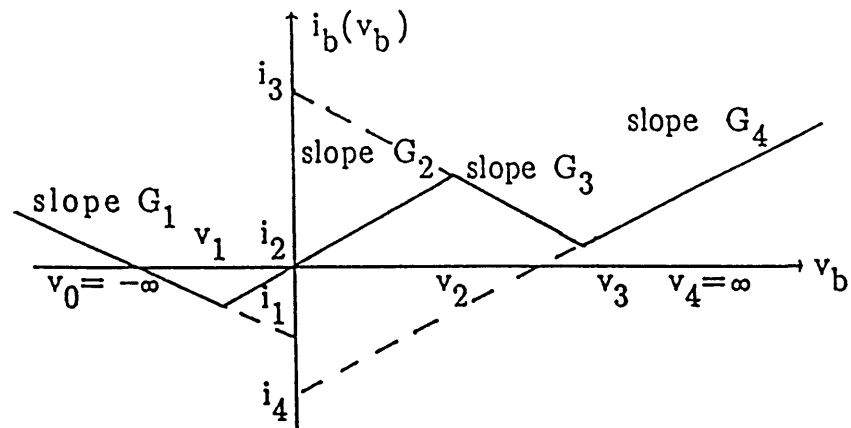
Fig. 3.4.1 Characteristic of a piecewise linear element.

In the ℓth segment, branch current i_b is described by a function of the branch voltage v_b

$$i_b(v_b) = i_\ell + G_\ell v_b \qquad \text{for} \qquad v_{\ell-1} \leq v_b \leq v_\ell , \qquad (3.4.13)$$

where G_ℓ is the equivalent admittance at this operating point and i_ℓ is the equivalent DC source at this point. Derivatives of the branch variables are

$$\frac{\partial i_b}{\partial v_b} = G_\ell , \qquad \frac{\partial i_b}{\partial i_\ell} = 1 , \qquad \text{and} \qquad \frac{\partial i_b}{\partial G_\ell} = v_b. \qquad (3.4.14)$$

The linear combination of segments of different elements is called a <u>region.</u> Denote r to be the region in which the network N_r operates, and replace all nonlinear elements by their equivalent admittance and current source at the operating point. The network N_r becomes a linearized network and the nodal equations have the form

$$Y_r V_r = I + I_r . \qquad (3.4.15)$$

where I_r is the vector of currents through the nonlinear elements.

The ℓth linear piecewise element can be represented by the linear admittance G_ℓ and equivalent current source i_ℓ as shown in Fig. 3.4.1. In this case, the sensitivities will be obtained by the method used in the linear network (3.4.11) and (3.4.7). When the branch is incident to the nodes 1 and j, we have

$$\frac{\partial V_r}{\partial G_\ell} = (v_i^a - v_j^a)(v_i - v_j) , \qquad (3.4.16)$$

and

$$\frac{\partial V_r}{\partial i_\ell} = - (v_i^a - v_j^a) . \qquad (3.4.17)$$

C. Sensitivity of the Magnitude of the Response

Using the frequency domain representation, the response V has a complex value. A complex variable can be expressed by its magnitude $|V|$ and phase φ,

$$V = |V|\ e^{j\varphi}\ .\tag{3.4.18}$$

Usually, the magnitude $|V|$ can be measured with high accuracy (measurement error $\leq$ 0.1%), but the phase measurement is less accurate. Most often we only measure the magnitude of the spectrum $|V|$. In this section we discuss how to find the sensitivity of measured $|V|$ after the sensitivity of the spectrum V has been computed. First let us change the test equation (3.4.2) to

$$\frac{\partial |V|}{\partial\ p}\ \Delta p = \Delta |V|\ ,\tag{3.4.19}$$

where $\Delta|V| = |V^*| - |V(p)|$. The magnitude of a variable can be computed by

$$|V| = \sqrt{V \cdot \tilde{V}}\ ,\tag{3.4.20}$$

where $\tilde{V}$ is the complex conjugate of V. Denote $\hat{S}$ to be the sensitivities of $|V|$ w.r.t. p. We can derive $\hat{S}$ as follows:

$$\hat{S}\ = \frac{\partial |V|}{\partial\ p} = \frac{\partial (V \cdot \tilde{V})^{1/2}}{\partial p}$$

$$= \frac{\partial (V \cdot \tilde{V})^{1/2}}{\partial (V \cdot \tilde{V})}\ \frac{\partial (V \cdot \tilde{V})}{\partial\ p}$$

$$= \frac{1}{2} \frac{1}{(V \cdot \tilde{V})^{1/2}} \left(\frac{\partial V}{\partial p} \tilde{V} + V \frac{\partial \tilde{V}}{\partial p} \right)$$

$$= \frac{1}{|V|} \text{Re} \left(\frac{\partial V}{\partial p} \tilde{V} \right) \qquad (3.4.21)$$

After the sensitivity of the spectrum $\dfrac{\partial V}{\partial p}$ is obtained, the sensitivity of the magnitude of the spectrum $\dfrac{\partial |V|}{\partial p}$ can be calculated from (3.4.21). It is obvious that the sensitivity $\dfrac{\partial |V|}{\partial p}$ is real.

D. Procedure to Generate and Solve Test Equations (AC case)

1. Measure the magnitude of the responses $|V^*|$ at all test frequencies.

2. Linearize the circuit elements at the operating point.

3. Calculate spectra of responses $V(p)$ from (3.4.4) and get $|V(p)|$.

4. Compute the adjoint matrix V^a.

5. Evaluate the sensitivity matrix S_ω (i.e. $\dfrac{\partial V}{\partial p}$) using (3.4.11–12) or (3.4.16–17).

6. Obtain the sensitivity of the magnitude of the response $\hat{S}_\omega$ (i.e. $\dfrac{\partial |V|}{\partial p}$) from (3.4.21).

7. Repeat Steps 3–6 for all test frequencies. If n_f is the number of test frequencies, the sensitivity matrix has the form

$$\hat{S} = [\hat{S}_1', \hat{S}_2', ..., \hat{S}_{n_f}']'.$$

8. Obtain element deviations Δp by solving

$$\hat{S} \, \Delta p = \Delta |V| \qquad (3.4.22)$$

3.4.2 Periodic Nonlinear Circuit Sensitivity

There are three ways to find the spectrum of response and its sensitivity in a nonlinear circuit. The first way is to find the steady state response and its sensitivity in time domain. Once the steady state x and $\frac{\partial x}{\partial p}$ are evaluated, the spectrum X and $\frac{\partial X}{\partial p}$ can be obtained by Fourier transformation. This is called the <u>time domain</u> method. The second way is to evaluate the spectrum X and its sensitivity $\frac{\partial X}{\partial p}$ directly in the frequency domain. This is called the <u>frequency domain</u> method. The third way is to partition a circuit into the linear and nonlinear part, and analyze the linear part in the frequency domain and the nonlinear part in time domain. This is called the <u>hybrid</u> method.

The following sections present different methods to evaluate the periodic circuit responses. These methods can be used to evaluate sensitivities, if the "original network" is replaced by the "sensitivity network" and the circuit response x is replaced by its sensitivity s $(\partial x/\partial p)$. The only difference is that several iterations are needed to obtain the response values, but only one step is needed to obtain the sensitivities. The procedure to generate and solve test equations is given in Part D.

A. Time Domain Methods

Many time domain methods are available for finding the steady state solution of a nonlinear circuit. The primary approach is to integrate the system

equations over many periods until the transients die out. Such an approach is probably the best for systems which quickly converge to the steady state. But many practical networks are such that the transients die out only after hundreds of periods.

To avoid expensive integration, several methods have been proposed in recent years. They can be classified into two basic categories: the shooting method and the finite—difference method. The shooting method treats the problem as an initial—value problem to be evaluated over one period. It tries to find an initial state that eliminates any transient behavior and results in periodicity. There are two ways to accelerate convergence of nonlinear iteration to the periodic solution. The first one is the so—called shooting by extrapolation method [Skelboe 1980]. The other approach is the so—called shooting by Newton—Raphson method [Trick et al. 1975].

The shooting by extrapolation method simulates the circuit over several periods. The final states of all periods are used to extrapolate the values of circuit states which result in the steady state. Extrapolated states may not result in the steady state, but they will be close. In such a case, the extrapolation procedure is repeated starting with the new states until the circuit reaches the steady state.

In the shooting by Newton—Raphson method, the circuit is simulated for one period and the final state is compared with the initial state. If two states match, then the circuit is in the steady state. Otherwise, the derivative of the

final state w.r.t. the initial state must be calculated and the Newton—Raphson algorithm is used to find the change in the initial state. The initial state is adjusted and the procedure is performed again in order to achieve the steady state.

In the finite—difference method, the differential equations are substituted by the finite—difference equations. The method tries to find the solution that satisfies the boundary condition. The finite difference methods can generate large number of system equations when either the number of unknown waveforms or the number of time points is large. However, this method has an advantage because of its robustness, which stems from performing the iterative process on the waveform rather than initial conditions.

B. Frequency Domain Methods

The second approach is to calculate spectrum response and sensitivity in frequency domain. The <u>power series</u> method is one approach to nonlinear circuit analysis in the frequency domain, in which both linear and the nonlinear elements are treated in the frequency domain. Frequency domain nonlinear analyses use functional expansions of the input—output characteristic of the nonlinear element, $y(t) = F(x(t))$. Generally, the input function, $x(t)$, is the summation of some basis functions, and the responses due to each functional component of the expansion are added to yield the total response of the system $y(t)$. The simplest functional expansion is the representation of $y(t)$ as a power series in $x(t)$. Conventional power series expansions can only be used with resistive systems having single valued input—output characteristics.

Volterra series, developed by Weiner in the 1950's, can be used with a large class of nonlinear systems. It can handle reactive systems with single valued input—output characteristics. But the method only works for circuits that have weak nonlinearities [Weiner and Spina 1980].

Steer and Khan (1983) developed the generalized power series method which is related to Volterra series analysis. However, it is not restricted to weakly nonlinear systems, as is Volterra series. The nonlinear elements are described using generalized power series while the linear elements are handled using the standard frequency domain nodal technique. The spectra of the terminal variables of nonlinear and linear circuits are balanced iteratively [Rhyne et al. 1988]. The solution can be found by minimizing the objective function derived from the application of Kirchhoff's current law. This method can be also called the spectral balance method.

C. Hybrid Method

A popular method for simulation of periodic nonlinear circuits is called the harmonic balance method [Nakhla and J.Vlach 1976, Curtice 1987, and Kundert and Sangiovanni—Vincentelli 1986]. The harmonic balance method analyzes linear circuits in the frequency domain and nonlinear circuits in the time domain, and transforms the solution of nonlinear circuits back to the frequency domain using the discrete Fourier transform. The harmonics of the terminal variables of nonlinear and linear circuits are balanced iteratively. Since the analysis of nonlinear circuits is explicitly done in the time domain, this method is more appropriately called the hybrid method.

The harmonic balance method is very useful in the simulation of microwave circuits [Wong 1988]. It can be also applied to almost—periodic circuits [Kundert, *et al.* 1988].

The methods discussed above are classified in Fig. 3.4.2.
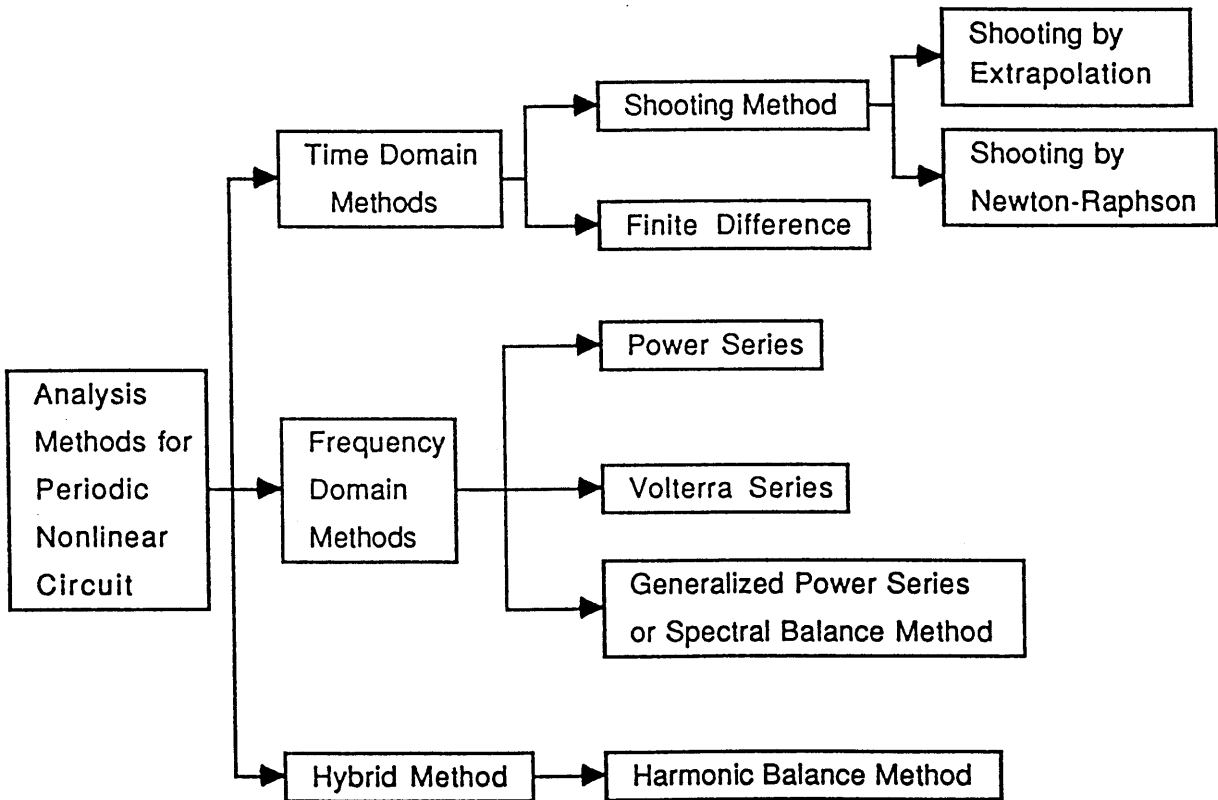
Fig. 3.4.2 Classification of analysis methods for periodic nonlinear circuits.

D. Procedure to Generate and Solve Test Equations (Nonlinear)

In order to test nonlinear circuits with periodic input functions, the following procedure can be implemented:

1. Measure the spectra of responses X^* at all harmonic frequencies.

2. Calculate the spectra of response X based on the nominal circuit using the time domain method, the frequency domain method or the hybrid method.

3. Evaluate the spectra of sensitivities $\frac{\partial X}{\partial p}$ using the same method that is used to find the spectra of response X.

4. The sensitivity matrix has the form

$$S = [S_1', S_2', ..., S_{n_h}']',$$

where ' stands for the matrix transpose and n_h is the number of harmonic frequencies.

5. Obtain element deviations Δp by solving the test equation

$$S \Delta p = X^* - X.$$

3.6 Summary

The sensitivity matrix method is currently the most popular fault identification technique. It can handle a broad category of networks and testing situations. Specialized formulas have been developed for this method when applied to linear and nonlinear networks or networks with reactive elements and switches. Different test equations are derived depending upon the type of measured responses such as time domain response, frequency response or harmonics of a periodic response.

As was mentioned in the previous sections, sensitivities are calculated in two stages: the network analysis stage and the sensitivity analysis stage. In the network analysis stage, equations of the "original network" are solved and the circuit responses are obtained. In the sensitivity analysis stage, equations of the "sensitivity network" are solved and the sensitivities of the circuit response are evaluated. The system matrix (Jacobian matrix) in the sensitivity analysis is the same as the system matrix at the convergence of iterations in the network analysis. Hence, the most important task is to evaluate the circuit response in the network analysis. Once the circuit response is evaluated, its sensitivities can be obtained by solving a system of linear equations.

The sensitivity matrix is the same as the test matrix in the sensitivity approach. Test points are directly selected by the QR factorization (QRF) based on the sensitivity matrix [Stenbakken and Souders 1987].

However, the method shows some serious drawbacks when applied to large scale circuits. The first drawback is its low speed. In order to derive the sensitivity matrix, a circuit must be analyzed using simulators based on Newton's method, a sparse matrix technique, and numerical integration. Since the computation time in these simulators is very long for large circuits, the size of circuits that can be tested practically using the sensitivity matrix approach is limited to a few hundred elements.

Another drawback is the low accuracy of the sensitivity matrix method. In addition to errors caused by the first order approximation, the method is very sensitive to inaccuracies in the circuit model and in the numerical integration

techniques, to parasitics introduced by the test equipment and errors of time synchronization [Dai and Souders 1989]. Serious problems are associated with determination of the rank of the sensitivity matrix, testability factors, and ambiguity groups [Stenbakken, Souders and Stewart 1988].

Finally, the sensitivity matrix method has large memory requirements, not only during the analysis but also at the solution of the test equations. Each transfer function is sensitive to variations of every network parameter. This causes the sensitivity matrix to be dense and makes numerical calculations expensive in the case of large networks. Since the obtained sensitivity matrix is dense, the memory required is at least proportional to the square of the number of network parameters. For example, a digital—to—analog converter model with 50 resistors required a 1024 x 50 sensitivity matrix which was close to the memory limits of the CDC Cyber—855 computer [Stenbakken and Souders 1987].

4. DECOMPOSITION APPROACH

This chapter presents a new testing method for large analog and mixed—mode circuits based on the decomposition approach. As we mentioned in the previous chapter, the sensitivity approach is a very popular fault identification technique which can be used for different networks and testing environments. However, the sensitivity approach shows serious drawbacks when it is applied to large circuits: 1) it needs large computation time and memory space, 2) it is sensitive to errors caused by the circuit model, numerical methods, and measurements, 3) it cannot be directly applied to the mixed mode circuits. In order to eliminate these drawbacks, the decomposition approach is now introduced.

It is well known that decomposition approaches to network analysis are very effective in reducing the amount of computation when the analyzed network becomes sizable [Starzyk *et al.* 1980, 1983 and M. Vlach 1985]. Salama *et al.* (1984) proposed the decomposition approach for fault location in large—scale networks using the fault verification technique. In this case it is assumed that the faulty elements are located within a small part of the network and the remaining part is fault—free. The decomposition of network into smaller subnetworks facilitate testing by localizing the effect of faults.

In their approach to fault location [Salama *et al.*, 1984], a network is decomposed into subnetworks at accessible nodes. For each subnetwork the terminal currents are computed from its terminal voltages assuming that the subnetwork is fault—free. The validity of this assumption is tested by checking

KCL at the accessible nodes. A test at an accessible node is passed if the computed terminal currents satisfy KCL at this node, and all the subnetworks connected to it are declared to be fault–free. If KCL is not satisfied, the test is failed, and at least one of the subnetworks connected to this node is faulty. The pass–or–fail results of different tests are analyzed, using logical diagnostic functions, to identify the faulty subnetworks.

The process can be performed hierarchically. The original network is decomposed into a small number of subnetworks, and these subnetworks which contain faults are identified. Each of these faulty subnetworks are then further decomposed into a small number of sub–subnetworks and again, the faulty sub–subnetworks are identified. The process is repeated until each fault is localized within a sufficiently small portion of the network. The logical fault analysis at each stage involves only a small number of subnetworks, therefore the computational effort needed to locate the fault is minimal. On the other hand, the parameters of subnetworks are necessary to compute the terminal currents which requires a great amount of computation. This computation can be done before the actual testing and stored in memory. This approach is attractive for on–line testing cases where a quick fault analysis is needed.

But Salama's method was developed only for fault location not for element identification. Element identification is more difficult than fault location since all parameter values in the circuit have to be evaluated. Therefore the need to develop a decomposition approach for element identification is of significant importance. This new approach developed in the course of this dissertation is presented in the following sections. The basic idea of this approach is as follows.

The network to be tested is partitioned into small subnetworks. Then the voltage measurements are taken at the partition points. Voltages and their sensitivities within each subnetwork can be computed independently and in parallel. The test equations are formulated on the basis of KCL equations at the measurement (partition) points. This results in a system matrix (test matrix) with a bordered block diagonal (BBD) structure. Because of the sparsity of the test matrix obtained, analysis of the test results is much easier. Test point selection and element evaluation are performed in parallel.

This chapter is organized as follows: Section 4.1 presents the nodal decomposition method and shows that the corresponding system matrix is a bordered block diagonal (BBD) structure. These results have been presented in the literature and are cited here in order to derive the new testing method based on the network decomposition. Section 4.2 formulates the system functions and test equations for the decomposed network. Then Section 4.3 derives a general formulation of the test matrix in time domain. Section 4.4 uses nodal equations as an example to illustrate the procedure for evaluating the test matrix in frequency domain. Section 4.5 presents the approximate method for a pre–test simulation and the exact method for a post–test calculation.

4.1 Nodal Decomposition and Structure of the System Matrix

Let N be the network under test. We assume voltage measurements only because direct measurement of currents is not possible in most cases of network diagnosis except perhaps at the input or output terminals of the network. The nodal decomposition is to decompose the network N into k subnetworks by

hypothetically breaking the connections (not actually cutting connecting wires) at accessible nodes (see Fig. 4.1.1). There must be no mutual coupling between any two subnetworks. We assume that all decomposition nodes are accessible for measurements. There are efficient algorithms for nodal decomposition based on the graph theory [Sangiovanni–Vincentelli, *et al.* 1977 and George and Liu 1981].
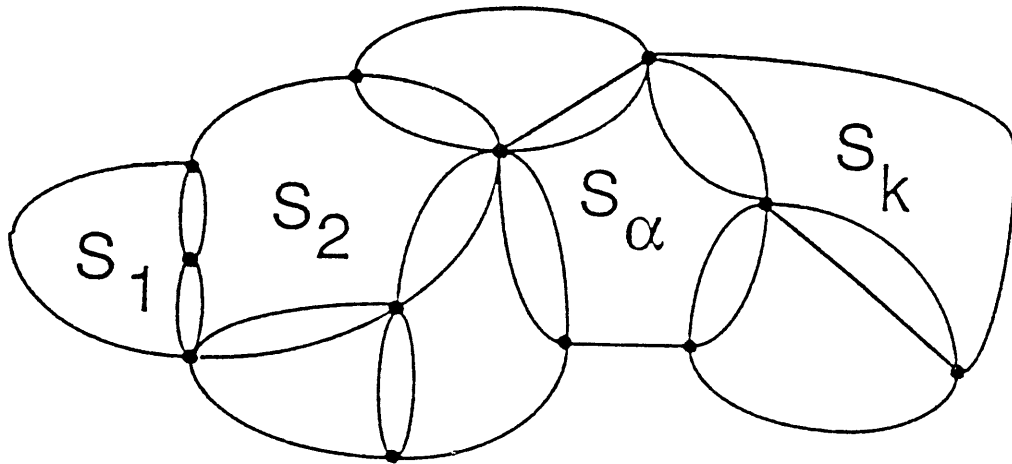
Fig. 4.1.1 Decomposition of Network N.

The entire network can be described by a nonlinear function

$$f(x, p) = 0 \quad , \qquad (4.1.1)$$

where the independent variables x represent voltages and currents. Let us partition the vector x into internal variables (those which are not associated with the test nodes) and external variables (those associated with the test nodes):

$$x = \begin{bmatrix} x^i \\ x^m \end{bmatrix} \quad . \qquad (4.1.2)$$

In a similar way, we can partition the network functions f into internal and external parts:

$$\mathbf{f} = \begin{bmatrix} \mathbf{f}^i \\ \mathbf{f}^m \end{bmatrix} . \qquad (4.1.3)$$

If nodal formulation is used, $\mathbf{f}^i$ consists of KCL equations for each internal node, and $\mathbf{f}^m$ consists of KCL equations for each external node.

The Jacobian of function (4.1.1) may be partitioned from (4.1.2) and (4.1.3) as

$$\mathbf{M} = \frac{\partial \mathbf{f}}{\partial \mathbf{x}} = \begin{bmatrix} \dfrac{\partial \mathbf{f}^i}{\partial \mathbf{x}^i} & \dfrac{\partial \mathbf{f}^i}{\partial \mathbf{x}^m} \\[2ex] \dfrac{\partial \mathbf{f}^m}{\partial \mathbf{x}^i} & \dfrac{\partial \mathbf{f}^m}{\partial \mathbf{x}^m} \end{bmatrix} = \begin{bmatrix} \mathscr{D} & \mathscr{C} \\[2ex] \mathscr{R} & \mathscr{E} \end{bmatrix} . \qquad (4.1.4)$$

where $\mathscr{D}$ stands for diagonal submatrix, $\mathscr{C}$ for column submatrix, $\mathscr{R}$ for row submatrix and $\mathscr{E}$ for external submatrix.

If the network is decomposed into k subnetworks, then the variables of each subnetwork can be partitioned into the internal part and external part:

$$\begin{bmatrix} \mathbf{x}^{i_1} \\ \mathbf{x}^{m_1} \end{bmatrix} , \begin{bmatrix} \mathbf{x}^{i_2} \\ \mathbf{x}^{m_2} \end{bmatrix} \cdots, \begin{bmatrix} \mathbf{x}^{i_\alpha} \\ \mathbf{x}^{m_\alpha} \end{bmatrix} \cdots, \begin{bmatrix} \mathbf{x}^{i_k} \\ \mathbf{x}^{m_k} \end{bmatrix} \qquad (4.1.5)$$

and the external variables of each subnetwork $\mathbf{x}^{m_\alpha}$ are the selected entries of $\mathbf{x}^m$.

$$\mathbf{x}^{m_\alpha} = \mathscr{S}^\alpha \mathbf{x}^m , \qquad (4.1.6)$$

where the $\mathscr{S}^\alpha$ is called a selector matrix whose rows are elementary unit vectors. (e.g. row i of $\mathscr{S}^\alpha$ is e_ℓ, corresponding to the selection $x_i^{m\alpha} = x_\ell^m$). Thus, the independent variables of the interconnected system (4.1.2) can be written as

$$\mathbf{x} = \begin{bmatrix} x^{i_1} \\ \cdots \\ x^{i_k} \\ x^m \end{bmatrix} . \qquad (4.1.7)$$

The selector matrix can be used to express the external functions of the entire network as the summation of the external functions of all subnetworks:

$$f^m = \sum_{\alpha=1}^{k} \mathscr{S}^{\alpha\prime} f^{m\alpha}(x^{i\alpha}, x^{m\alpha}) \qquad (4.1.8)$$

where ' stands for the matrix transpose operation.

The system of equations (4.1.1) can be written as

$$f(\mathbf{x}) = \begin{bmatrix} f^{i_1}(x^{i_1}, x^{m_1}) \\ \cdots \\ f^{i_k}(x^{i_k}, x^{m_k}) \\ f^m(x^i, x^m) \end{bmatrix} = \begin{bmatrix} f^{i_1}(x^{i_1}, \mathscr{S}^1 x^m) \\ \cdots \\ f^{i_k}(x^{i_k}, \mathscr{S}^k x^m) \\ \sum_{\alpha=1}^{k} \mathscr{S}^{\alpha\prime} f^{m\alpha}(x^{i\alpha}, \mathscr{S}^\alpha x^m) \end{bmatrix}. \qquad (4.1.9)$$

since

$$\frac{\partial f^{i\alpha}}{\partial x^m} = \frac{\partial f^{i\alpha}}{\partial x^{m\alpha}} \frac{\partial x^{m\alpha}}{\partial x^m} = \frac{\partial f^{i\alpha}}{\partial x^{m\alpha}} \mathscr{S}^\alpha , \qquad (4.1.10)$$

the Jacobian matrix (4.1.4) becomes

$$
\mathbf{M} = \frac{\partial\ \mathbf{f}}{\partial\ \mathbf{x}} =
\begin{bmatrix}
\dfrac{\partial \mathbf{f}^{i_1}}{\partial \mathbf{x}^{i_1}} & & & & \dfrac{\partial \mathbf{f}^{i_1}}{\partial \mathbf{x}^{m_1}}\ \mathscr{S}^{1} \\
& \cdots & & & \cdot\ \cdot\ \cdot \\
& & \dfrac{\partial \mathbf{f}^{i_k}}{\partial \mathbf{x}^{i_k}} & & \dfrac{\partial \mathbf{f}^{i_k}}{\partial \mathbf{x}^{m_k}}\ \mathscr{S}^{k} \\
\mathscr{S}^{1},\ \dfrac{\partial \mathbf{f}^{m_1}}{\partial \mathbf{x}^{i_1}} & \cdots & \mathscr{S}^{2},\ \dfrac{\partial \mathbf{f}^{m_k}}{\partial \mathbf{x}^{i_k}} & \displaystyle\sum_{\alpha=1}^{k} \mathscr{S}^{\alpha},\ \dfrac{\partial \mathbf{f}^{m_\alpha}}{\partial \mathbf{x}^{m_\alpha}}\ \mathscr{S}^{\alpha}
\end{bmatrix}.
\tag{4.1.11}
$$

Let us denote

$$
\mathscr{D}^{\alpha} = \frac{\partial\ \mathbf{f}^{i_\alpha}}{\partial\ \mathbf{x}^{i_\alpha}}\ , \qquad\qquad
\mathscr{C}^{\alpha} = \frac{\partial\ \mathbf{f}^{i_\alpha}}{\partial\ \mathbf{x}^{m_\alpha}}\ \mathscr{S}^{\alpha}\ ,
$$

$$
\mathscr{R}^{\alpha} = \mathscr{S}^{\alpha},\ \frac{\partial\ \mathbf{f}^{m_\alpha}}{\partial\ \mathbf{x}^{i_\alpha}} \qquad \text{and} \qquad
\mathscr{E}^{\alpha} = \mathscr{S}^{\alpha},\ \frac{\partial\ \mathbf{f}^{m_\alpha}}{\partial\ \mathbf{x}^{m_\alpha}}\ \mathscr{S}^{\alpha}
$$

$$
\text{for } \alpha = 1,2,\ ...,\ k
\tag{4.1.12}
$$

The Jacobian matrix (4.1.11) can be simplified to

$$
\mathbf{M} =
\begin{bmatrix}
\mathscr{D}^{1} & & & & & \mathscr{C}^{1} \\
& \mathscr{D}^{2} & & & & \mathscr{C}^{2} \\
& & \cdots & & & \cdot\ \cdot\ \cdot \\
& & & \mathscr{D}^{\alpha} & & \mathscr{C}^{\alpha} \\
& & & & \cdots\ \mathscr{D}^{k} & \cdot\ \cdot\ \cdot\ \mathscr{C}^{k} \\
\mathscr{R}^{1}\ \mathscr{R}^{2} & ...\ \mathscr{R}^{\alpha} & ...\ \mathscr{R}^{k} & & & \displaystyle\sum_{\alpha=1}^{k} \mathscr{E}^{\alpha}
\end{bmatrix}
=
\begin{bmatrix}
\mathscr{D} & \mathscr{C} \\
\\
\mathscr{R} & \mathscr{E}
\end{bmatrix}.
\tag{4.1.13}
$$

For a single level interconnection, the Jacobian matrix has the bordered block diagonal (BBD) structure as shown (4.1.13). If we decompose the network hierarchically, the Jacobian matrix will have the recursive bordered block diagonal form as follows:

$$\mathbf{M} = \qquad . \qquad\qquad (4.1.14)$$

An efficient implementation of a decomposition algorithm for such a matrix was presented in [M. Vlach, 1986]. The method is very useful for parallel and vector computation. Simulating large electronic circuits with n nodes, $O(n^3)$ computations are needed if the direct analysis method is used, whereas only $O(n*\ln(n))$ computations are needed for the hierarchical decomposition method.

4.2 System Solutions and Test Equations

System solutions used in testing techniques are based on first order approximations. Both the sensitivity approach and the decomposition approach belong to this category. We have presented the sensitivity approach in Chapter 3. After the decomposition approach is discussed, we can compare these two techniques and point out the most essential advantages of the decomposition approach. We can also point out how the decomposition method can be used to test mixed mode circuits.

We see that the critical step in the formulation of the test equations for the sensitivity approach is that both the nominal solution vector x and the sensitivity matrix s have to be calculated first. Usually several iterations are needed to obtain the system solution x when the circuit is nonlinear. Also, the obtained sensitivity matrix s is dense, since all variables in x depend on all parameters p.

It is obvious from the discussion of the sensitivity approach that the most time consuming step in sensitivity evaluation is the solution of the original system. This is also the most inaccurate step in sensitivity evaluation. Inaccuracies in the system model, approximations of nonlinear integration and solutions of nonlinear algebraic equations introduce errors in the sensitivity analysis. The decomposition method significantly reduces these deficiencies. As a result, analog testing strategies can be developed and implemented for networks many times larger than those which can be handled by existing methods (including the sensitivity approach).

In the decomposition method, we attempt to reduce computation time and the need for large memory storage both in the evaluation of the solution vector **x** and the vector of parameter deviations Δ**p**. The approach is realized in two major steps:

1. Network analysis — to calculate the solution vector **x** and to evaluate sensitivities of the internal voltages w.r.t. network parameters.

2. Formulation and solution of test equations — to evaluate parameter deviations Δ**p**.

4.2.1. Network Analysis

In the decomposition approach, the voltage measurements must be taken at the external nodes of each subnetwork. After the test has been completed, the external variables $\mathbf{v}^m$ have known values. In this case, the deviation of measured voltages $\Delta\mathbf{v}^m$ are zero

$$\Delta\mathbf{v}^m = 0 \qquad (4.2.1)$$

and since the measured voltages do not vary with the assumed or computed parameter values, sensitivities of the external variables to the parameters are zero,

$$\mathbf{s}^m = \frac{\partial \; \mathbf{x}^m}{\partial \; \mathbf{p}} = 0 \quad . \qquad (4.2.2)$$

Due to simplification resulting from (4.2.1) and (4.2.2), the system solution vector $\mathbf{x}^i$ and the sensitivities $\mathbf{s}^i$ can be easily computed. When the circuit is decomposed into a number of small subnetworks, all computations for $\mathbf{x}^i$ and $\mathbf{s}^i$ can be implemented in parallel within each subnetwork.

A. Internal System Solutions

As a result of (4.2.1), the deviations of circuit variables contain only the internal part

$$\Delta x = \begin{bmatrix} \Delta x^i \\ \Delta x^m \end{bmatrix} = \begin{bmatrix} \Delta x^i \\ 0 \end{bmatrix} , \qquad (4.2.3)$$

so only the internal system equations f^i are used for solving internal variables Δx^i. If we use the Newton–Raphson iteration process, then the Jacobian matrix M is replaced by the internal submatrix $\mathscr{D}$. Therefore equation (3.3.7) becomes

$$\mathscr{D} \Delta x^i = - f^i , \qquad (4.2.4)$$

where

$$\mathscr{D} = \frac{\partial f^i}{\partial x^i} , \qquad (4.2.5)$$

and

$$f^i = f^i(x_0^i, x^m, p^0) . \qquad (4.2.6)$$

here x_0^i are the assumed internal variables and p^0 are the nominal parameter values. It is known from (4.1.13) that the internal part of the Jacobian matrix $\mathscr{D}$ is the block diagonal matrix. Therefore, equation (4.2.4) can be written as

$$\begin{bmatrix} \mathscr{D}^1 & & & & \\ & \mathscr{D}^2 & & & \\ & & \cdots & & \\ & & & \mathscr{D}^\alpha & \\ & & & & \cdots & \\ & & & & & \mathscr{D}^k \end{bmatrix} \begin{bmatrix} \Delta x^{i_1} \\ \Delta x^{i_2} \\ \cdots \\ \Delta x^{i_\alpha} \\ \cdots \\ \Delta x^{i_k} \end{bmatrix} = - \begin{bmatrix} f^{i_1} \\ f^{i_2} \\ \cdots \\ f^{i_\alpha} \\ \cdots \\ f^{i_k} \end{bmatrix} , \qquad (4.2.7)$$

and it can be solved independently in each block.

$$\mathscr{D}^{\alpha} \Delta x^{i\alpha} = - f^{i\alpha},$$ (4.2.8)

The internal variables $x^{i\alpha}$ are evaluated using the measured variables $x^{m\alpha}$ and the nominal parameter values p^{α} of each subnetwork ($\alpha=1,2,...,k$). All the internal variables $x^{i\alpha}$ can be computed in parallel.

When the iterative process converges, the KCL equations are satisfied at the internal nodes. i.e.,

$$f^i(\bar{x}^i, x^m, p^0) = 0$$ (4.2.9)

where the internal variables $\bar{x}^i$ obtained from (4.2.4) are different than the actual values of x^{i*}. The reason is that the iterations were performed based on the nominal parameters p^0 rather than the actual parameters p^*.

B. Internal System Sensitivities

In order to evaluate the test matrix $\mathscr{S}$, the sensitivities $\dfrac{\partial x^i}{\partial p}$ of the internal variables x^i w.r.t. parameters p should be evaluated first. Differentiating both sides of (4.2.9) w.r.t. p, we obtain

$$\frac{d\ f^i}{d\ p} = \frac{\partial\ f^i}{\partial\ x^i} \frac{\partial\ x^i}{\partial\ p} + \frac{\partial\ f^m}{\partial\ x^m} \frac{\partial\ x^m}{\partial\ p} + \frac{\partial\ f^i}{\partial\ p} = 0 \ .$$ (4.2.10)

Substituting (4.2.2) and putting the last term to the right hand side, we get

$$\frac{\partial\ f^i}{\partial\ x^i} \frac{\partial\ x^i}{\partial\ p} = - \frac{\partial\ f^i}{\partial\ p} \ .$$ (4.2.11)

Let us denote

$$s^i = \frac{\partial \, x^i}{\partial \, p}, \qquad \text{and} \qquad f^i_p = \frac{\partial \, f^i}{\partial \, p} \ . \tag{4.2.12}$$

then (4.2.11) can be written as

$$\mathscr{D} \, s^i = - \, f^i_p \ . \tag{4.2.13}$$

It is clear that the internal variables $x^i{}_\alpha$ and the internal system functions $f^i{}_\alpha$ of the αth subnetwork depend only on these parameters from the vector p which belong to the same subnetwork S_α i.e.

$$s^i = \left\{ \begin{array}{ll} \frac{\partial x^i{}_\alpha}{\partial p} & \text{if } p \in S_\alpha \\ 0 & \text{otherwise} \end{array} \right. \qquad \text{and} \qquad f^i_p = \left\{ \begin{array}{ll} \frac{\partial f^i{}_\alpha}{\partial p} & \text{if } p \in S_\alpha \\ 0 & \text{otherwise} \end{array} \right. \ . \tag{4.2.14}$$

Let

$$s^i{}_\alpha = \frac{\partial \, x^i{}_\alpha}{\partial \, p_\alpha} \ , \qquad \text{and} \qquad f^i_{p_\alpha} = \frac{\partial \, f^i{}_\alpha}{\partial \, p_\alpha} \ , \tag{4.2.15}$$

p_α are the parameters in the αth subnetwork. Thus, the (4.2.13) becomes

$$\begin{bmatrix} \mathscr{D}^1 & & & & & \\ & \mathscr{D}^2 & & & & \\ & & \cdots & & & \\ & & & \mathscr{D}^\alpha & & \\ & & & & \cdots & \\ & & & & & \mathscr{D}^k \end{bmatrix} \begin{bmatrix} s^i{}_1 & & & & & \\ & s^i{}_2 & & & & \\ & & \cdots & & & \\ & & & s^i{}_\alpha & & \\ & & & & \cdots & \\ & & & & & s^i{}_k \end{bmatrix} = - \begin{bmatrix} f^i_{p_1} & & & & & \\ & f^i_{p_2} & & & & \\ & & \cdots & & & \\ & & & f^i_{p_\alpha} & & \\ & & & & \cdots & \\ & & & & & f^i_{p_k} \end{bmatrix} \ . \tag{4.2.16}$$

Since matrices $\mathscr{D}$, s^i and f^i_p are of the block diagonal structure, the internal sensitivity can be solved in each subnetwork independently

$$\mathscr{D}^\alpha \, s^i{}_\alpha = - \, f^i_{p_\alpha} \ . \tag{4.2.17}$$

Note that $\mathscr{D}^{\alpha}$ has the LU factored form obtained when the system solution (4.2.8) converges. Only one forward and backward substitution is needed to solve (4.2.17).

4.2.2 Test Matrix and Test Equations

After the analysis stage, the system equations will be satisfied at the internal points, but in general they will not be satisfied at the partition points

$$f(\overline{x}^i, x^m, p^0) = \begin{bmatrix} f_j^i \\ f_j^m \end{bmatrix} = \begin{bmatrix} 0 \\ f_j^m \end{bmatrix} \quad . \tag{4.2.18}$$

This results from a mismatch between the assumed (in our case nominal) parameter values p^0 for which iterations (4.2.4) were performed, and the actual parameter values p^* for which the measurements were taken. In other words, the reason that the external system equations cannot be satisfied is that the parameter values p^* deviate from their nominal values p^0. Thus, the actual parameter values can be evaluated when the external system equations are satisfied. We define external system functions f^m as test functions

$$f^m = f^m(x^i, x^m, p) \quad . \tag{4.2.19}$$

The corresponding test matrix is

$$\mathscr{T} = \frac{\partial f^m}{\partial p} \quad , \tag{4.2.20}$$

and the test equation is

$$\mathscr{T} \Delta p = - f^m \quad . \tag{4.2.21}$$

This can be compared to the sensitivity approach in which test functions are the differences between measured and nominal responses (3.1.1), and test

matrix is the sensitivity matrix (3.1.2) resulting in test equation (3.1.3). Because of the differences shown in Table 4.2.1, the sensitivity and the decomposition approaches have different numerical properties.

Table 4.2.1 Comparison of sensitivity approach and decomposition approach

	sensitivity approach	decomposition approach
test function	$\phi = x(p) - x^*$	$\phi = f^m(x^i, x^m, p)$
test matrix	$s = \dfrac{\partial x}{\partial p}$	$\mathcal{J} = \dfrac{\partial f^m}{\partial p}$
test equation	$s \Delta p = \Delta x$	$\mathcal{J} \Delta p = - f^m$

In the following discussion, we want to show that the test matrix in the decomposition approach has BBD structure. From (4.2.20)

$$\mathcal{J} = \frac{d\ f^m}{d\ p} = \frac{\partial\ f^m}{\partial\ x^i}\frac{\partial\ x^i}{\partial\ p} + \frac{\partial\ f^m}{\partial\ x^m}\frac{\partial\ x^m}{\partial\ p} + \frac{\partial\ f^m}{\partial\ p}\ . \qquad (4.2.22)$$

Let us denote

$$f^m_p = \frac{\partial\ f^m}{\partial\ p} \qquad (4.2.23)$$

and recall (4.1.4), (4.2.2) and (4.2.12). The test matrix (4.2.22) can be simplified as

$$\mathcal{J} = \mathcal{R}\ s^i + f^m_p \qquad (4.2.24)$$

or written in the block form as

$$
\begin{bmatrix} \mathcal{T}^1 & & & & \\ & \mathcal{T}^2 & & & \\ & & \ddots & & \\ & & & \mathcal{T}^\alpha & \\ & & & & \ddots \\ & & & & & \mathcal{T}^k \end{bmatrix} = \begin{bmatrix} \mathcal{R}^1 & & & & \\ & \mathcal{R}^2 & & & \\ & & \ddots & & \\ & & & \mathcal{R}^\alpha & \\ & & & & \ddots \\ & & & & & \mathcal{R}^k \end{bmatrix} \begin{bmatrix} {}_s^{i_1} & & & & \\ & {}_s^{i_2} & & & \\ & & \ddots & & \\ & & & {}_s^{i_\alpha} & \\ & & & & \ddots \\ & & & & & {}_s^{i_k} \end{bmatrix} + \begin{bmatrix} f_{p_1}^{m_1} & & & & \\ & f_{p_2}^{m_2} & & & \\ & & \ddots & & \\ & & & f_{p_\alpha}^{m_\alpha} & \\ & & & & \ddots \\ & & & & & f_{p_k}^{m_k} \end{bmatrix}.
$$

$$(4.2.25)$$

The matrix s^i is a block diagonal matrix (there is no overlap between any two blocks on the basis of (4.2.14)). The matrices $\mathcal{R}$ and f_p^m are nonzero only for those parameters in the subnetworks which are incident to selected measurement nodes. As the result, the matrix $\mathcal{T}$ is a bordered block diagonal matrix.

The test matrix can be evaluated within each subnetwork in parallel as

$$
\mathcal{T}^\alpha = \mathcal{R}^\alpha \, s^{i_\alpha} + f_{p_\alpha}^{m_\alpha} , \qquad (4.2.26)
$$

and the test equation in the block form is

$$
\begin{bmatrix} \mathcal{T}^1 & & & & \\ & \mathcal{T}^2 & & & \\ & & \ddots & & \\ & & & \mathcal{T}^\alpha & \\ & & & & \ddots \\ & & & & & \mathcal{T}^k \end{bmatrix} \begin{bmatrix} \Delta p_1 \\ \Delta p_2 \\ \cdot\cdot \\ \Delta p_\alpha \\ \cdot\cdot \\ \Delta p_k \end{bmatrix} = - \begin{bmatrix} f^{m_1} \\ f^{m_2} \\ \cdot\cdot \\ f^{m_\alpha} \\ \cdot\cdot \\ f^{m_k} \end{bmatrix} . \qquad (4.2.27)
$$

The structures of matrices $\mathcal{T}$ and $\mathcal{D}$ are different. The matrix $\mathcal{D}$ is of the block diagonal (BD) structure, but the matrix T is of the bordered block diagonal (BBD) structure as shown in Fig. 4.2.1. In the block diagonal matrix,
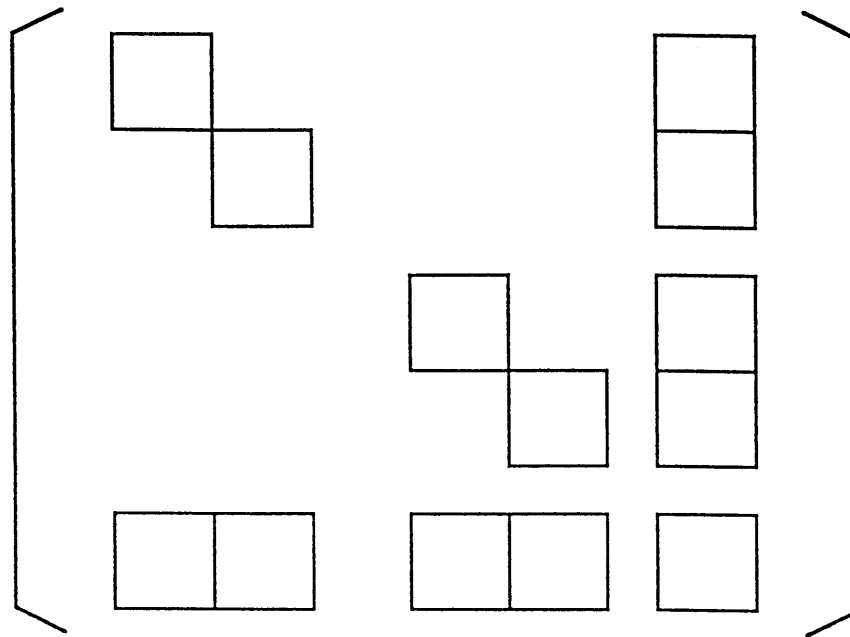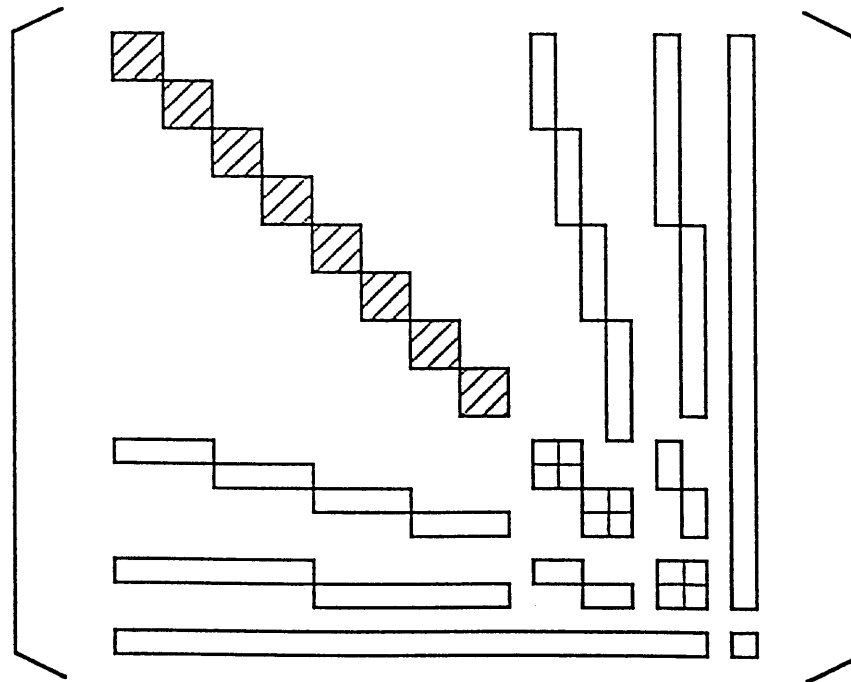
Fig. 4.2.1 (a) Bordered block diagonal matrix of single—level decomposition.

(b) Bordered block diagonal matrix of multi—level decomposition.

blocks are independent from each other (no overlap between any two blocks). So the system equations can be solved independently in each block, e.g. the solutions of the interconnected systems (4.2.7) and (4.2.16) can be obtained by solving the subnetwork systems (4.2.8) and (4.2.17) respectively. In the bordered block diagonal matrix, there are some overlaps between the blocks. The solution of such a system can not be obtained as simply as the solution of a block diagonal system, but such equations can be solved very efficiently using the sparse matrix technique or parallel processing. Due to the bordered block diagonal structure, it is possible to identify individual parameters locally using only measurements from a given subnetwork or adjacent subnetworks.

4.2.3 Procedure to Generate and Solve Test Equations (DC case)

The formulation and solution of the test equation in the DC case can be organized as follows:

1. Decompose the tested network N into k subnetworks.

2. Perform measurements at the partition nodes to obtain x^m for all DC excitation levels.

3. Assume the initial parameter values p^0.

4. Assume initial internal variables x_0^i for a given DC level.

5. For each subnetwork do the following steps in parallel ($\alpha=1,2,...,k$)

   a. Calculate the internal variables $x^{i\alpha}$ by solving the internal system equations. Use the Newton–Raphson iterative process

$$\mathscr{D}^{\alpha} \Delta x^{i\alpha} = - f^{i\alpha} \tag{4.2.28}$$

   b. Keep $\mathscr{D}^{\alpha}$ in LU factored form when $x^{i\alpha}$ converges.

c.   Compute sensitivities $\overset{i}{s}{}^{\alpha}$ of the internal variables $\overset{i}{x}{}^{\alpha}$ w.r.t. the parameters p_{α} of the subnetwork S_{α} by solving the linear equations

$$\mathcal{D}^{\alpha} \, \overset{i}{s}{}^{\alpha} = - \overset{i}{f}{}^{\alpha}_{p_{\alpha}} \tag{4.2.29}$$

d.   Evaluate the test matrix $\mathcal{T}^{\alpha}$

$$\mathcal{T}^{\alpha} = \mathcal{R}^{\alpha} \, \overset{i}{s}{}^{\alpha} + \overset{m}{f}{}^{\alpha}_{p_{\alpha}} \tag{4.2.30}$$

6.   Form the test matrix $\mathcal{T}$ by combining test matrices $\mathcal{T}^{\alpha}$ of all subnetworks.

7.   Repeat Steps 4–6 for each DC excitation level. The test matrix has the form

$$\mathcal{T} = [\; \mathcal{T}'_1 \; \mathcal{T}'_2, \; ..., \; \mathcal{T}'_T]' \tag{4.2.31}$$

where ' represents the matrix transpose operation.

8.   Estimate parameter deviations Δp by solving the test equation of the entire system

$$\mathcal{T} \Delta p = - f^{m} \; . \tag{4.2.32}$$

The test matrix $\mathcal{T}$ is a bordered block diagonal matrix. Sparse matrix technique, a parallel algorithm and vector computation can be used to reduce computational time and memory requirements.

9.   Update the parameter values and repeat steps 3–8 if Δp is large.

This procedure is summarized in Fig. 4.2.2.
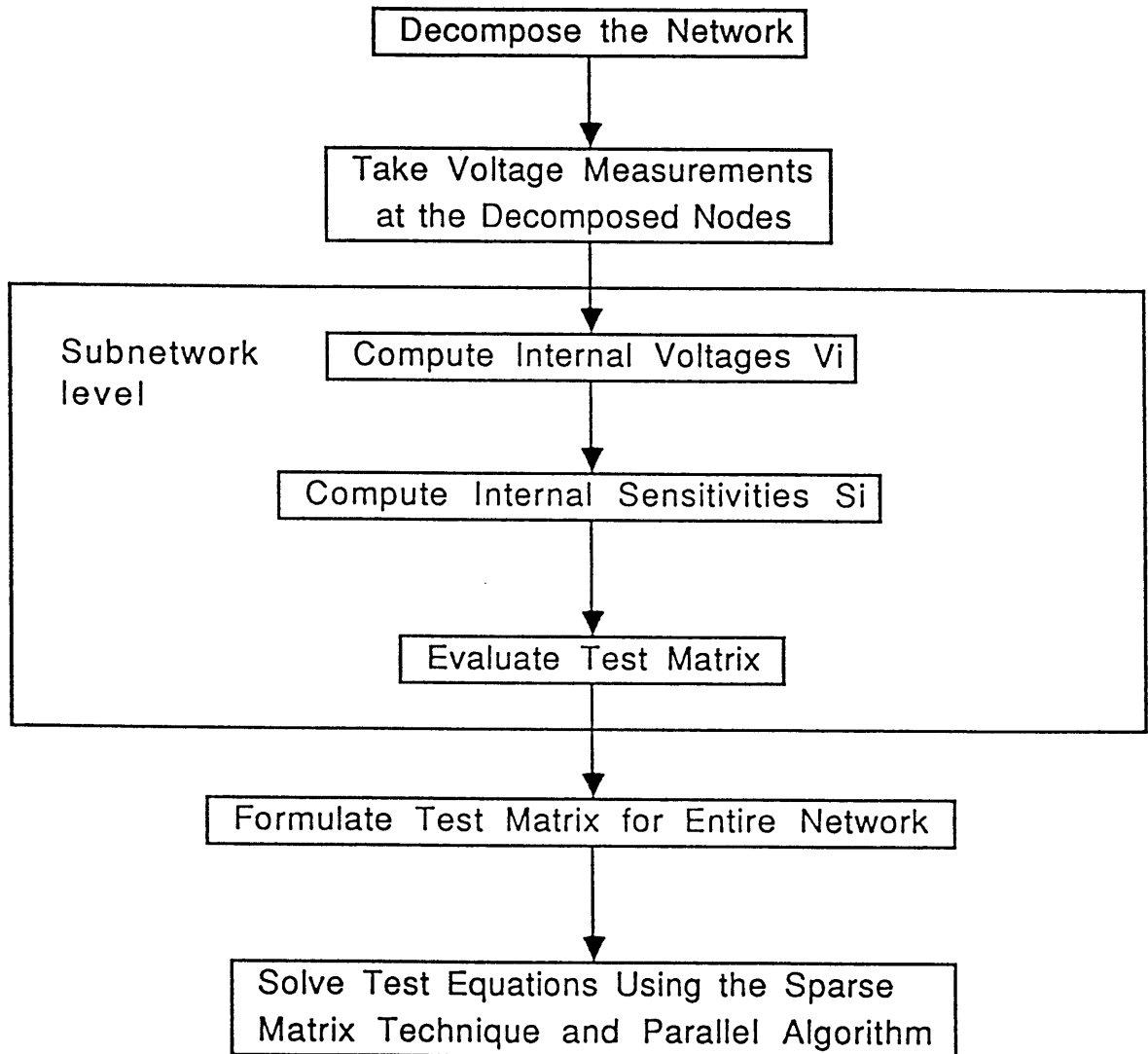
Fig. 4.2.2 Flowchart for generation and solution of test equation in DC case.

4.3 Time Domain Test Equations

In time domain the system is described by an algebraic–differential equation

$$f(\dot{x},x,p,t) = 0 . \tag{4.3.1}$$

At a certain time instant t_j, (4.3.1) becomes an algebraic equation

$$f(\dot{x}_j,x_j,p) = 0 . \tag{4.3.2}$$

From (3.3.6), the Jacobian matrix of functions (4.3.2) has the form

$$M_j = (\frac{\partial f}{\partial \dot{x}} a_0 + \frac{\partial f}{\partial x})_j , \tag{4.3.3}$$

where

$$\frac{\partial f}{\partial \dot{x}} \Big|_j = \begin{bmatrix} \frac{\partial f^i}{\partial \dot{x}^i} & \frac{\partial f^i}{\partial \dot{x}^m} \\ \frac{\partial f^m}{\partial \dot{x}^i} & \frac{\partial f^m}{\partial \dot{x}^m} \end{bmatrix}_j = \begin{bmatrix} \dot{\mathcal{D}} & \dot{\mathcal{C}} \\ \dot{\mathcal{R}} & \dot{\mathcal{E}} \end{bmatrix}_j . \tag{4.3.4}$$

Let us denote

$$\dot{\mathcal{D}}^\alpha = \frac{\partial f^{i\alpha}}{\partial \dot{x}^{i\alpha}} , \qquad \dot{\mathcal{C}}^\alpha = \frac{\partial f^{i\alpha}}{\partial \dot{x}^{m\alpha}} \mathcal{A}^\alpha ,$$

$$\dot{\mathcal{R}}^\alpha = \mathcal{A}^{\alpha_1} \frac{\partial f^{m\alpha}}{\partial \dot{x}^{i\alpha}}, \quad \text{and} \quad \dot{\mathcal{E}}^\alpha = \mathcal{A}^{\alpha_1} \frac{\partial f^{m\alpha}}{\partial \dot{x}^{m\alpha}} \mathcal{A}^\alpha .$$

$$\text{for } \alpha = 1,2, ..., k \tag{4.3.5}$$

The matrix (4.3.4) can be written as

$$\frac{\partial f}{\partial \dot{x}} \bigg|_j = \begin{bmatrix} \dot{\mathscr{D}}^1 & & & & & & \dot{\mathscr{C}}^1 \\ & \dot{\mathscr{D}}^2 & & & & & \dot{\mathscr{C}}^2 \\ & & \cdots & & & & \vdots \\ & & & \dot{\mathscr{D}}^\alpha & & & \dot{\mathscr{C}}^\alpha \\ & & & & \cdots & & \vdots \\ & & & & & \dot{\mathscr{D}}^k & \dot{\mathscr{C}}^k \\ \dot{\mathscr{R}}^1 & \dot{\mathscr{R}}^2 & \cdots & \dot{\mathscr{R}}^\alpha & \cdots & \dot{\mathscr{R}}^k & \sum_{\alpha=1}^{k} \dot{\mathscr{C}}^\alpha \end{bmatrix}_j . \qquad (4.3.6)$$

So the Jacobian matrix in time domain also has the bordered block diagonal (BBD) structure.

4.3.1. Network Analysis

A. Internal System Solutions

At a certain time step j, the internal variable x_j^i can be evaluated by solving the internal system equations using the N–R iterations

$$M_j^i \, \Delta x_j^i = - f_j^i \quad , \qquad (4.3.7)$$

where the internal part of the Jacobian matrix has two terms (refer to (4.3.3))

$$M_j^i = \dot{\mathscr{D}}_j \, a_0 + \mathscr{D}_j \quad . \qquad (4.3.8)$$

From (4.2.7) and (4.3.6), it is clear that the internal Jacobian matrix is of the block diagonal structure, so that (4.3.7) can be solved in each subnetwork

independently. For $\alpha = 1,2,...,k$.

$$M_j^{i\alpha} \Delta \dot{x}_j^{i\alpha} = - f_j^{i\alpha} , \qquad (4.3.9)$$

where

$$M_j^{i\alpha} = \dot{\mathscr{D}}_j^{\alpha} a_0 + \mathscr{D}_j^{\alpha} , \qquad (4.3.10)$$

B. Internal System Sensitivities

Differentiating (4.3.2), we obtain

$$\frac{d \; f_j^i}{d \; p} = \frac{\partial f_j^i}{\partial \dot{x}_j^i} \frac{\partial \dot{x}_j^i}{\partial p} + \frac{\partial f_j^i}{\partial x_j^i} \frac{\partial x_j^i}{\partial p} + \frac{\partial f_j^i}{\partial p} = 0 \quad . \qquad (4.3.11)$$

Using the backward differentiation formula (BDF) , it becomes

$$\frac{\partial f_j^i}{\partial \dot{x}_j^i} \sum_{\ell=0}^{k_j} a_\ell \frac{\partial x_{j-\ell}^i}{\partial p} + \frac{\partial f_j^i}{\partial x_j^i} \frac{\partial x_j^i}{\partial p} + \frac{\partial f_j^i}{\partial p} = 0 , \qquad (4.3.12)$$

Substituting (4.2.5), (4.2.12) and (4.3.5) into (4.3.12), we have

$$\dot{\mathscr{D}}_j \sum_{\ell=0}^{k_j} a_\ell s_{j-\ell}^i + \mathscr{D}_j s_j^i + f_{pj}^i = 0 , \qquad (4.3.13)$$

from which we can find the internal sensitivities s_j^i by solving

$$M_j^i s_j^i = - \mathscr{D}_j , \qquad (4.3.14)$$

where

$$M_j^i = \dot{\mathscr{D}}_j a_0 + \mathscr{D}_j , \qquad (4.3.15)$$

and

$$\dot{\mathscr{B}}_j = \dot{\mathscr{D}}_j \sum_{\ell=1}^{k_j} a_\ell \, s_{j-\ell}^i + f_{pj}^i \, . \tag{4.3.16}$$

The matrices M_j^i and $\mathscr{B}_j$ are of the block diagonal structure. Equation (4.3.14) can be solved in each subnetwork independently.

$$M_j^{i\alpha} \, s_j^{i\alpha} = - \, \mathscr{B}_j^\alpha \, , \tag{4.3.17}$$

where

$$M_j^{i\alpha} = \dot{\mathscr{D}}_j^\alpha \, a_0 + \mathscr{D}_j^\alpha \, , \tag{4.3.18}$$

and

$$\mathscr{B}_j^\alpha = \dot{\mathscr{D}}_j^\alpha \sum_{\ell=1}^{k_j} a_\ell \, s_{j-\ell}^{i\alpha} + f_{p_\alpha j}^{i\alpha} \, . \tag{4.3.19}$$

Note that M^α is in LU factored form, obtained when the solution of (4.3.9) converges. Only one forward and backward substitution is needed to solve (4.3.17).

4.3.2. Test Matrix and Test Equations

The test matrix $\mathscr{I}_j$ can be evaluated from the following equation:

$$\mathscr{I}_j = \frac{d \, f_j^m}{d \, p} = \frac{\partial \, f_j^m}{\partial \, \dot{x}_j^i} \frac{\partial \, \dot{x}_j^i}{\partial \, p} + \frac{\partial \, f_j^m}{\partial \, x_j^i} \frac{\partial \, x_j^i}{\partial \, p} + \frac{\partial \, f_j^m}{\partial \, p} \, . \tag{4.3.20}$$

Using BDF (3.3.2), it becomes

$$\mathscr{I}_j = \left[\frac{\partial f_j^m}{\partial \dot{x}_j^i} \sum_{\ell=1}^{k_j} a_\ell \frac{\partial x_{j-\ell}^i}{\partial p} + \frac{\partial f_j^m}{\partial x_j^i} \frac{\partial x_j^i}{\partial p} + \frac{\partial f_j^m}{\partial p} \right]. \qquad (4.3.21)$$

Similar to (4.3.13), we have

$$\mathscr{I}_j = \dot{\mathscr{R}}_j \sum_{\ell=0}^{k_j} a_\ell s_{j-\ell}^i + \mathscr{R}_j s_j^i + f_{pj}^m, \qquad (4.3.22)$$

and the <u>test matrix</u> of each subnetwork can be evaluated in parallel

$$\mathscr{I}_j^\alpha = \dot{\mathscr{R}}_j^\alpha \sum_{\ell=0}^{k_j} a_\ell s_{j-\ell}^{i\,\alpha} + \mathscr{R}_j^\alpha s_j^{i\,\alpha} + f_{p\,\alpha j}^{m\,\alpha}. \qquad (4.3.23)$$

The <u>test equations</u> at the time instance j will be

$$\mathscr{I}_j \Delta p = - f_{pj}^m. \qquad (4.3.24)$$

4.3.3 Procedure to Generate and Solve Test Equations (Time Domain)

Test equations in time domain can be formulated and solved using the following procedure:

1. Decompose the tested network N into k subnetworks.

2. Perform the test measurements at the partition nodes to obtain x^m within the time interval $(0-\tau)$.

3. Assume the initial parameter values p^0.

4. Assume the initial values of internal variables x_0^i.

5. For each subnetwork do the following steps in parallel $(\alpha=1,2,...,k)$

    a. Predict $x_j^{i\,\alpha}$ using the forward differentiation formula.

    b. Calculate $\dot{x}_j^{i\,\alpha}$ using the backward differentiation formula.

c.   Evaluate the internal variables $\overset{i}{\mathbf{x}}{}^{\alpha}$ by solving the internal system equations. Use the Newton–Raphson iterative process

$$\overset{i}{\mathbf{M}}{}^{\alpha}_{j} \, \Delta \overset{i}{\mathbf{x}}{}^{\alpha}_{j} = - \overset{i}{\mathbf{f}}{}^{\alpha}_{j} \, . \tag{4.3.25}$$

d.   Keep $\mathbf{M}^{\alpha}_{j}$ in LU factored form when $\overset{i}{\mathbf{x}}{}^{\alpha}_{j}$ converges.

e.   Compute the sensitivity $\overset{i}{\mathbf{s}}{}^{\alpha}_{j}$ of the internal variables $\overset{i}{\mathbf{x}}{}^{\alpha}_{j}$ w.r.t. the parameters $\mathbf{p}_{\alpha}$ of the subnetwork by solving the linear equation

$$\overset{i}{\mathbf{M}}{}^{\alpha}_{j} \overset{i}{\mathbf{s}}{}^{\alpha}_{j} = - \overset{i}{\mathscr{B}}{}^{\alpha}_{j} \, . \tag{4.3.26}$$

f.   Evaluate the test matrix $\mathbf{T}^{\alpha}_{j}$

$$\mathscr{T}^{\alpha}_{j} = \dot{\mathscr{R}}^{\alpha}_{j} \overset{k_{j}}{\underset{\ell=0}{\Sigma}} a_{\ell} \overset{i}{\mathbf{s}}{}^{\alpha}_{j-\ell} + \mathscr{R}^{\alpha}_{j} \overset{i}{\mathbf{s}}{}^{\alpha}_{j} + \overset{m}{\mathbf{f}}{}^{\alpha}_{p_{\alpha}j} \, . \tag{4.3.27}$$

6.   Formulate the test matrix $\mathscr{T}_{j}$ by combining test matrices $\mathscr{T}^{\alpha}_{j}$ of all subnetworks.

7.   Repeat Steps 5–6 for each time instance within $(0,\tau)$. The test matrix has the form

$$\mathscr{T} = [\mathscr{T}'_{1} \ \mathscr{T}'_{2}, \ ..., \ \mathscr{T}'_{\tau}]' , \tag{4.3.28}$$

where $'$ stands for the matrix transpose operation.

8.   Estimate the parameter deviations $\Delta \mathbf{p}$ by solving the test equations of the interconnected system

$$\mathscr{T} \Delta \mathbf{p} = - \mathbf{f}^{m} \, . \tag{4.3.29}$$

The test matrix $\mathscr{T}$ is of the bordered block diagonal structure. The sparse matrix technique, parallel algorithm and vector computation can be used to reduce the computational time and the memory requirements.

9.   Update the parameter values and repeat steps 4–8 if $\Delta \mathbf{p}$ is large.

This procedure is summarized in Fig. 4.3.1.
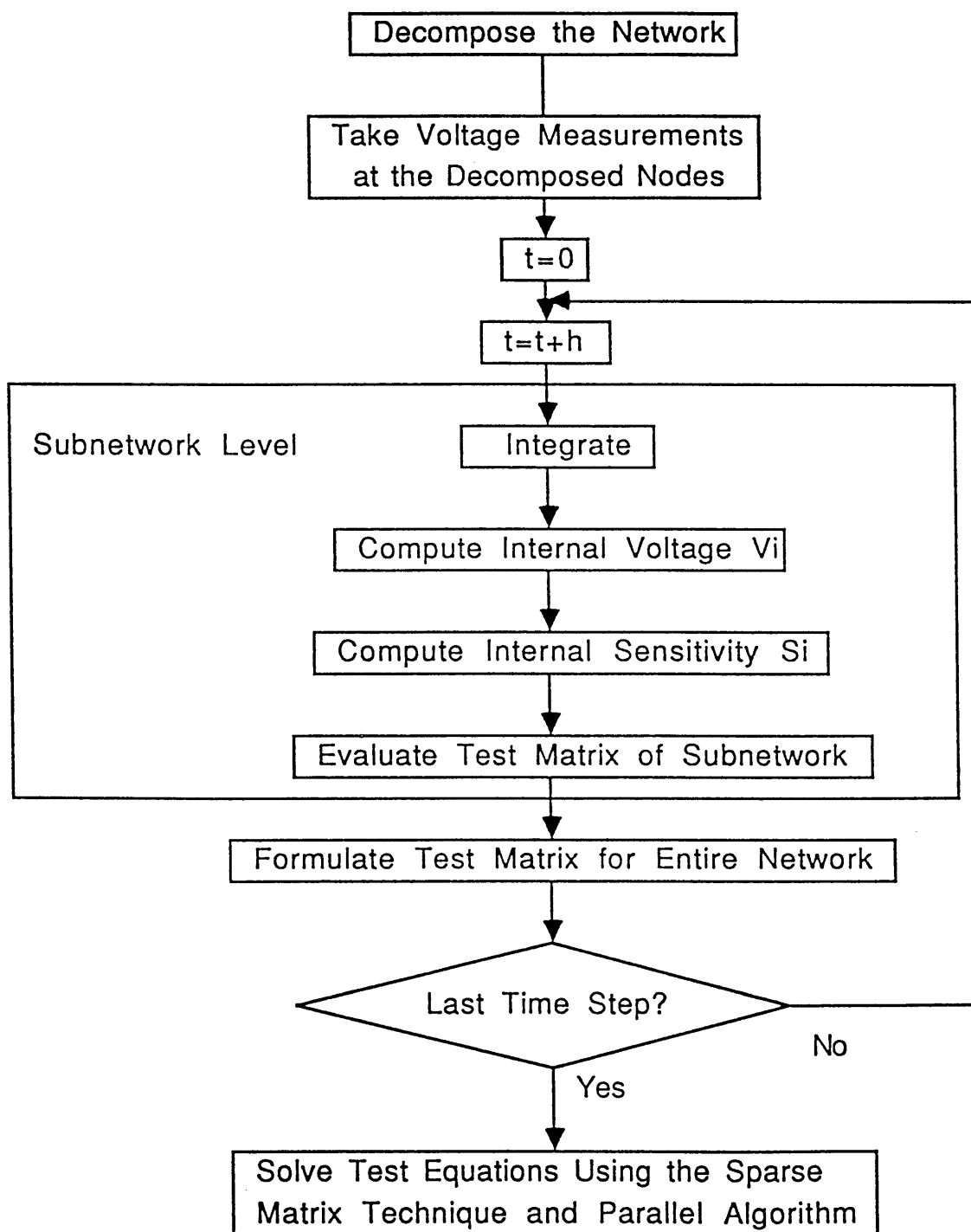
Fig. 4.3.1 Flowchart of generation and solution of test equation in time domain.

Remarks

1. The Jacobian matrix M^i_j for the nonlinear iterations (4.3.7) is block diagonal, so the circuit analysis is much easier than the corresponding analysis in the sensitivity approach [see (3.3.7)].

2. Each subnetwork can be analyzed independently, therefore, parallel processing can be implemented, which further reduces the analysis time.

3. In the case of a linear subnetwork, a solution vector can be obtained in one step; no iterations are necessary. Note that if a linear subnetwork is a part of a nonlinear network, such a simplification of analysis cannot be achieved by other approaches. Even in the popular harmonic balance approach [Kundert and Sangiovanni–Vincentelli, 1986], in which linear subnetworks are separated from the nonlinear part, several iterations are necessary to balance the mismatch between the solutions of nonlinear and linear parts.

4. Jacobian matrix M^i_j is the block diagonal with LU factorization which was known from the solution of (4.3.9). Therefore the sensitivities $s^{i \alpha}_j$ can be easily obtained from (4.3.17).

5. It is obvious from the block diagonal form of M^i_j that the internal variables x^i_j of a subnetwork depend only on these parameters from the vector p which belong to the same subnetwork. Also, one can observe that derivatives of f^m_j w.r.t. x^i_j or $\dot{x}^i_j$ are nonzero only for these variables or their derivatives in the subnetworks which are incident to the selected measurement nodes. As a result, the test matrix $\mathscr{T}_j$ (4.3.22) has a block matrix structure. Due to this structure it is possible to identify individual parameters locally using only measurements from a given subnetwork or two adjacent subnetworks.

4.4 Frequency Domain Test Equations

In this section, the general method described in Section 4.2 is applied to frequency domain testing. In order to acquire a better understanding of the method, nodal analysis is used to obtain the system equations. First, we consider the case in which small sinusoidal signals are applied to the tested circuit. The circuit can be linearized at the operating point. Therefore both simulation and test can be implemented in the frequency domain. In Sections 4.4.1–4.4.3, we show that the internal system solutions and their sensitivities can be evaluated within each subnetwork in parallel, and that the test matrix is of the BBD form for the hierarchically decomposed network. Second, we consider the case in which arbitrary periodical signals are applied to the tested circuit. When the circuit is nonlinear, the real test is implemented in the frequency domain. However, the simulation can be implemented either in the frequency domain or in time domain depending on the method used. The methods that deal with nonlinear circuits are presented in Section 4.4.4.

4.1 Network Analysis

Consider a linearized network N. Let n+1 be the number of nodes of N. The system functions based on the nodal equations are

$$F = Y_n V^n - I^n ,\qquad\qquad (4.4.1)$$

where Y_n is the nodal admittance matrix, V^n is the nodal voltage vector and I^n is the nodal current vector. Assume that m is the number of measurement

nodes (or external nodes) and i is the number of internal nodes. Label the external nodes first and then the internal nodes, in which case the network function (4.4.1) can be written as

$$\begin{bmatrix} F^m \\ F^i \end{bmatrix} = \begin{bmatrix} Y_{mm} & Y_{mi} \\ Y_{im} & Y_{ii} \end{bmatrix} \begin{bmatrix} V^m \\ V^i \end{bmatrix} - \begin{bmatrix} I^m \\ 0 \end{bmatrix} . \tag{4.4.2}$$

Then the network is divided hierarchically into k subnetworks. The corresponding nodal admittance matrix has a bordered block diagonal (BBD) form as shown in Fig. 4.4.1. In fact, Fig. 4.4.1 shows the worst case situation since in practice both internal blocks (shaded areas) as well as interconnection parts are sparse.

For each subnetwork, the nodal equations are

$$F_\alpha = Y_{n_\alpha} V^{n_\alpha} - I^{n_\alpha} . \tag{4.4.3}$$

or

$$\begin{bmatrix} F^{m_\alpha} \\ F^{i_\alpha} \end{bmatrix} = \begin{bmatrix} Y_{m_\alpha m_\alpha} & Y_{m_\alpha i_\alpha} \\ Y_{i_\alpha m_\alpha} & Y_{i_\alpha i_\alpha} \end{bmatrix} \begin{bmatrix} V^{m_\alpha} \\ V^{i_\alpha} \end{bmatrix} - \begin{bmatrix} I^{m_\alpha} \\ 0 \end{bmatrix} \tag{4.4.4}$$

where m_α and i_α are the number of the external and internal nodes of the subnetwork S_α respectively. The admittance matrix has the structure as shown in Fig. 4.4.2.
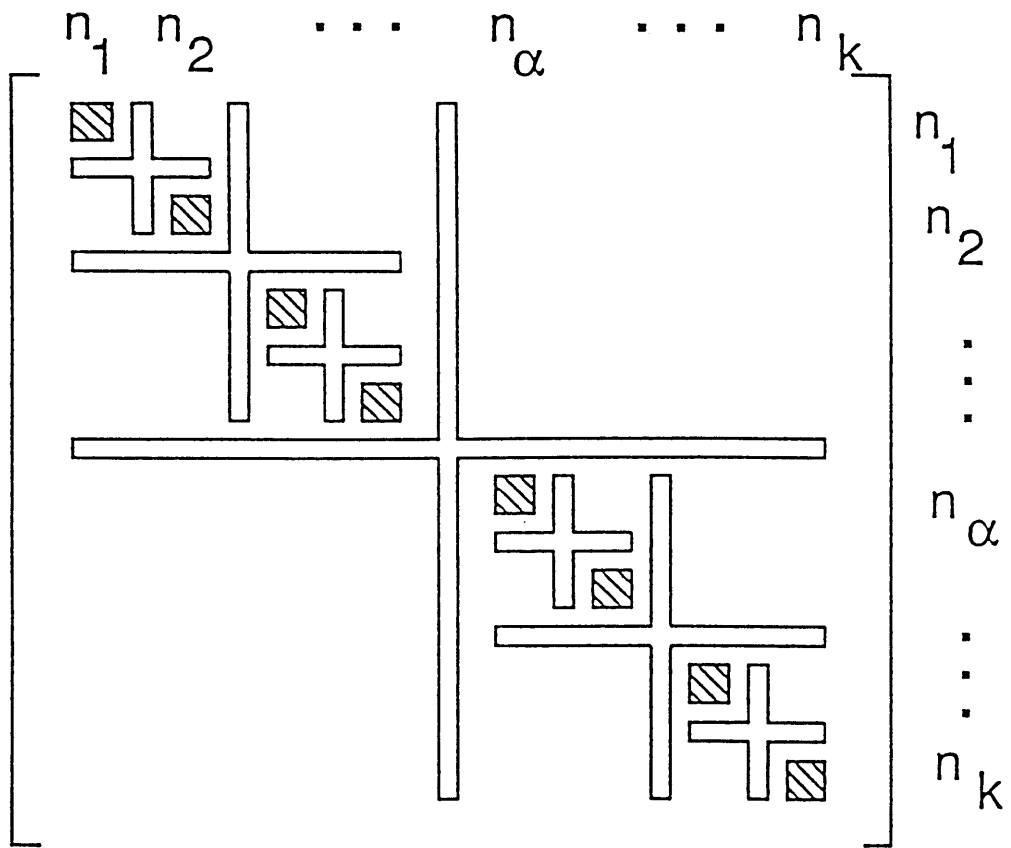
Fig. 4.4.1 The nonzero pattern of matrix Y of the decomposed N.
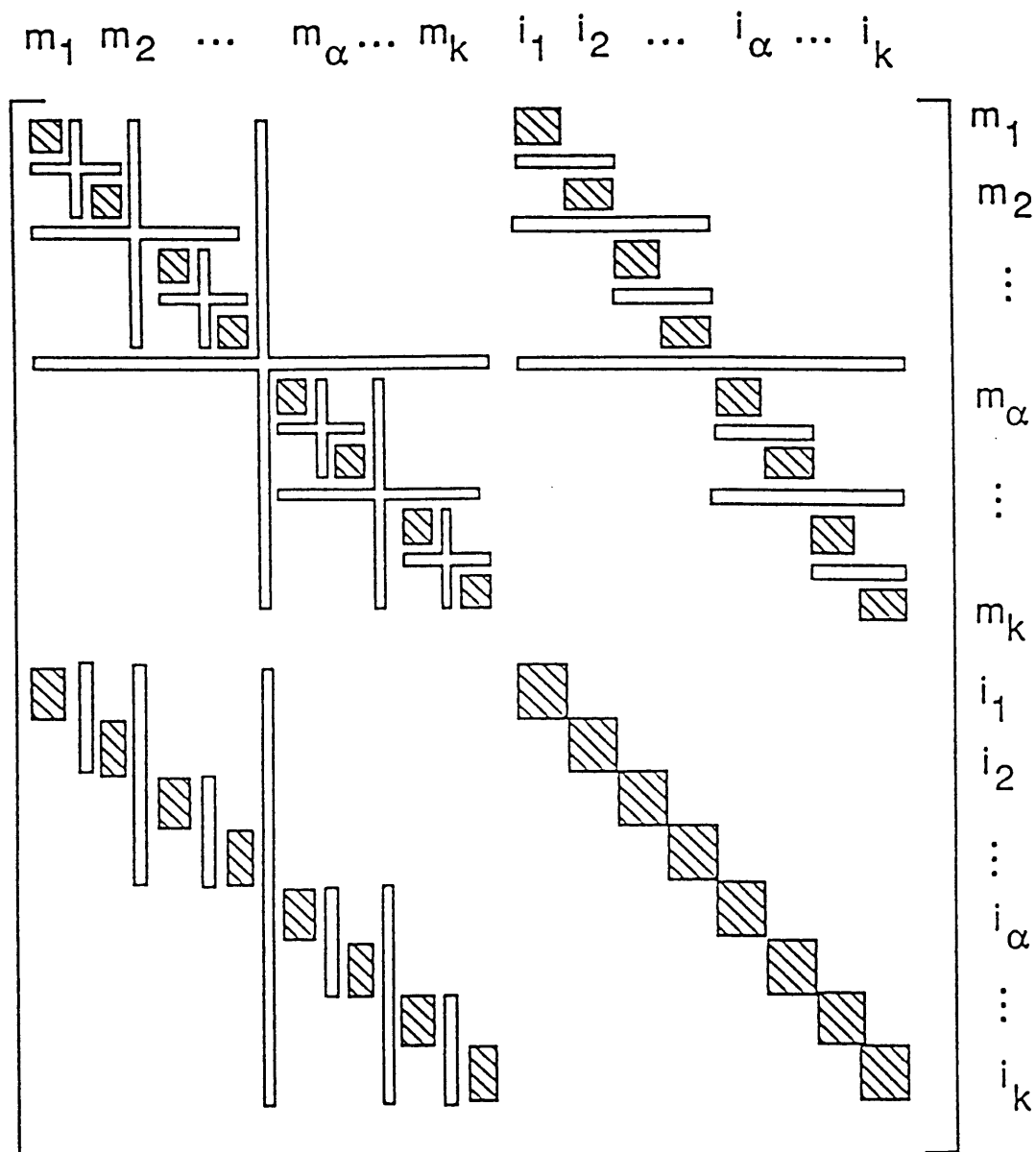
Fig. 4.4.2 The nonzero pattern of reordered matrix Y in Fig. 4.4.1.

A. Internal System Solutions

The internal system functions are used to solve the internal voltages V^i. From (4.4.2), we have

$$F^i = Y_{im} V^m + Y_{ii} V^i .$$

(4.4.5)

When KCL equations are satisfied at the internal nodes

$$F^i = 0 ,$$

(4.4.6)

we get the internal voltages by solving

$$V^i = - Y_{ii}^{-1} Y_{im} V^m .$$

(4.4.7)

In fact, the internal voltages of each subnetwork can be solved independently using

$$V^{i_\alpha} = - Y_{i_\alpha i_\alpha}^{-1} Y_{i_\alpha m_\alpha} V^{m_\alpha} .$$

(4.4.8)

B. Internal System Sensitivities

Differentiating the both sides of (4.4.5) w.r.t. parameters p, we obtain

$$\frac{\partial F^i}{\partial p} = \frac{\partial Y_{im}}{\partial p} V^m + Y_{im} \frac{\partial V^m}{\partial p} + \frac{\partial Y_{ii}}{\partial p} V^i + Y_{ii} \frac{\partial V^i_i}{\partial p} = 0 .$$

(4.4.9)

Since the V^m is the vector of measured voltages, we have

$$\frac{\partial V^m}{\partial p} = 0 .$$

(4.4.10)

The sensitivity of the internal voltage w.r.t. the parameter is

$$S^i = \frac{\partial V^i}{\partial p} = -Y_{ii}^{-1} [\frac{\partial Y_{im}}{\partial p} V^m + \frac{\partial Y_{ii}}{\partial p} V^i] .$$

(4.4.11)

or

$$S^i = \frac{\partial V^i}{\partial p} = -Y_{ii}^{-1} \left[\frac{\partial Y_{in}}{\partial p} V^n\right] .$$ (4.4.12)

It can be acquired by computing the internal sensitivities of each subnetwork in parallel,

$$S^{i_\alpha} = \frac{\partial V^{i_\alpha}}{\partial p} = -Y_{i_\alpha i_\alpha}^{-1} \left[\frac{\partial Y_{i_\alpha n_\alpha}}{\partial p} V^{n_\alpha}\right] .$$ (4.4.13)

Note that $Y_{i_\alpha i_\alpha}^{-1}$ has been computed when the internal voltages V^{i_α} are obtained from (4.4.8).

4.4.2 Test Matrix and Test Equations

Define the external functions as test functions. From (4.4.2), we have

$$F^m = Y_{mm} V^m + Y_{mi} V^i - I^m .$$ (4.4.14)

The test matrix is

$$T = \frac{\partial F^m}{\partial p} = \frac{\partial Y_{mm}}{\partial p} V^m + Y_{mm} \frac{\partial V^m}{\partial p} + \frac{\partial Y_{mi}}{\partial p} V^i + Y_{mi}\frac{\partial V^i}{\partial p} - \frac{\partial I^m}{\partial p}.$$ (4.4.15)

Since

$$\frac{\partial V^m}{\partial p} = 0 \quad \text{and} \quad \frac{\partial I^m}{\partial p} = 0$$ (4.4.16)

The second term and the last term vanish. Substituting (4.4.12) into (4.4.15), we get

$$T = \frac{\partial \, Y_{mm}}{\partial \, p} \, V^m + \frac{\partial \, Y_{mi}}{\partial \, p} \, V^i - Y_{mi} \, Y_{ii}^{-1} \, [\frac{\partial \, Y_{in}}{\partial \, p} \, V^n]$$

$$= \, [\frac{\partial \, Y_{mn}}{\partial \, p} \, V^n \,] - Y_{mi} \, Y_{ii}^{-1} \, [\frac{\partial \, Y_{in}}{\partial \, p} \, V^n]$$

$$= \, [\, U_{mm} - Y_{mi} \, Y_{ii}^{-1} \,] \frac{\partial \, Y_n}{\partial \, p} \, V^n \, . \qquad (4.4.17)$$

where U_{mm} stands for the mxm identity matrix.

Let

$$\underset{\sim}{H} = [\, \underset{\sim}{U}_{mm} \, | \, - \underset{\sim}{Y}_{mi} \, \underset{\sim}{Y}_{ii}^{-1} \,] \, , \qquad (4.4.18)$$

so that the test matrix T can be expressed as

$$T = \frac{\partial \, F^m}{\partial \, p} = \, H \frac{\partial \, Y_n}{\partial \, p} \, V^n \, . \qquad (4.4.19)$$

Note that the test matrix (4.4.19) is the product of three matrices and is similar to the sensitivity matrix (3.4.10) except that the H matrix of (4.4.19) replaces the V^a matrix in (3.4.10). The derivative $\dfrac{\partial Y_n}{\partial p}$ can be easily evaluated by direct differentiation of all entries in Y_n which contain the variable p (in most formulation methods not more than four).

To show the structure of the test matrix (4.4.19), we investigate the structure of the matrix $\underset{\sim}{H}$.

$$H = [\, U_{mm} \, | \, W \,] \, . \qquad (4.4.20)$$

where

$$W = - \, Y_{mi} \, Y_{ii}^{-1} \qquad (4.4.21)$$

Y_{mi} and Y_{ii} are sparse matrices that have the block structure as shown in Fig. 4.4.2. Since $(Y_{ii})^{-1}$ is a block diagonal matrix, it is easy to show that the matrix W — the product of ($Y_{mi}\ Y_{ii}^{-1}$) — has a block structure identical to that of Y_{mi}. Therefore, H has the block structure as shown in Fig. 4.4.3., where

$$W_\alpha = -\ Y_{m_\alpha i_\alpha}\ Y_{i_\alpha i_\alpha}^{-1}\ . \qquad (4.4.22)$$

We can define

$$H_\alpha = [\ U_{m_\alpha m_\alpha}\ |\ W_\alpha\ ]\ , \qquad (4.4.23)$$

where $\alpha=1,2,...k$. Equations (4.4.22) and (4.4.23) can be computed in parallel within each subnetwork and H can be obtained by adding different H_α. With this approach the computations can be kept to a minimum.

The test matrix can be evaluated in each subnetwork independently

$$T_\alpha = H_\alpha\ \frac{\partial Y_{n_\alpha}}{\partial\ p}\ V^{n_\alpha}\ . \qquad (4.4.24)$$

An alternative way to see that a test matrix is a sparse matrix is as follows. Suppose that p is the element incident to the nodes i and j in the subnetwork S_α. Let f_{qr} be the sum of currents at node q (q=1,2,...,m) when an excitation is applied at node r. Since H has the block nonzero pattern and $\frac{\partial Y}{\partial p}$ has four or less nonzero elements, we can see that the derivative of f_{qr} w.r.t. p (qr–th element of T) is not equal to zero only if the node q is a node of the subnetwork S_α. Individual sensitivities can be obtained from (4.4.19).
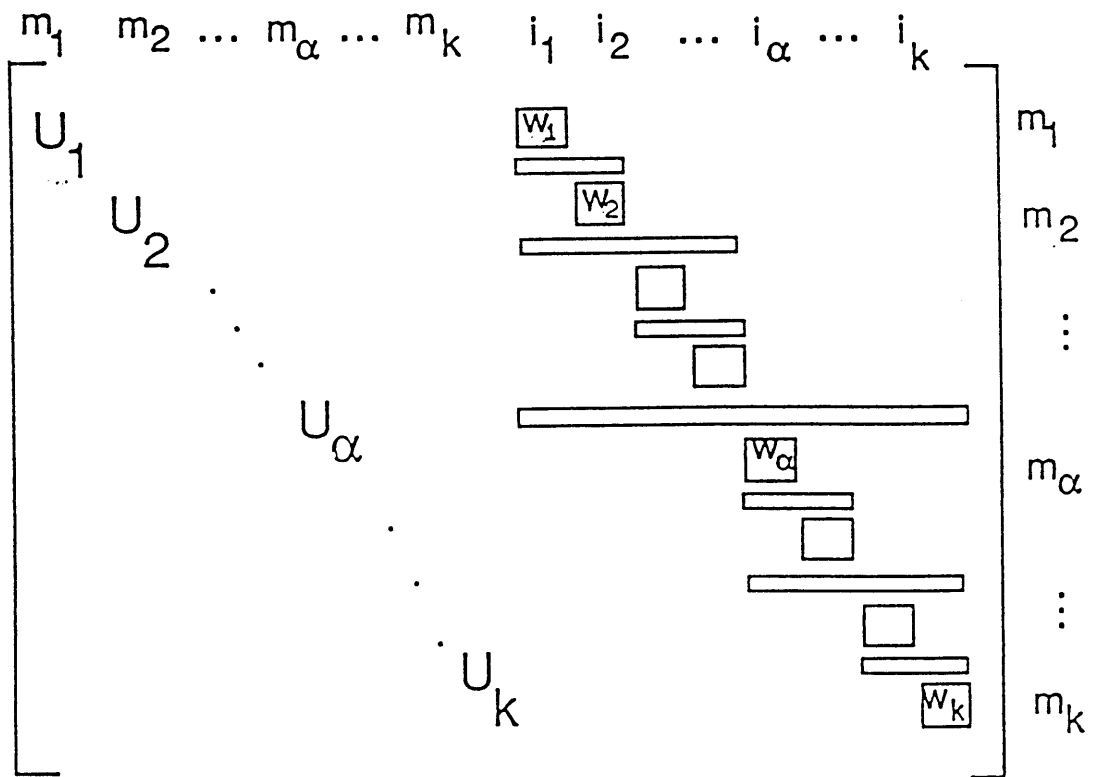
Fig. 4.4.3 The nonzero pattern of matrix H.

The result closely resembles formulas for sensitivities derived in [J. Vlach, 1983], that is

$$\frac{\partial f_{qr}}{\partial p} = \begin{cases} (h_{qi} - h_{qj})(v_{ir} - v_{jr}) & \text{when node } q \; \epsilon \; S_\alpha \\ 0 & \text{otherwise} \end{cases} \qquad (4.4.25)$$

In general, when an element p appears in the coefficient matrix Y_n at the intersection of rows i,j and columns k,l,

$$\frac{\partial f_{qr}}{\partial p} = \begin{cases} (h_{qi} - h_{qj})(v_{kr} - v_{lr}) & \text{when node } q \; \epsilon \; S_\alpha \\ 0 & \text{otherwise} \end{cases} \qquad (4.4.26)$$

The test matrix T is a block matrix of the size $m \times n_p$ where m is the product of the number of external nodes used for measurements multiplied by the number of excitations, and n_p is the number of elements in the network. When the external nodes and all the elements are labeled based on the order of subnetworks in which they are included, the test matrix has the block structure as shown in Fig. 4.4.4. If the sparsity of the test matrix is properly used, then the computation speed at pre—test as well as post—test stages can be increased.
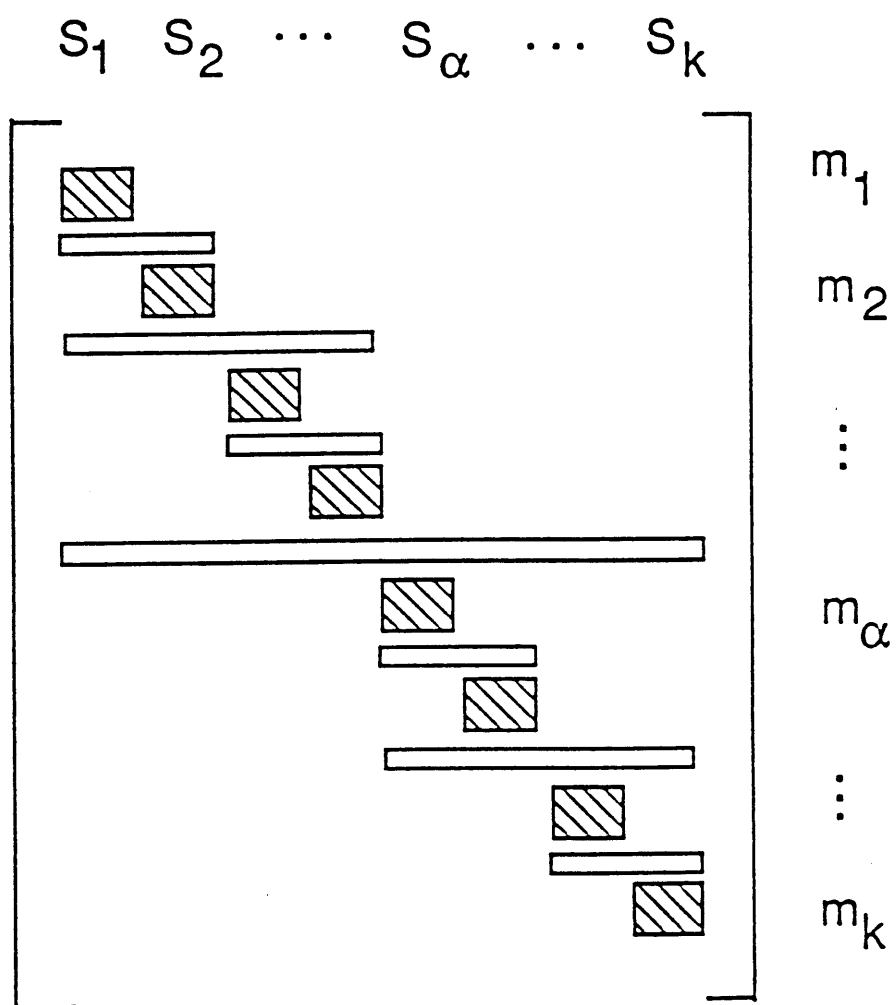
Fig. 4.4.4 The nonzero pattern of matrix T.

4.4.3. Procedure to Generate and Solve Test Equations (Frequency Domain)

1. Decompose the tested circuit N into k subnetworks.

2. Perform the test measurements at the partition nodes to obtain V^m in the interested frequency range.

3. Assume initial parameter values p^0 and V_0^i.

4. Do the following steps for each subnetwork in parallel $(\alpha=1,2,...,k)$

    a. Evaluate the internal voltages V^{i_α} by solving the internal system equations.

$$V^{i_\alpha} = -Y_{i_\alpha i_\alpha}^{-1} \, Y_{i_\alpha m_\alpha} \, V^{m_\alpha} \, . \tag{4.4.27}$$

    b. Compute sensitivities S^{i_α} of the internal voltages V^{i_α} w.r.t. the parameters p of the subnetwork S_α using

$$S^{i_\alpha} = \frac{\partial V^{i_\alpha}}{\partial p} = -Y_{i_\alpha i_\alpha}^{-1} \left[\frac{\partial Y_{i_\alpha n_\alpha}}{\partial p} V^{n_\alpha} \right] \, . \tag{4.4.28}$$

    f. Evaluate the test matrix T_j^α of the subnetwork

$$T^\alpha = H_\alpha \frac{\partial Y_{n_\alpha}}{\partial p} V \, . \tag{4.4.29}$$

5. Formulate the test matrix T by combining test matrices T^α of all subnetworks.

6. Repeat Steps 4–5 for each test frequencies $(\omega_1, \; \omega_2, \; ...\omega_{n_f})$. The test matrix has the form

$$T = [\; T_1' \; T_2', \; ..., \; T_{n_f}']' \tag{4.4.30}$$

where ' stands for the matrix transpose operation.

7. Estimate parameter deviations Δp by solving the test equation of the

interconnected system

$$T \; \Delta p = - \; F^m \; .$$ (4.4.31)

The test matrix T has the bordered block diagonal structure. The sparse matrix technique, a parallel algorithm and vector computation can be used to reduce the computational time and the memory requirements.

8.   Update the parameter values and repeat steps 4–7 if Δp is large.

4.5. Approximate Method and Exact Method

In the previous sections, we assumed that the test matrix was formulated after the measurements had been taken. In order to perform the test point selection and to measure testability before the test, the test matrix should be formulated in the pre–test stage. It is required, then, to simulate the solution vector of the entire network which includes both external and internal nodes, based on the nominal model, i.e.,

$$x = x(p^0)$$ (4.5.1)

This method is called the <u>approximate</u> method. The solution will be obtained by the Newton–Raphson iterative process

$$M \; \Delta x = - \; f \; .$$ (4.5.2)

From the discussion in Section 4.1., when the network is decomposed hierarchically to a number of small subnetworks, the corresponding Jacobian matrix M is of the bordered block diagonal (BBD) structure. The equation (4.5.2) can be solved by parallel processing and a vector computation algorithm.

The test matrix will be evaluated based on the solution vector obtained form (4.5.2). The procedure will be the same as discussed before. The test

matrix of each of the subnetworks T_α can be computed in parallel, and the test matrix of the entire network T is formed by combining all T_α. The test point selection is performed by QRF based on the obtained test matrix T. In the next chapter, we will present the method needed to perform QRF in parallel.

After the test is performed at the test points selected by QRF, the test equations are formulated, and the deviations of parameters Δp can be estimated. Since external variables (i.e. the measured voltages at the partition nodes) are known, the internal node voltages can be computed using the function of measured external voltages as (4.2.4), (4.3.7) and (4.4.6). Taking a linearized circuit in the frequency domain as an example, the voltage matrix can be evaluated more accurately than in the case when all voltages are obtained by simulation.

$$\overline{V}^n = \begin{bmatrix} V^{m*} \\ -Y_{ii}^{-1} \, Y_i \, V^{m*} \end{bmatrix} = \begin{bmatrix} V^{M*} \\ \overline{V}^{\,i} \end{bmatrix} . \qquad (4.5.3)$$

This way of evaluating the voltage matrix is called the <u>exact</u> method. The advantage of (4.5.3) is that it provides a more accurate solution to the element evaluation problem.

In summary:

before the test	$V^n = V^n(p^0)$	approximate method
after the test	$V^n = \overline{V}^n$.	exact method

Before the test, the approximate method can be used to evaluate the test matrix. The QR factorization is implemented on the test matrix in order to select test points and measure circuit testability. After the test, the exact

method can be used to evaluate the test matrix in order to obtain the solution of test equations. The difference between these two methods is only in the values of the voltage vectors. Hence, the test matrices formulated by both methods have the same structure.

The test procedure for the decomposition approach is given in Fig. 4.5.1.

In this chapter we have developed a decomposition approach to element identification and demonstrated its advantages. It reduces the computation time and enhances the test performance. Large circuits can be tested. It increases the accuracy of the solutions. Inaccuracies in the circuit model, numerical methods and measurement techniques affect only the local computations of subnetworks so they do not affect the test results of remote subnetworks. In addition it can be directly applied to test mixed mode circuits. A network can be decomposed into analog and digital subnetworks. At the boundaries of the analog and digital subnetworks, analog signals can be converted to the digital signal form, and digital testing procedures can be implemented [Cha 1979, Miczo 1986, Cox and Rajski, 1988]. In the next Chapter, test strategies for large analog circuits are developed.
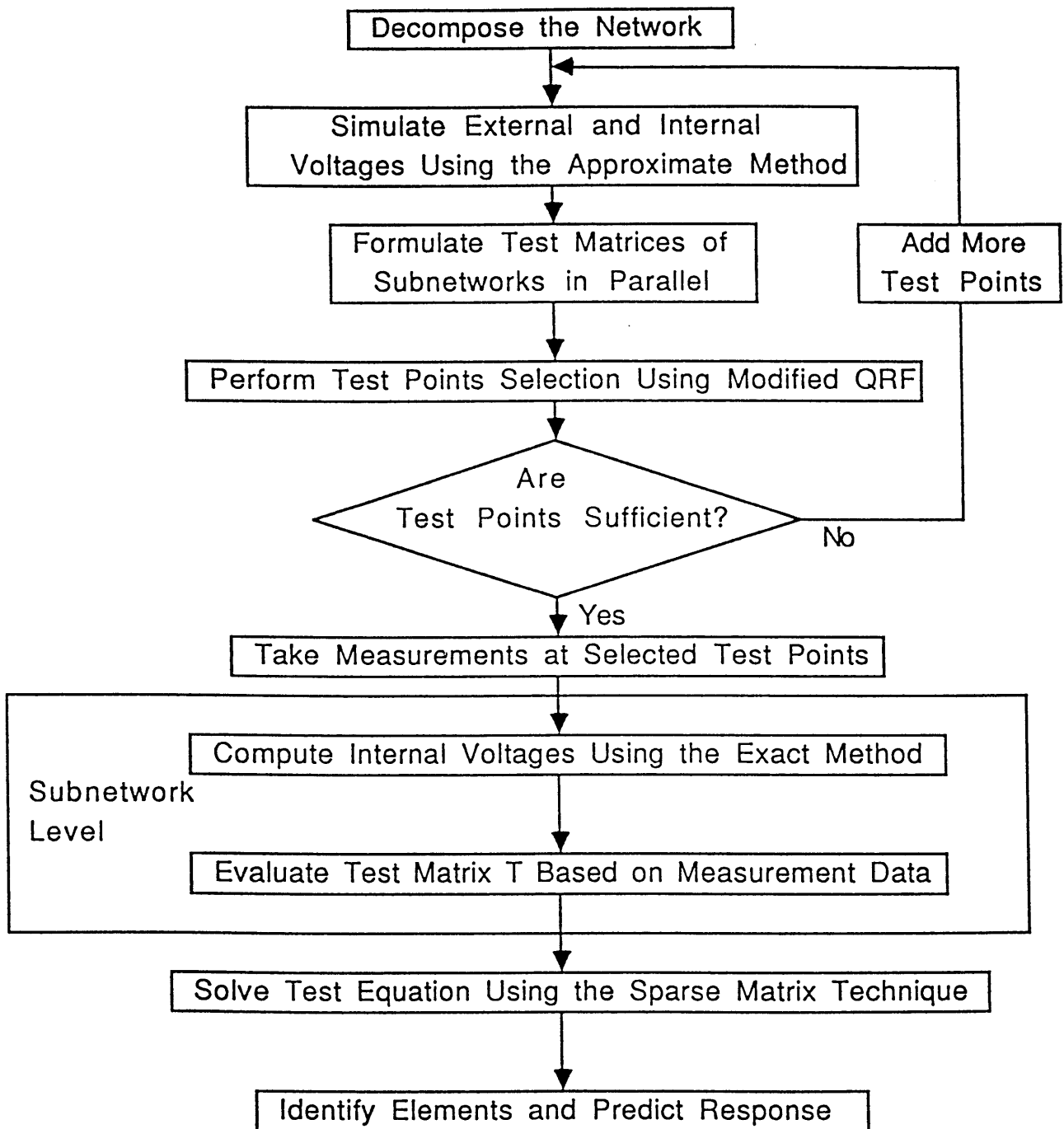
Fig. 4.5.1 Test procedure for the decomposition approach.

5. TESTING STRATEGIES

In this chapter testing strategies for fault diagnosis and calibration of analog circuits are presented. Testing strategies enable test engineers to perform reliable and cost—effective tests. They can be used to design testable circuits by affecting circuit architecture and providing access to the selected test points. Design, which incorporates a testing strategy, is known as "design for testability".

Testing strategies include the following aspects:

— determination of the test method depending on the type of faulty elements and the type or size of the tested system;

— determination of the test environment (such as DC testing, frequency domain testing, or time domain testing) depending on the type of the tested circuit. For each test environment, there are several ways to increase the number of independent measurements.

— test point selection and testability measurement to ensure a reliable and inexpensive test.

— prediction of the circuit's response in order to obtain the accurate response in very efficient way.

— consideration of the effect of the measurement errors on the element estimation and response prediction.

— elimination of the ambiguity groups in order to estimate parameter values.

— estimation of the time skew effect on element evaluation.

In Sections 5.1—5.7, all aspects of testing strategies will be presented in a

general way. The QR factorization process, which is a key point for test point selection, testability measurement, element estimation and response prediction, is time consuming for a large circuit. In Section 5.8, the modified QRF process, which can be performed in parallel within each subnetwork, is developed and used for the decomposition approach. Hence the computational speed is increased and the memory requirement is decreased in this method. This strengthens our claim that the decomposition approach is suitable for large systems.

5.1 Test Methods

Fault diagnosis and calibration of analog circuits are related. When the changes in the network's element values are small, the first order approximation method can be applied. A relationship between measurement and parameter deviations can be expressed through the sensitivity matrix. With a sufficient number of test points, all elements can be evaluated. This allows one to diagnose a faulty circuit or calibrate a working one by tuning its elements to the desired settings. For a large scale system, a decomposition approach has to be used to increase reliability and to reduce test costs.

5.2 Test Environments

Usually the number of accessible nodes in a circuit is limited. Different techniques can be used to increase the number of measurements depending on the type of circuit. By changing operating points (DC excitation level), test frequencies, sampling time points and input signal waveforms, a sufficient

number of candidate test points can be obtained. However, not all candidate test points are independent. In this section, the upper bounds of the independent measurements from all the test candidates are estimated. In the following sections, efficient methods in selecting independent measurements from all test candidates will be given.

5.2.1 Multi—Excitation Testing

For a linear resistive circuit, multi—excitation testing can be used. Voltage measurements are taken with excitations applied to the accessible nodes. The number of transfer functions depends on the number of excitations and measurements. If the n_m is the number of measurement nodes and n_e is the number of excitation nodes, then the number of rows of the test matrix is $n_m \cdot n_e$. However, the upper bound of the number of independent functions for a reciprocal circuit was given by Navid and Willson (1979) as

$$R_{max} \leq \frac{1}{2} \bar{n}_m (\bar{n}_m + 1), \quad \text{where } \bar{n}_m = \max (n_m, n_e) . \tag{5.2.1}$$

5.2.2 Multi—Frequency Testing

When a circuit contains reactive elements, multi—frequency voltage measurements can be used [Sen and Seaks 1979, and Rapisarda and DeCarlo 1983]. A test circuit is excited with sinewave excitations. Deviations of the steady—state voltage responses from their nominal values are measured. If n_f is the number of test frequencies, the number of rows of the test matrix can be up to $n_m \cdot n_e \cdot n_f$. The number of harmonics generated from the nonlinear circuit

is greater than the number of test frequencies. If n_h is the number of harmonics generated, then the number of rows of the test matrix is $n_m \cdot n_e \cdot n_h$. The upper bound on the number of independent transfer functions was estimated by Berkowitz (1962),

$$R_{max} = n_m \cdot n_e \ (n_{react} + 1) + n_{react} \qquad (5.2.2)$$

where n_{react} is the number of the reactive elements. Or more exactly,

$$R_{max} = n_m \cdot n_e \ (N_{order} + 1) + N_{order} \qquad (5.2.3)$$

where N_{order} is the order of complexity of the network, which is defined as the order of the polynomial of complex variable s describing the determinant of the transfer function. The order of complexity is determined by the number of reactive elements and their location in the network. Therefore, it is related to the network topology [Starzyk and Dai 1987].

5.2.3. Multi–Operating–Point Testing

When a circuit contains nonlinear elements, multi–operating–point testing can be used. Voltage measurements are taken when the circuit is operated at different DC levels. Different DC excitation levels bring the nonlinear elements to different operating points. The effect of nonlinearities on the rank of the test matrix is similar to the effect of the multifrequency measurements in the linear reactive network. If n_l is the number of DC excitation levels, then the number of rows of the test matrix is $n_m \cdot n_e \cdot n_l$. If nonlinear elements are represented by their piecewise linear segments, the linear combinations of the

piecewise linear segments can be mapped to different linear regions. If n_r is the number of linear regions, then the number of rows of the test matrix is $n_m \cdot n_e \cdot n_r$. Since the voltage measurements are taken at different linear regions of the piecewise characteristics, the equivalent branch admittances G_i will change their values acting as variable parameters. An effect of these changes can be compared to changes caused by variable frequency, therefore this method is called the pseudo–frequency approach [Swamy and Roytman 1984].

Let ΔG_{lin} be the vector of deviations of linear elements from their nominal values and ΔG_ℓ, ΔI_ℓ the vectors of deviations in nonlinear segments description (changes in i_α and G_α in each segment for each nonlinear element). Changing the region causes the number of unknowns to increase since new values for ΔG_ℓ and ΔI_ℓ have to be added. If n_s is the number of piecewise linear segments, the total number of parameters will be $n_{lin} + 2 \cdot n_s$. However, since the circuit is linearized, the multi–frequency testing can be used when the circuit contains reactive elements. Then we gain additional system information. In such case we will be able to evaluate all the unknowns.

The number of rows of the test matrix is $n_m \cdot n_e \cdot n_f \cdot n_r$. Let $m = n_m \cdot n_e \cdot n_f$. The test matrix has the following pattern

$$(5.2.4)$$

5.2.4. Multi—Time—Point Testing

In time domain testing, the waveform recorder is used to sample, digitize and store the time response. If n_t is the number of time points at which the response is sampled and recorded, the number of rows of the test matrix is up to $n_m \cdot n_e \cdot n_t$. Different test signals, e.g. step function, ramp function, pulse function or any arbitrary function, can be applied since different input functions affect the output differently. If n_w is the number of input signals applied to the circuit, the number of rows of the test matrix is $n_m \cdot n_e \cdot n_t \cdot n_w$.

The maximum number of candidate test points for different cases is summarized in Table 5.2.1.

Table 5.2.1 The maximum number of candidate test points

test environment	test circuit	number of test points
DC	linear	$n_m \cdot n_e$
	nonlinear	$n_m \cdot n_e \cdot n_l$
	piecewise linear	$n_m \cdot n_e \cdot n_r$
Frequency domain	linear	$n_m \cdot n_e \cdot n_f$
	nonlinear	$n_m \cdot n_e \cdot n_f \cdot n_l$
	piecewise linear	$n_m \cdot n_e \cdot n_f \cdot n_r$
Time domain	linear	$n_m \cdot n_e \cdot n_t$
	nonlinear	$n_m \cdot n_e \cdot n_t \cdot n_l$
	piecewise linear	$n_m \cdot n_e \cdot n_t \cdot n_r$

5.3. Test Point Selection and Testability Measure

A key factor in solving fault diagnosis problems is the selection of appropriate measurements. This is often referred to as the test point selection problem. An important related concern is circuit testability, which indicates the percentage of components that can be identified.

Seaks, Visvanathan and Sangiovanni–Vincentelli discussed the subject of testability measures on the basis of the rank of the test matrix [Seaks at el 1981, and Visvanathan and Sangiovanni–Vincentelli 1981]. The effect of the network topology, type of network elements, and test points on the rank of the test matrix has been discussed in several papers addressing problems of network testability [Iuculano et al. 1986 and Starzyk and Dai 1987].

Stenbakken and Souders have considered the problem of selecting test points, as well as practical aspects of testability related to measurement and computation errors. Analyzing the sensitivity matrix with the help of the QR algorithm, they have selected a sub–optimum set of test points. The selected test points can be used to evaluate circuit elements with minimum computational effort and high numerical accuracy. Using the same technique, the effect of measurement errors and element tolerances can be studied with sufficient statistical confidence.

The QRF algorithm is primarily used as a robust, linear–systems solving technique [Leon 1980]. However, Stenbakken and Souders (1987) have shown that the QRF algorithm with pivoting is also a powerful technique for the test

point selection, estimation of prediction variances, and element testability. In order to select the optimum set of test points, the largest major of the test matrix must be identified. In the QRF with pivoting, this selection is performed in a multi—stage process. First, we choose the column of the largest norm and orthogonalize all remaining columns to the selected one. Then the column of the largest norm of those remaining is selected and the orthogonalization step is repeated. The process continues until the norms of all the remaining columns are less than a preset threshold.

To measure testability, the QRF is performed on the original sensitivity matrix. The selected pivot column vectors correspond to the parameters which are testable under the given test nodes or test conditions. The reduced column number is equal to the column rank r, which indicates the number of the elements that can be estimated. If the column reduced sensitivity matrix is denoted by s_c, then the test equation becomes

$$s_c \, \Delta p_{sel} = \Delta v \qquad (5.3.1)$$

where Δp_{sel} represents the deviations of the selected elements.

To select the test points, the QRF is performed again on the column reduced sensitivity matrix s_c. The selected pivot row vectors correspond to the test points at which the actual measurements will be taken. The row and column reduced sensitivity matrix is denoted by s_{rc}, which is a rxr square matrix. After that, the real measurements are taken at the selected test nodes, resulting in Δv_r. The test equation can be reduced to a system of r equations

and the parameter deviations of the selected elements Δp_{sel} can be obtained by solving

$$s_{cr} \, \Delta p_{sel} = \Delta v_r \qquad (5.3.2)$$

5.4 Response Prediction

Prediction of the circuit's response from known information without taking the actual measurements is known as response prediction. There are two kinds of response prediction. One is called <u>linear response prediction</u> and the other is <u>nonlinear response prediction</u>.

5.4.1. Linear Response Prediction

Linear response prediction is used to predict the circuit's response at all candidate test points from measurements made at the selected points. This is based on the sensitivity approach. The procedure LINRESPRED used for linear response prediction is organized as follows.

Procedure LINRESPRED:

1. Simulate the response vector $v(p)$ of the nominal circuit and formulate its sensitivity matrix s at all candidate test points.

2. Perform the QRF process on the sensitivity matrix in order to select test points

3. Perform the measurements at the selected test points.

4. Estimate the parameter values from the equation (5.3.2).

5. Calculate the response deviations at all candidate test points

$$\Delta v_{pre} = s \, \Delta p \, . \qquad (5.4.1)$$

6.   Predict the circuit response by adding the nominal response simulated in Step 1 and the deviation of response Δv_{pre} calculated in Step 5.

$$v_{pre} = v(p) + \Delta v_{pre} \, . \qquad (5.4.2)$$

In this method, the deviation of response Δv_{pre} is the product of the sensitivity matrix and the estimated parameter deviations (Step 5). Since only linear equations are dealt with, it is a linear method. This method is very useful in predicting the frequency response, which is an important characteristic for a wide variety of circuits and systems. Usually, measurements have to be taken at all candidate test frequencies in the entire interested range in order to obtain an accurate response. Even if the candidate test frequencies can be spread on the log scale, the number of frequencies is still large, making it difficult to measure the frequency response accurately. The linear method is a very efficient and accurate method for predicting the frequency response for linear time invariant systems [Stenbakken and Souders 1985].

The linear response prediction method is very useful not only for frequency domain testing, but also for the general case testing. For example, this method can be used for data converter testing [Souders and Stenbakken 1985]. The response at the 1024 codes of the 10 bits D/A converter can be predicted based on the 37 selected measurements. If we extend this method to the time domain testing, the circuit's response within the entire time interval can be predicted based on a few measurements at the selected sampling time points [Dai and Souders 1989].

5.4.2. Nonlinear Response Prediction

The nonlinear response prediction is used to predict the circuit's response to an arbitrary input signal, based on the updated parameter values obtained from the measurements of the circuit's response to the standard input signal. The procedure NONRESPRED which utilizes nonlinear response prediction is organized as follows.

Procedure NONRESPRED:

1. Apply the standard input signal to the circuit and measure the response.

2. Estimate the deviation of parameters Δp by solving (5.3.2).

3. Update the element parameters by

$$p_u = p_0 + \Delta p \qquad (5.4.3)$$

the iterative process could be used if Δp is large.

4. Simulate the circuit's response to an arbitrary input signal w_{ar} based on the updated parameter values p_u obtained in Step 3. The circuit's response can be obtained by solving the system equations

$$f(v_{ar}, \dot{v}_{ar}, t, p_u, w_{ar}) = 0 \qquad (5.4.4)$$

The circuit simulator such as SPICE or SABER can be used to simulate v_{ar}.

Since the system of nonlinear equations is used in Step 4, this method is referred to as a nonlinear method. In practice, the step input signal can be chosen as a standard input because it can be accurately generated and the step response can be obtained directly through an automatic test equipment. However, some arbitrary input signals are difficult to be accurately generated and their response cannot be easily recorded. We can solve this problem by

employing the nonlinear response prediction method. In order to test the circuit, we apply the step input signal and measure the step response. Then we evaluate the parameter values and update the circuit model based on the step response measurement. Instead of measuring the response to an arbitrary input signal, we can simulate the response based on the updated model. Therefore we can predict the time domain response to an arbitrary input signal or the frequency domain response based on the step response measurement. This is a general method for linear and nonlinear circuits.

5.5 Measurement Errors

According to statistics, a commonly used optimization criterion is to minimize the variances of the response predictions caused by measurement errors [Box and Draper 1971]. If we assume that the measurement errors are normally distributed, uncorrelated, with zero mean, and have a variance of σ^2_{err}, then the variances of the parameter estimation are

$$\sigma^2_{\Delta p} = \text{diag} \left[\left(s'_{rc} \, s_{rc} \right)^{-1} \sigma^2_{err} \right] \qquad (5.5.1)$$

which determine the confidence of the parameter estimation (5.3.2). The variances of the response predictions are

$$\sigma^2_{\Delta v} = \text{diag} \left[s \left(s'_{rc} \, s_{rc} \right)^{-1} s' \, \sigma^2_{err} \right] \qquad (5.5.2)$$

which determine the confidence of the response prediction (5.4.1).

Stenbakken and Souders (1987) took the measurement errors into account. They defined testability factor as the ratio of the variance of the measurement errors σ_{err} to the variance of the parameter estimation $\sigma_{\Delta p}$ as follows:

$$tf_j = \frac{\sigma_{err}}{\sigma_{\Delta p_j}} \tag{5.5.3}$$

where j stands for the jth component. To understand the testability factors, we substitute (5.5.1) into (5.5.3)

$$tf_j = \frac{\sigma_{err}}{\sigma_{\Delta p_j}} = \sqrt{\operatorname*{diag}_j [s'_{rc} \, s_{rc}]} \tag{5.5.4}$$

As we mentioned above, the QRF process gives a suboptimal maximization of $|s'_{rc} s_{rc}|$. Therefore, the variances of the response prediction and parameter estimation are minimized, and testability factor tf is maximized. Equations (5.3.1–5.3.4) not only provide reasonable optimization criteria for the test point selection, but also provide a definition of testability which takes measurement errors into account.

5.6. Ambiguity Groups Elimination

In a typical circuit, it is common for the column rank of a test matrix to be less than the actual number of circuit parameters. This is due to the presence of ambiguity groups in the circuit [Stenbakken, Souders and Steward 1989]. Ambiguity groups are groups of components which cannot be

distinguished from each other by measurements made at the designated test nodes and test conditions. Consequently, their sensitivity vectors are dependent, the test matrix is singular, and a unique solution of the test equation cannot be found. However, even with full numerical rank the test matrix may still be nearly singular due to near–ambiguity groups. In these cases, the solution is unstable, and will be extremely sensitive to small errors in the model, and to measurement errors. In short, the testability factor will be poor. If ambiguity groups exist in the circuit, then the parameter values can not be evaluated. The effects of ambiguity groups have been shown to be very important for parameter estimation.

There are several ways in which ambiguity groups, or near–ambiguity groups can be eliminated.

First, addition of new test nodes or test conditions is often effective. These test conditions can be DC excitation levels, test frequencies, or input waveforms.

Second, it is possible to add components of known value into the tested circuit and take measurements with and without the added components. The sensitivity matrix consists of two parts: the test matrix obtained from measurements taken at the original circuit $s_{original}$ and the test matrix obtained from measurements taken at the circuit with additional components s_{added}. The new test matrix s is formed by combining the two as follows:

$$s_{new} = \begin{bmatrix} s_{original} \\ s_{added} \end{bmatrix} . \qquad (5.6.1)$$

It was shown through the computer simulation that the rank of the new test matrix is larger than the rank of the original test matrix. When the sufficient components are added, the full rank can be achieved. In this case, all ambiguity groups are broken up and all element values can be identified. This approach can be an attractive compromise between functional testing and traditional bed–of–nails, in circuit testing.

Finally, if these approaches fail or are not feasible, the column dimension of the test matrix is reduced to the column rank. This is accomplished by performing the QRF process. Only one element from each ambiguity group is selected by the QRF. Remaining elements in each ambiguity group are fixed to their nominal values artificially, i.e., deviations of the remaining element values are assumed to be zero. In this case the selected element values can be obtained from

$$s_c \, \Delta p_{sel} = \Delta v \qquad (5.6.2)$$

where s_c is the column reduced sensitivity and Δp_{sel} correspond to the deviation of the selected element values. Of course, the values of the selected parameters can be estimated relative to the remaining parameters.

The level of ambiguity permitted (and hence the testability of the selected components) is set by a factor ϵ, provided by the user. By setting ϵ larger, fewer components may be included in the test matrix, but the testability factors of the selected components will be higher. Consequently, response predictions made by substituting the estimated parameter values back into the original model may be more accurate.

5.7 Time Skew Estimation

In order to obtain accurate parameter estimates from the first order approximation, it is critical that the timing relationship between the output and input data record be accurately known. In cases where the output and input waveforms are synchronously sampled, this may not be particularly difficult if the external electrical delays are kept equal. On the other hand, it is often convenient to apply a standard input waveform, e.g., a step, which is known to be nearly ideal, and then sample only the output waveform. In this case, only one recording channel is required. However, with asynchronous triggering, the timing may be in error by as much as one half the sampling period. This amount of timing error is often intolerable. For example, it has been found that in some cases as little as 1 ns of time skew can cause changes in parameter estimates of up to 50%. The problem can be overcome, however, by adding a time skew parameter to the model. We accomplish this by adding Δt to the parameter vector Δp, and an column vector, s_t, to the test matrix. The test equation becomes

$$[\; s \; s_t \;] \begin{bmatrix} \Delta p \\ \Delta t \end{bmatrix} = \Delta v \; , \qquad (5.7.1)$$

where

$$s_t = \frac{dv}{dt} \; . \qquad (5.7.2)$$

At the jth time instance, the vector s_t is easily computed by taking the first difference of the response vector, i.e.,

$$s_{tj} = \frac{v_j - v_{j-1}}{t_j - t_{j-1}} \; . \qquad (5.7.3)$$

It is has been verified experimentally that this approach makes the parameter estimates relatively insensitive to the actual time skew.

5.8 Modified QR Factorization for the Decomposition Approach

The optimum set of test points should be selected to minimize the variances of response prediction and parameter evaluation. An efficient approach to test point selection is based on the QR factorization (QRF) of the system test matrix as we mentioned in the previous sections.

5.8.1 Group Test Point Selection

In the KCL–based method, the test equations are formulated using voltage measurements at the partition points. Since all the partition voltages (at least in one subnetwork) must be known to formulate even a single test equation, it is necessary to modify the QRF process. In each step, instead of selecting a vector with the largest norm, we look for the best group of vectors. Each candidate group consists of a set of rows of the test matrix that correspond to all the partition points at a single test frequency or sampling time point. The QR factorization is run on the candidate group to evaluate a product of diagonal elements of the R matrix. Partial products are evaluated only for those elements of R which correspond to the selected rows. The group with the largest partial product is our pivot. The remaining rows in the Jacobian are orthogonalized w.r.t. the pivot rows.

It may happen that not all rows in the selected group are independent. This will be indicated by small values on the diagonal positions in R that correspond to the dependent vectors. Using a user–defined threshold, we can eliminate such vectors from the selected group. Since different groups may have

a different number of selected vectors, we must compare their partial products appropriately. Rather than using a partial product for all diagonal elements in the group, we construct a vector of partial products as follows:

$$
\mathbf{R}_{pp} = \begin{bmatrix} r_1 \\ r_2 \\ \vdots \\ r_{g_i} \end{bmatrix} = \begin{bmatrix} R_{i_1} \\ \prod\limits_{k=1}^{2} R_{i_k} \\ \vdots \\ \prod\limits_{k=1}^{g_i} R_{i_k} \end{bmatrix} , \tag{5.8.1}
$$

where R_{i_k} represents the k–th diagonal element of the $\mathbf{R}$ matrix in the ith group, and g_i is the number of elements in this group that are larger than the threshold value. Comparing two groups (say ith and mth) we first select

$$
g = \min(g_i, g_m) \tag{5.8.2}
$$

and choose the one with the larger r_g as a pivot.

The computer simulation shows that this selection reduces the number of excitations (and frequencies) with only a small decrease in the accuracy of the solution (see Tables 6.1.4–6.1.6).

5.8.2 Parallel QR Factorization

The test matrix based on the sensitivity approach is a dense matrix since the deviations of the measured voltages are taken as test functions. In such a

case, considerable computational effort for the QRF is required. On the other hand, the test matrix based on the decomposition approach is sparse. In what follows we present the modified QRF process. Its purpose is to preserve the sparsity of the test matrix during the vector orthogonalization.

For simplicity, we divide the network into 2^n subnetworks hierarchically using n levels of decomposition. Fig. 5.8.1 shows an example of a network partitioned hierarchically into 8 subnetworks (n=3). Here c_i represents the set of common nodes between the subnetworks on different levels of the hierarchical partition. The hierarchical levels are illustrated in Fig. 5.8.2 where r_α represents the remaining external nodes of the subnetwork S_α (the external nodes excluding the common nodes).

The test matrix for this example has the same nonzero pattern as the one shown in Fig. 4.4.4. To select test points, the QR factorization is performed on the T' (where ' stands for the matrix transpose operator) . Columns of T' are reordered according to the hierarchical levels as shown in Fig. 5.8.3.

The test matrix has a block structure, and blocks at the same level are independent of each other. Therefore, the QR process can be implemented in parallel within these blocks, level by level, to speed up the computations. There are four levels in this example. Level 1 has 8 blocks corresponding to the nodes r_1, r_2,...,r_8. Level 2 has 4 blocks corresponding to the nodes c_7, c_6, c_5, c_4. Level 3 has 2 blocks corresponding to the nodes c_3 and c_2, and level 4 has one block corresponding to the nodes c_1. The QRF runs from level 1 to level 4 performing parallel computations at each level.
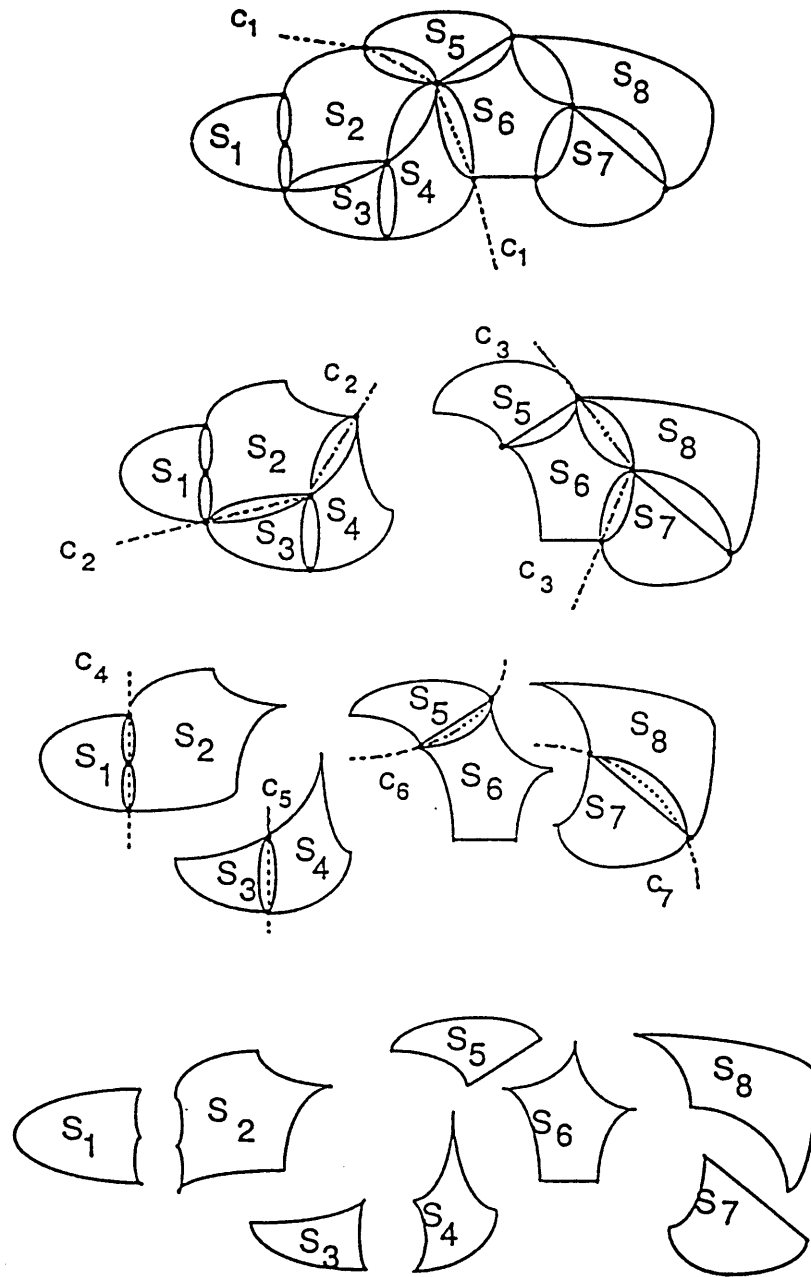
Fig. 5.8.1 An example of the hierarchical decomposition.
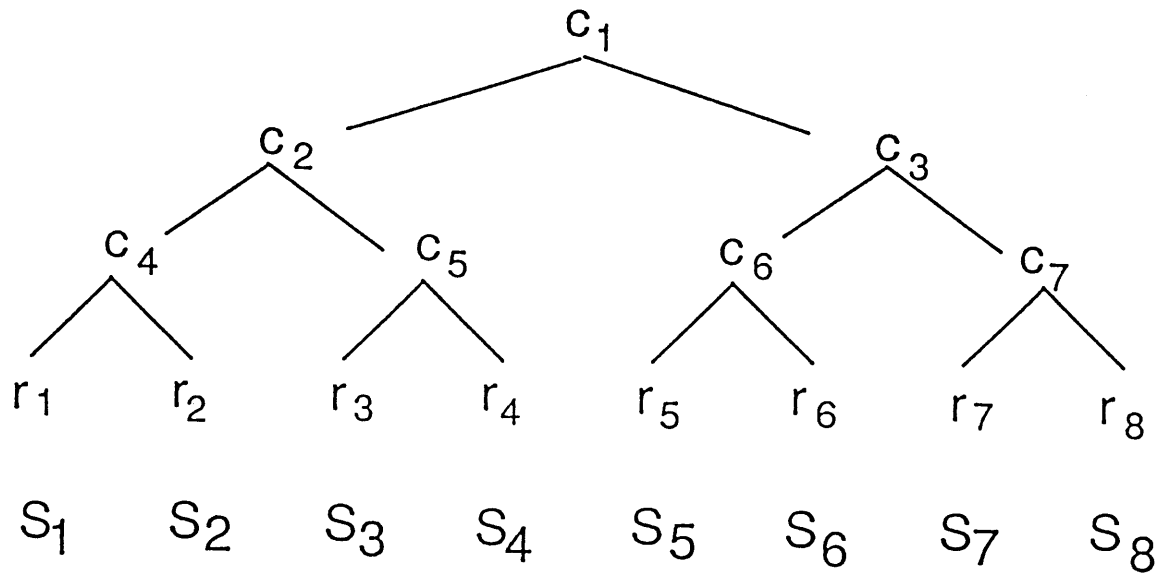
Fig. 5.8.2 The hierarchical levels.
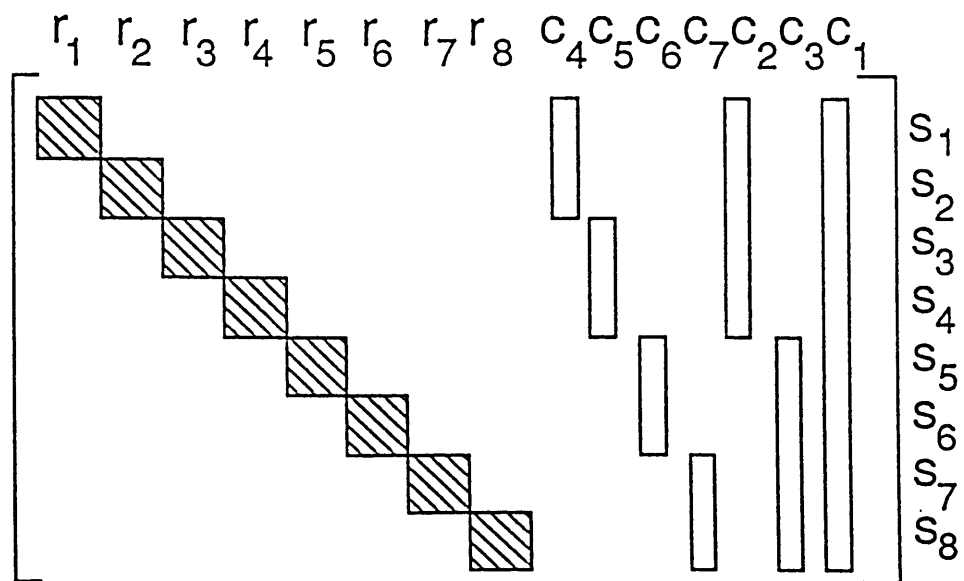
Fig. 5.8.3 The reordered test matrix T'.

The resulting Jacobian matrix T'_{QRF} has the same nonzero pattern as shown in Fig. 5.8.3. It can be seen that T_{QRF} is a sparse matrix as well. Since the corresponding test matrix has a block structure, it is possible to solve the test equations locally. Parallel processing can be used to find the element values in each subnetwork. This increases the computation speed. Furthermore, higher accuracy can be expected because the numerical errors decrease when computation operations are performed in the smaller matrices.

6. COMPUTER SIMULATION AND EXPERIMENTAL RESULTS

The software for the decomposition approach was developed and tested on a transistor amplifier circuit. Results obtained from the decomposition approach are compared with those obtained from the sensitivity approach. A piecewise linear circuit is used to illustrate how all parameters in a nonlinear circuit can be estimated by the multi–operating–point and multi–frequency testing methods. The effect of nonlinearities of the nonlinear circuit on circuit testability is shown on a small nonlinear circuit example.

A time domain testing system was set up at the National Institute of Standards and Technology, U.S. Department of Commerce. Time domain testing was implemented on two example circuits: an amplifier/attenuator circuit and a bandpass filter circuit. Testing strategies presented in Chapter 5 were applied to time domain testing.

6.1 A Transistor Amplifier Circuit

A linearized transistor amplifier circuit shown in Fig. 6.1.1 is selected as an example to illustrate the decomposition approach presented in Chapter 4. Voltage measurements are taken at nodes 1, 2, 4, 5 and 6. The circuit is decomposed at the measurement nodes into three subnetworks as shown in Fig. 6.1.2. Nodes 1, 6 and 5 are the internal measurement nodes of S_1, S_2 and S_3 respectively. Node 2 is the common node between S_1 and S_2, and node 4 is the common node between S_2 and S_3. The system of test equations is formed based
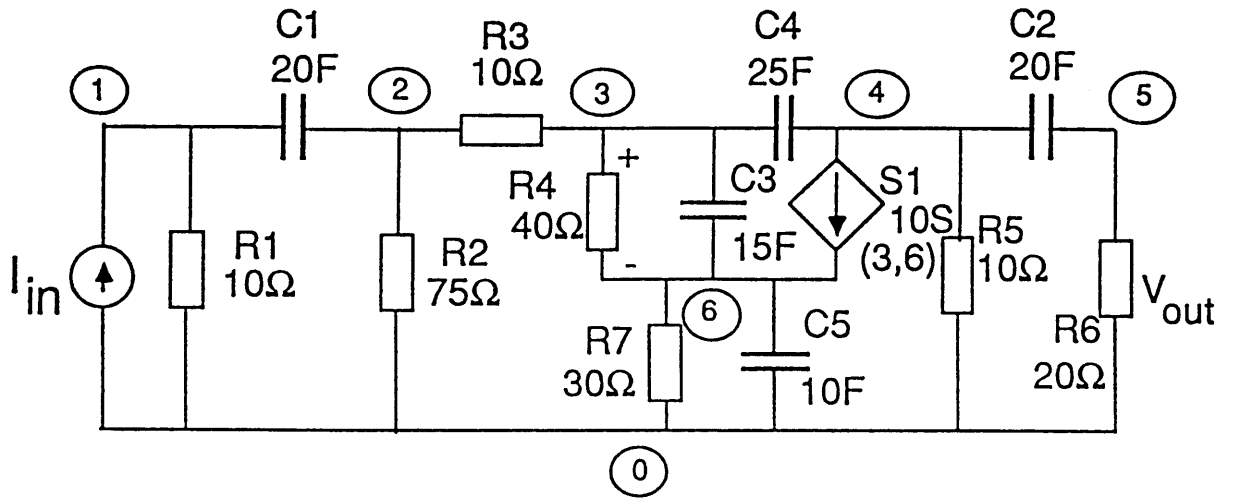
Fig. 6.1.1 A linearized transistor amplifier circuit.
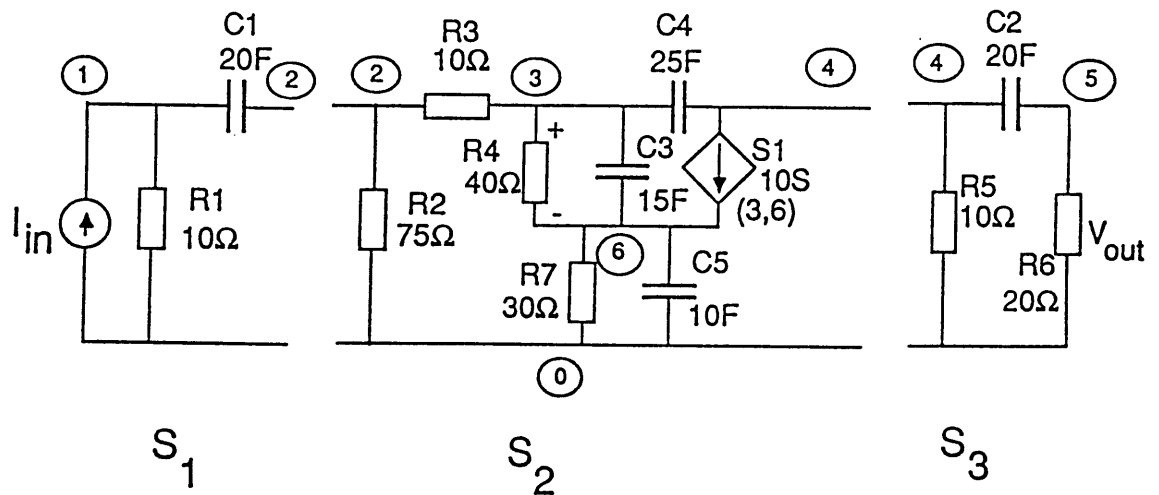
Fig. 6.1.2 Network decomposition of the example circuit.

on the KCL equations at these five nodes. The corresponding test matrix has the block structure as shown in Fig. 6.1.3 where the shaded areas represent the nonzero pattern of T.

The nominal and faulty parameter values are listed in Table 6.1.1. The actual element deviation in percent is denoted by d. The purpose of testing is to estimate the parameter deviations Δp. In what follows, the computed deviations obtained by different methods are compared.

$$
\begin{array}{c}
R_1 \quad C_1 \quad R_2 \quad R_3 \quad R_4 \quad C_4 \quad C_3 \quad R_7 \quad C_5 \quad S_1 \quad R_5 \quad C_2 \quad R_6
\end{array}
$$
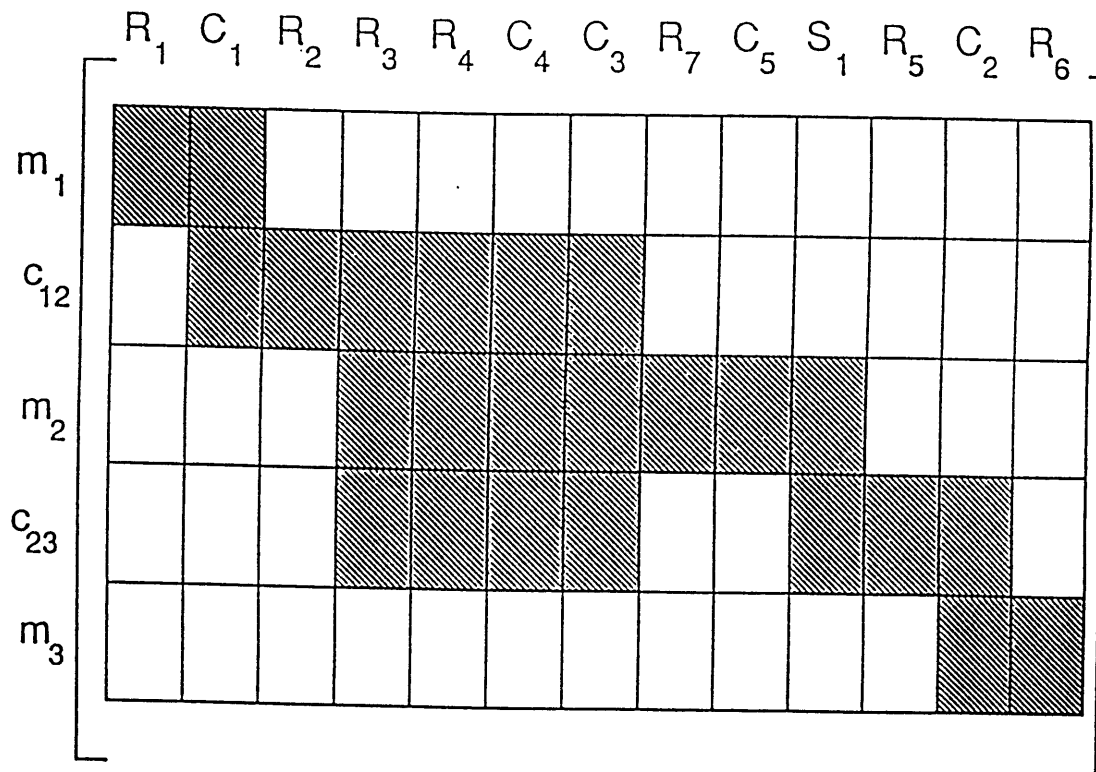
Fig. 6.1.3 Nonzero pattern of the test matrix.

6.1.1   Comparison of the Sensitivity and Decomposition Approaches in Frequency Domain

In frequency domain testing, the candidate set of test frequencies consists of 31 frequencies equally spaced on a logarithmic scale, giving 155 possible test measurements. We compare the results obtained from the decomposition approach described in Section 4.4 with those of the sensitivity approach described in Section 3.4 in Tables 6.1.2–6.1.6.

In Table 6.1.2 , the first and second columns list the estimated errors in element deviations obtained by the approximate method and the exact method respectively, which are the two methods of the decomposition approach described in Section 4.5. The last column represents results obtained from the sensitivity approach. The results in Table 6.1.2 are obtained by the real variables computation (refer to Section 3.4.1 C) and the results in Table 6.1.3 are obtained by the complex variables computation. As we can see, element deviations calculated using the decomposition approach are comparable with those obtained using the sensitivity approach.

In Tables 6.1.4 − Table 6.1.6 we compare results of the QR factorization with the single test and the group test selections discussed in Section 5.8. The single test selection uses orthogonalized vectors with the largest norm, while the group test selection uses the partial products (5.8.1). We compare the results of different selections for the test matrix obtained using the decomposition approach and the sensitivity approach. Tables 6.1.4 and Table 6.1.5 show the selected test nodes and the test frequencies. The accuracies of the solution

obtained in the single and the group test selection are compared in Table 6.1.6. Note that the number of test frequencies selected by the group test selection is less than that selected by the single test (Table 6.1.4), but the accuracy of the solutions obtained by both methods are equivalent. Therefore, the group test selection reduces the test effort without any notable decrease in accuracy.

6.1.2 Comparison of Sensitivity and Decomposition Approaches in Time Domain

In time domain testing, the candidate set of test time sampling points consists of 40 time points distributed in the log scale, giving 200 possible test measurements.

Table 6.1.7 gives the comparison of results obtained by the decomposition approach and the sensitivity approach. Column a lists the actual element deviations. Columns b and c give the element deviations computed by the decomposition approach and the sensitivity approach, respectively. From the table we can see that the results are comparable for both approaches.

6.1.3. Comparison of Time Domain Testing with Frequency Domain Testing

To understand the effect of measurement errors on element estimation and testability factors, the results obtained by the sensitivity approach were studied. Table 6.1.8 compares results obtained by time domain and frequency domain methods. Column a lists true element deviations from the nominal values. Two cases are considered. In the first case deviations are calculated based on the assumption that there are no measurement errors (standard deviations of

measurement errors $\sigma = 0$). Test results are listed in columns b and d. In the second case, random measurement errors were simulated with $\sigma = 0.1$ %. This random error simulation was repeated 20 times. Test results are listed in columns c and e. Table 6.1.9 gives testability factors computed using the time domain and the frequency domain methods.

From the results of the computer simulation, it is obvious that the accuracy obtained by the time domain and the frequency domain methods are comparable, and testability factors computed by these methods are equivalent. Since the time domain measurements can be obtained easily by using automatic test equipment (ATE), the time domain method preferred over the frequency domain method in practical testing.

Table 6.1.1 Data for Example

$$d = \frac{p^* - p^0}{p} \times 100$$

element	nominal values p^0	faulty values p^*	actual deviations d (%)
R1	10Ω	10.05Ω	0.5
C1	20F	19.00F	-5.0
R2	75Ω	76.92Ω	2.5
R3	10Ω	10.20Ω	2.0
R4	40Ω	42.67Ω	6.6
C4	25F	24.00F	-4.0
R7	30Ω	29.40Ω	-2.0
C3	15F	14.00F	-6.6
C5	10F	9.50F	-5.0
R5	10Ω	9.80F	-2.0
C2	20F	19.00F	-5.0
R6	20Ω	20.60F	3.0
S1	10S	9.50S	-5.0

The normalized frequency points (in Hz) are as follows:

f_1	0.0001	f_2	125.892E–6	f_3	158.489E–6
f_4	199.526E–6	f_5	251.188E–6	f_6	316.227E–6
f_7	398.107E–6	f_8	501.187E–6	f_9	630.960E–6
f_{10}	794.328E–6	f_{11}	100.000E–5	f_{12}	125.890E–5
f_{13}	158.490E–5	f_{14}	199.530E–5	f_{15}	251.190E–5
f_{16}	316.230E–5	f_{17}	398.110E–5	f_{18}	501.190E–5
f_{19}	630.960E–5	f_{20}	794.330E–5	f_{21}	100.000E–4
f_{22}	125.893E–4	f_{23}	158.489E–4	f_{24}	199.526E–4
f_{25}	251.188E–4	f_{26}	361.228E–4	f_{27}	398.107E–4
f_{28}	501.187E–4	f_{29}	630.960E–4	f_{30}	794.328E–4
f_{31}	100.000E–3				

Table 6.1.2 Estimated Errors $\Delta\mathbf{d}$ (real case, in percent)

$$\Delta\mathbf{d} = \mathbf{d}_{calculated} - \mathbf{d}_{actual}$$

| element | decomposition approach | | sensitivity approach |
	approximate	exact	
C4	–0.00081	–0.00026	–0.00166
C1	–0.00243	0.0	–0.00168
R1	–0.00017	–0.00002	–0.00005
R3	0.00002	–0.00049	–0.00010
S1	–0.00046	–0.00339	–0.00304
C3	–0.00407	0.00037	0.00379
C2	0.11372	–0.01011	–0.00124
R7	–0.05968	–0.00660	–0.00195
C5	–0.00171	–0.00523	0.00203
R5	0.08824	0.00626	–0.00171
R2	0.00078	0.00074	0.00067
R6	–0.11573	0.00946	–0.00027
R4	0.60676	0.10454	–0.16485

Table 6.1.3 Estimated Errors $\Delta\mathbf{d}$ (complex case, in percent)

$$\Delta\mathbf{d} = \hat{\mathbf{d}}_{cal} - \mathbf{d}_{actual}$$
$$\mathbf{d}_{cal} = \mathrm{Re}(\mathbf{d}_{cal}) + j\mathrm{Im}(\mathbf{d}_{cal})$$
$$\hat{\mathbf{d}}_{cal} = \mathrm{sgn}\,[\,\mathrm{Re}(\mathbf{d}_{cal})\,]\sqrt{\mathrm{Re}^2(\mathbf{d}_{cal}) + \mathrm{Im}^2(\mathbf{d}_{cal})}$$

| element | decomposition approach | | sensitivity approach |
	approximate	exact	
C4	–0.00076	0.00040	–0.00097
R1	–0.00005	–0.00002	0.00002
C1	–0.00233	0.0	–0.00183
S1	–0.00104	0.00026	–0.01461
R3	–0.00044	–0.00050	–0.00004
C5	–0.00108	0.00053	–0.00144
C3	–0.00256	–0.00020	–0.01371
R5	0.00906	0.00047	–0.00053
R7	0.00893	0.00064	–0.00007
C2	0.01389	0.01195	0.00281
R2	0.00336	0.00080	–0.00049
R6	–0.00498	–0.01075	–0.00451
R4	0.04449	0.03748	0.16446

Table 6.1.4 Test frequencies in the single and group test selections.
Decomposition approach (exact method, real case)

Nodes	Test frequencies													
	Single test									Group test				
	1	2	3	4	5	6	7	8	9	1	2	3	4	5
1	f_{31}	f_1								f_{10}	f_{31}			
2	f_{31}	f_1								f_{10}	f_{31}			
3			f_{17}	f_5	f_9	f_{29}				f_{10}	f_{31}	f_{17}		f_4
4	f_{31}		f_{17}				f_3	f_8		f_{10}	f_{31}	f_{17}	f_5	
5									f_{13}	f_{10}				

Table 6.1.5 Test frequencies in the single and group test selections.
Sensitivity approach (real case)

Nodes	Test frequencies											
	Single test								Group test			
	1	2	3	4	5	6	7		1	2	3	4	5
1	f_1	f_5		f_{11}	f_{29}				f_4	f_{29}	f_{11}		
2	f_1								f_4		f_{11}		
3	f_1	f_5	f_{31}						f_4	f_{29}			
4	f_1		f_{31}			f_{22}			f_4			f_{31}	f_{30}
5	f_1						f_{13}		f_4	f_{29}	f_{11}		

Table 6.1.6 Estimated element deviations in the single and group test selections.
(real case, in percent)

element	Decomposition approach single test	group test	sensitivity approach single test	group test
C4	0.00026	0.00068	–0.00166	–0.00078
C1	0.0	0.0	–0.00168	–0.00185
R1	–0.00002	–0.00002	–0.00005	–0.00018
R3	–0.00049	–0.00094	–0.00010	–0.00047
S1	–0.00339	–0.00267	–0.00304	–0.00194
C3	0.00037	0.00074	–0.00379	–0.00364
C2	–0.01011	–0.00539	–0.00124	0.00359
R7	–0.00660	–0.00847	–0.00195	–0.00117
C5	–0.00523	–0.00427	–0.00203	–0.00189
R5	0.00626	0.00805	–0.00171	–0.00047
R4	0.10454	0.10399	–0.16485	–0.04327
R2	0.00074	0.00406	0.00067	0.00445
R6	0.00946	0.00463	–0.00027	–0.00526

Table 6.1.7 Deviations from nominal (time domain)

Element	True	sensitivity approach	decomposition approach
	a	b	c
R1	0.500	0.490	0.505
R3	2.00	1.98	2.00
C1	–5.00	–5.18	–5.00
C5	–5.00	–5.15	–5.04
C4	–4.00	–4.11	–4.02
R5	–2.00	–2.08	–2.64
R7	–2.00	–2.05	–2.72
R6	3.00	2.37	2.03
R2	2.56	2.68	2.21
C2	–5.00	–4.57	–4.14
S1	–5.00	–5.45	–5.04
C3	–6.67	–7.03	–6.76
R4	6.68	–7.65	9.11

Table 6.1.8 Deviations from nominal
(Sensitivity approach)

Element	True	Time Domain		Frequency Domain	
		$\sigma = 0$	$\sigma = 0.1\%$	$\sigma = 0$	$\sigma = 0.1\%$
	a	b	c	d	e
R1	0.500	0.490	0.456	0.495	0.435
R3	2.00	1.98	2.02	2.00	1.99
C1	−5.00	−5.18	−5.27	−5.16	−5.31
C5	−5.00	−5.15	−5.14	−5.12	−5.16
C4	−4.00	−4.11	−3.98	−4.15	−3.51
R5	−2.00	−2.08	−3.03	−2.16	−1.49
R7	−2.00	−2.05	−1.83	−2.15	−0.79
R6	3.00	2.37	4.05	3.22	2.61
R2	2.56	2.68	3.14	2.50	2.89
C2	−5.00	−4.57	−6.97	−5.39	−5.10
S1	−5.00	−5.45	−11.2	−5.41	−17.0
C3	−6.67	−7.03	−42.9	−6.69	−25.6
R4	6.68	−7.65	0.023	2.75	413.

Table 6.1.9 Estimated testability factors
(Sensitivity approach)

Element	Time Domain	Frequency Domain
R1	0.67	0.65
R3	0.14	0.082
C1	0.12	0.17
C5	0.052	0.038
C4	0.085	0.026
R5	0.032	0.024
R7	0.045	0.017
R6	0.0068	0.0086
R2	0.024	0.013
C2	0.0070	0.0081
S1	0.0039	0.0024
C3	0.0015	0.0010
R4	0.00015	0.000095

6.2 A Piecewise Linear Circuit

This example is used to illustrate how the multi–operating–point testing and multi–frequency testing methods work. As mentioned in Chapter 5, nonlinearities of circuit elements can effect the circuit testability. When different DC excitation levels are applied to a tested circuit, the circuit is driven to different operating points. Therefore more independent measurements can be obtained. For a piecewise linear circuit, the nonlinear elements are represented by a number of linear segments and a linear combination of segments of different piecewise linear elements can be mapped into a region. One region is equivalent to a specific operating point. Multi–region testing in a piecewise linear circuit is similar to the multi–operating–point testing in a nonlinear circuit.

When the circuit operating point changes from one region to another, the number of unknown variables for each piecewise linear element increases by 2 (an equivalent admittance and a current source of a new segment). However the number of linear elements does not change. If the number of additional test points obtained in multi–region testing is two times larger than the number of piecewise elements, then it is possible to solve all element values. The common way to increase the number of test points is to use multifrequency testing at each region so that the reactive elements can be identified.

As an example, consider the nonlinear circuit shown in Fig. 6.2.1. Its equivalent piecewise linear circuit is shown in Fig. 6.2.2, and the characteristics of the piecewise linear elements g_1 and g_2 are given in Fig. 6.2.3. Voltage measurements are taken at the nodes 1,2 and 3. Each piecewise linear element has two segments and the parameter space is divided into four regions as follows:

r_1 (segment A and C): $v_3 < 1.0$ and $v_4 < 0.5$;

r_2 (segment B and D): $v_3 > 1.0$ and $v_4 > 0.5$;

r_3 (segment B and C): $v_3 < 1.0$ and $v_4 > 0.5$;

r_4 (segment A and D): $v_3 > 1.0$ and $v_4 < 0.5$.

The operating point can be moved from one region to another by changing the level of the DC current excitation

r_1: $J_s = -2.0$ A,

r_2: $J_s = 3.0$ A   and

r_3: $J_s = 15.0$ A .

In each region, a small AC signal is applied at two test frequencies:

$f_1 = 0.075$ Hz   and

$f_2 = 0.01$ Hz.
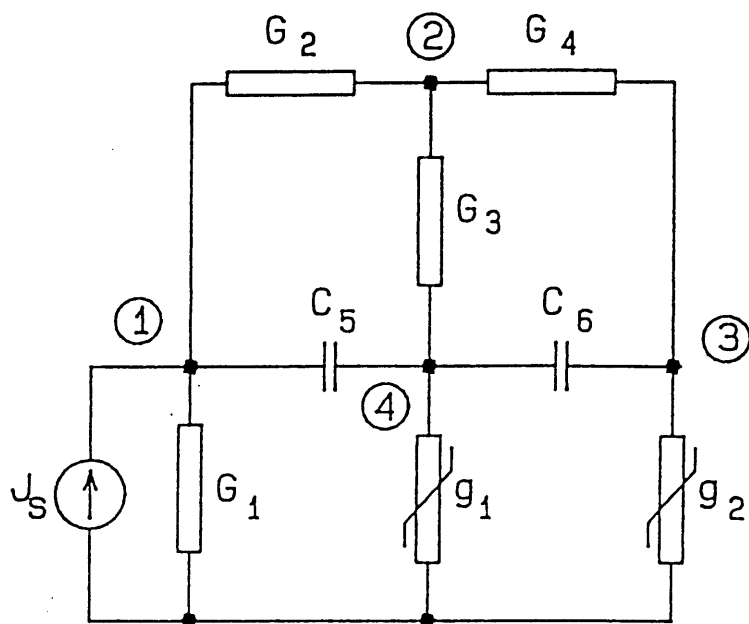
Fig. 6.2.1 A nonlinear circuit
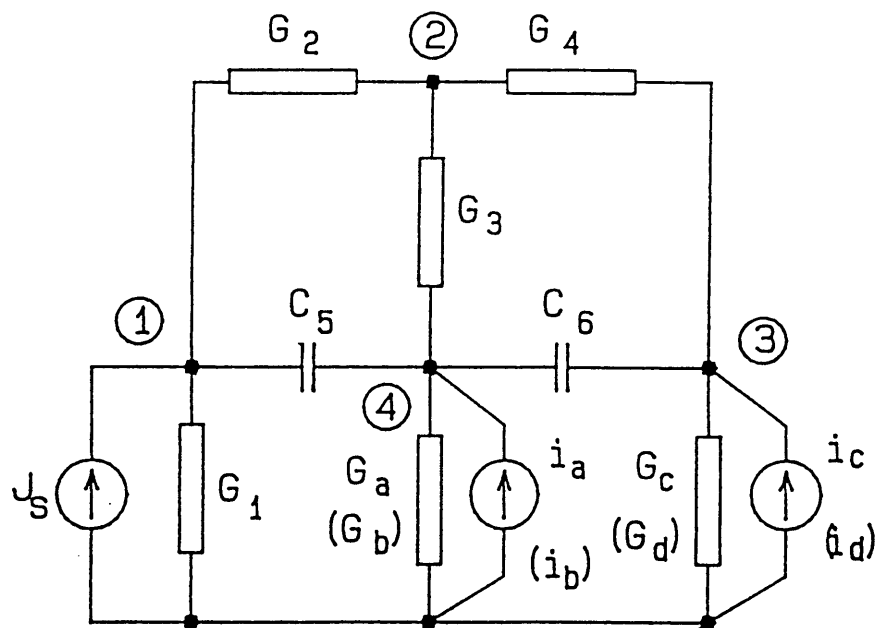
Fig. 6.2.2. Equivalent piecewise linear circuit
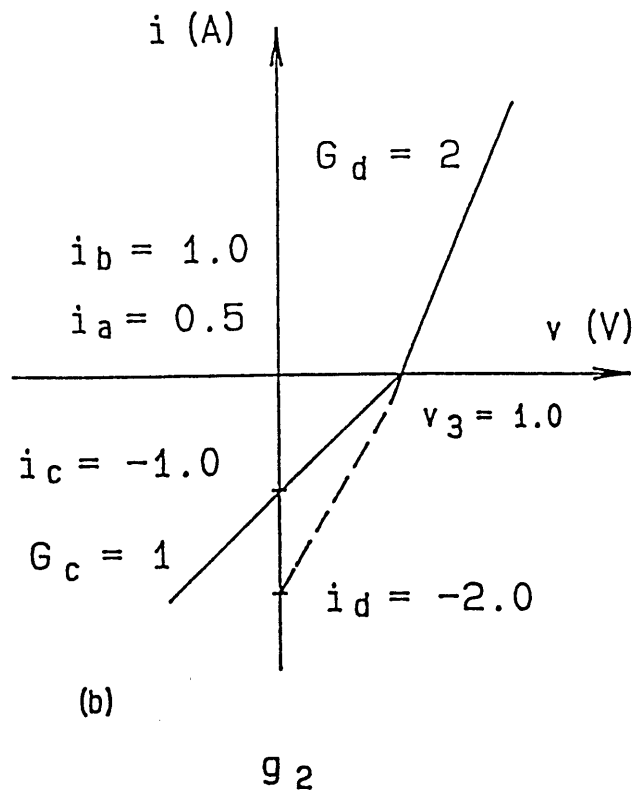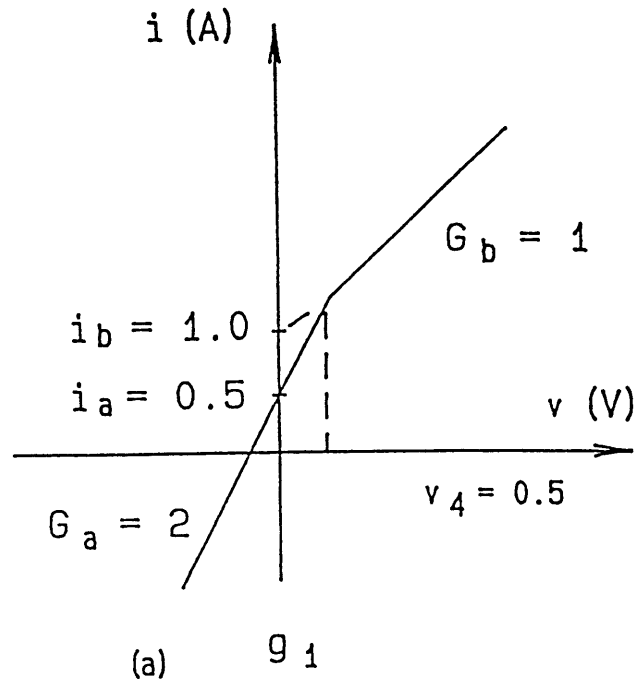
Fig. 6.2.3. Characteristics of piecewise linear elements.

Assume that deviations of element values **d** ($\Delta p/p$) are small (0.5%–23%). The QR algorithm was run on the test matrix to select 14 test points. Then the element deviations were computed. The results of the computer simulation are listed in Table 6.2.1.

Table. 6.2.1. Computer Results

Element		Deviations Computed d_c	Actual d_a	Differences $\Delta d = d_c - d_a$
1	G_1	−0.00973	−0.010	0.00027
2	G_2	0.00447	0.005	−0.00053
3	G_3	−0.02129	−0.020	−0.00205
4	G_4	−0.01070	−0.010	−0.00069
5	C_5	0.00784	0.010	−0.00216
6	C_6	−0.02205	−0.020	−0.00205
7	G_a	−0.05150	−0.050	−0.00150
8	I_a	0.22660	0.226	0.00060
9	G_b	0.01986	0.020	−0.00014
10	I_b	−0.01973	−0.020	−0.00150
11	G_c	−0.01069	−0.010	−0.00069
12	I_c	−0.01070	−0.010	−0.00070
13	G_d	0.00444	0.005	−0.00056
14	I_d	0.00435	0.005	−0.00065

6.3 A Nonlinear Circuit

In the previous example, a piecewise linear circuit was tested by the multi—operating—point method and the multi—frequency method in frequency domain. It showed that the nonlinearity of circuit elements can be used to increase circuit testability. In this section, a nonlinear circuit is tested by the multi—operating—point method and the multi—time points method in time domain. Similar results are observed.

Let us take the example from Section 3.3.3. Assume that the step function signal is applied to node 1 and the step response is measured at node 2. When we use only one excitation level, the rank of the sensitivity matrix is 3. One of the elements cannot be determined. When we use two excitation levels, the rank increases to 4. The procedure developed in Section 3.3.3 was used to estimate parameter deviations in this circuit. The true and computed deviations are listed in Table 6.3.1.

Table 6.3.1. Deviations from nominal (d in percent)

| Element | Actual | Computed | |
		$j = 1$ A	$j = 1$ A and $j = 2$ A
C	2.00	2.24	2.17
G	−3.00	−3.51	−3.34
I_s	10.00	undetermined	9.73
C_n	−5.00	−4.85	−5.02

Testing results discussed in Sections 6.1 through 6.3 were based entirely on the computer simulation. Both faults and measurements were simulated and then the test problem was solved. The remaining part of this chapter deals with experimental results and related problems. We first describe the organization of the time domain testing system.

6.4. Time Domain Testing System

Time domain testing of nonlinear circuits is very useful for the following reasons:

(1) Dynamic response is an important characteristic of nonlinear systems.

(2) Discrete measurements can be accurately obtained by the automatic test equipment in a fraction of the time needed for other tests (e.g., frequency domain test).

(3) The frequency domain response of a circuit can be estimated with sufficient accuracy from the discrete step response as discussed in [Souders and Flach, 1987].

(4) Time domain testing is essential for calibration and fault diagnosis of analog/digital mixed signal systems.

For the above reasons, we conducted experiments in time domain in order to implement the testing strategies developed in the previous chapters. The time domain testing system was set up as shown in the Fig. 6.4.1. During the real test, reference time domain input signals were applied to the circuits under test using signal levels selected in the pre—test stage. A waveform recorder was used to sample, digitize and store the output responses at the test points determined

in the pre—test stage. Data was transferred to the computer system for the post—test processing.

The following sections present experimental results based on the data collected at the National Institute of Standards and Technology.
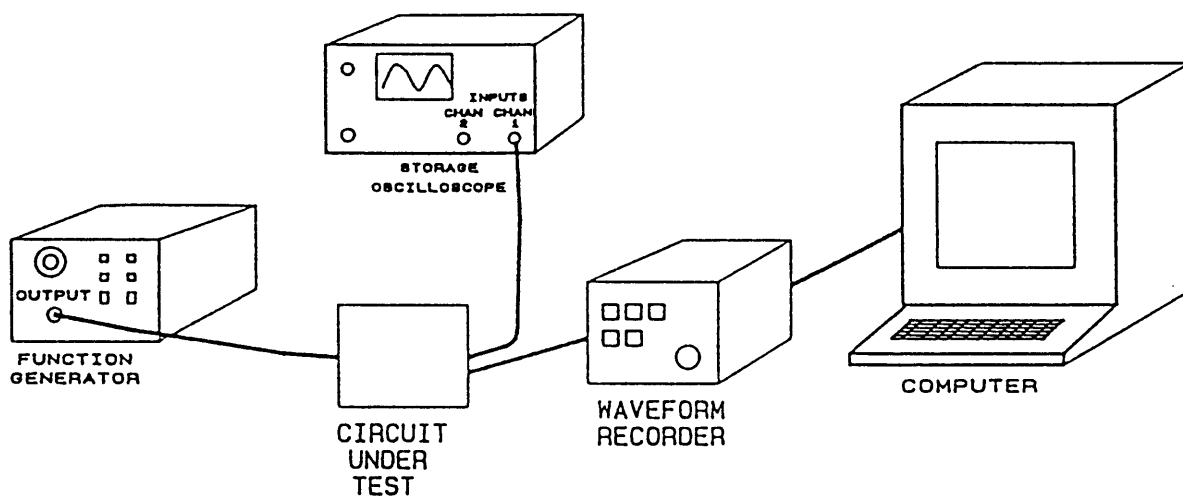

Fig. 6.4.1. Time domain testing system.

6.5. An Amplifier/Attenuator Circuit

An amplifier/attenuator circuit, which comprises the front end of a wide band sampling wattmeter developed at the National Institute of Standards and Technology (NIST), was the first circuit tested. It was designed to have a bandwidth of about 5 MHz and a flat response up to 300 kHz. A precision programmable step generator developed at NIST was used as the input waveform. The voltage step from this generator has a transition duration (rise time) of approximately 6 ns and settles smoothly to 0.1 percent in 17 ns. The waveform recorder used to sample, digitize, and store the step response was a commercial 10—bit instrument. The fastest sampling frequency is 60 MHz and the total number of sampling points is 4096. The output response from 0 to 1 ms was obtained by combining data at 4 MHz and 60MHz sampling frequencies. The lumped element model of the circuit is shown in Fig. 6.5.1.

6.5.1 Variable Step Integration and Time Skew Estimation

The step response was simulated based on this model. For greater simulation accuracy, we have used variable size time steps in the numerical integration procedure. Since the step response changes rapidly during the transition, and stabilizes after three to four times the circuit time constant, we have used an integration step of 16.6 ns (1/60 MHz). In this case a total of 45 time points are needed in the time interval 0—1 ms. The time skew parameter discussed in Section 5.7 was included in the test matrix.
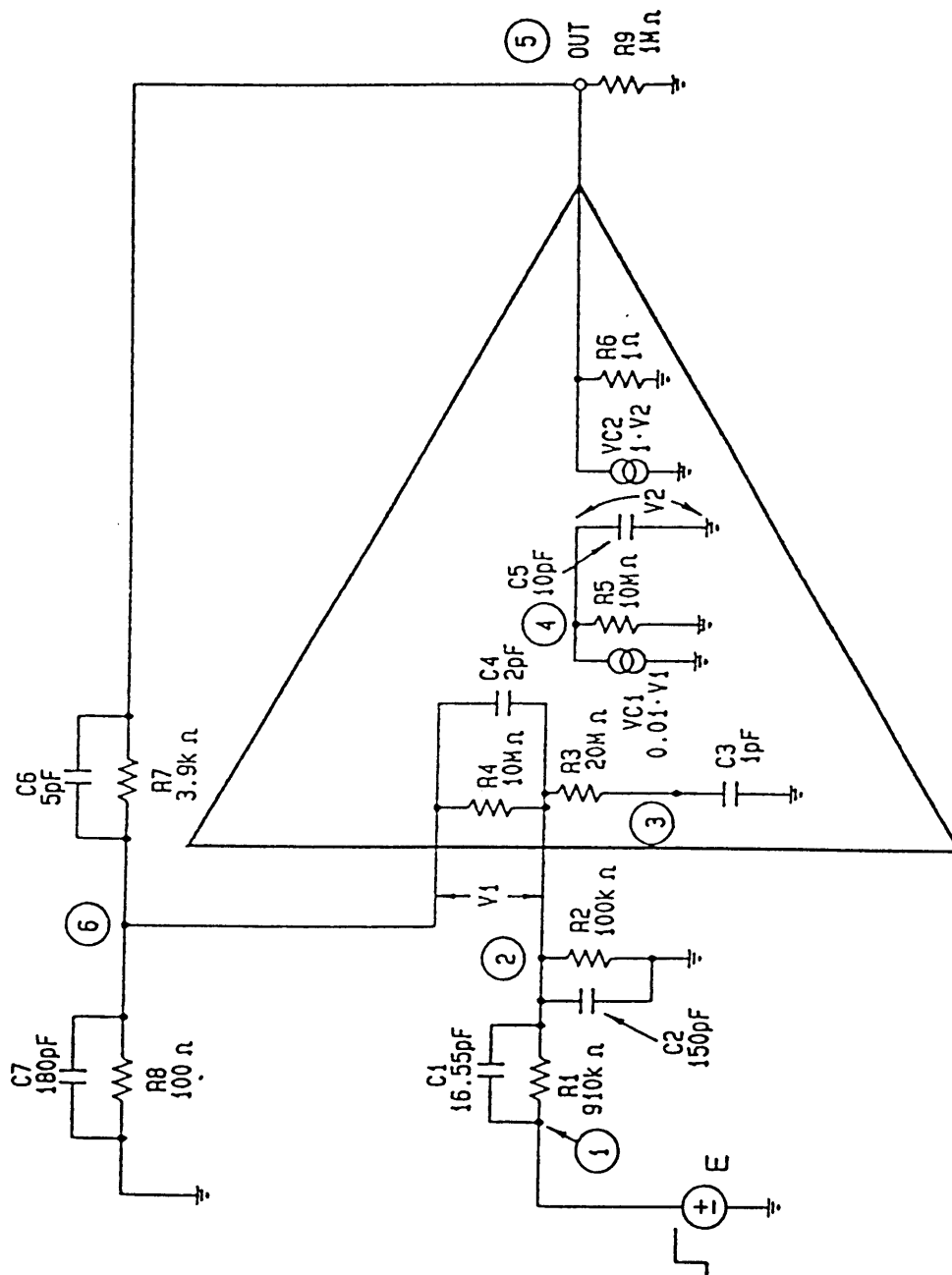
Fig. 6.5.1. Lumped element model of amplifier—attenuator network.

Fig. 6.5.2 shows the measured (solid) step response, and the step response computed from the nominal model (dashed), for two different time scales. Note that the measured response has an overshoot following the transition, while the computed one does not. The overshoot is caused by a mismatch between the time constants of the input circuits.

6.5.2 Testability Analysis and Ambiguity Groups

The testability analysis of this circuit showed that many ambiguity groups are present when node 5 (the output) is the only measurement. For example, (R1, R2) and (C1, C2) are ambiguity groups. Unfortunately for this circuit, nodes 3 and 4 are inaccessible, node 2 and node 6 are almost redundant because V1 $\cong$ 0, and both nodes are easily perturbed by small amounts of test probe capacitance.

Table 6.5.1 gives results of the computer simulation. Although results of the computer simulation in this example are satisfactory, the testability factors are very low (t < 0.001). In such a case the estimation errors will be relatively large, i.e., 1000 times the measurement errors. In the real testing, the accuracy of the waveform recorder is about 0.1%. Thus the component errors are usually large due to the inaccuracies of circuit modeling, temperature variations, and measurement errors.
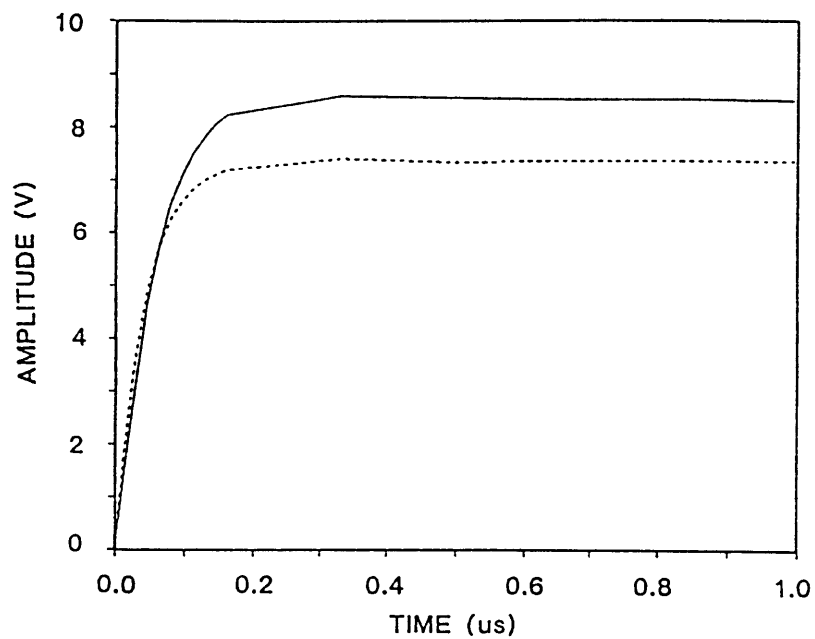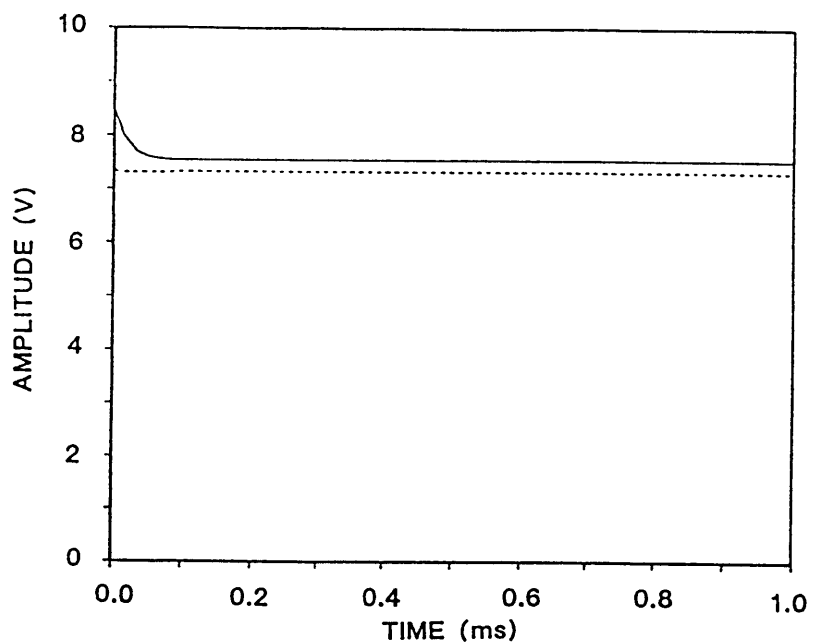
Fig.6.5.2 Step response of amplifier/attenuator network, over 1 μs (a) and 1 ms (b) time intervals. Solid curves give the measured response, and dashed curves give the response computed from the nominal model.

6.5.3 Unambiguous Component Selection and Linear Response Prediction

Using the third approach to eliminate the effect of ambiguity groups discussed in Section 5.6, we set a value of ϵ to 0.001 (the test node was still node 5). Four unambiguous components were found $(R_8,\ C_1,\ R_1,\ C_6)$ and their testability factors were higher than that in Table 6.5.1. Consequently, four out of the 45 candidate time points were selected for Δv measurements. Deviations Δp of the four chosen elements were computed by solving (5.3.2); then the step response for the entire time period was predicted based on Δv_{pred} calculated from (5.4.1). Fig. 6.5.3 shows the measured and the predicted responses, for the same time scales shown in Fig. 6.5.2. The maximum difference between the two curves over all time points, is 0.08 V, or 1% of the peak response.

Table 6.5.1. Element deviations and testability factors from computer simulation

Element	Nominal value	Deviations True	Computed	Testability factor
1	91 KΩ	–0.549	–0.616	0.003122
14	3.9 KΩ	–0.256	–0.25	0.0004687
11	10 pF	1.00	0.98	0.0005038
16	100 Ω	1.00	0.99	0.003726
4	150 pF	–0.67	–0.75	0.0003946
3	10 KΩ	0.80	0.80	0.0004071
5	20 MΩ	–0.50	–0.50	0.0004001
15	5 pF	1.00	0.98	0.0004862
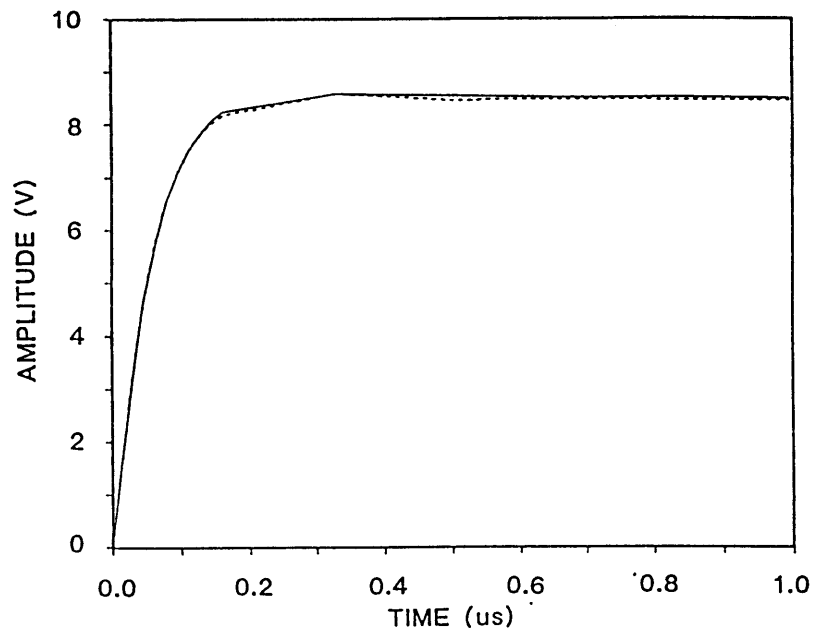
(a)
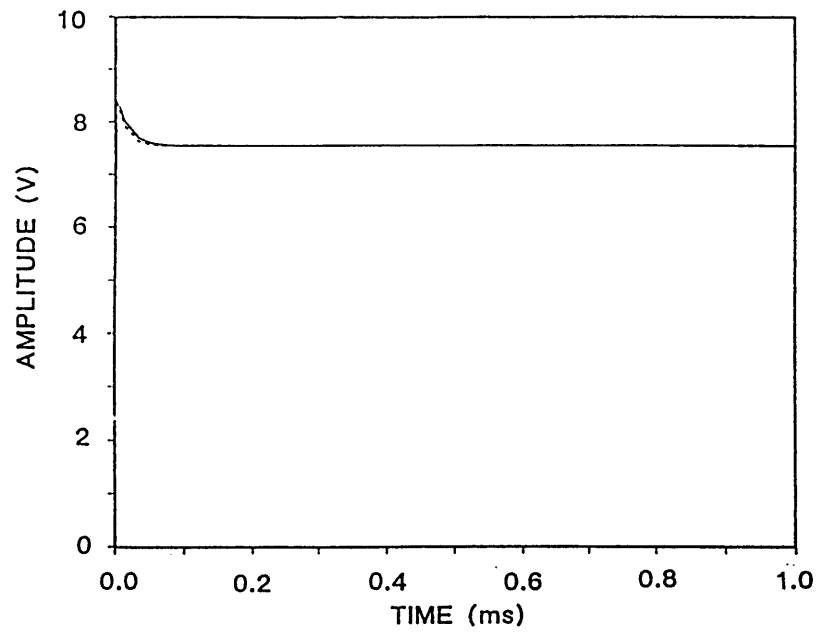
(b)

Fig. 6.5.3 Measured (solid) and predicted (dashed) step response of amplifier–attenuator network, over 1 μs (a) and 1 ms (b).

6.6. A Band Pass Filter

In this example, the second—order filter shown in Fig. 6.6.1 was used. The filter was designed to have a nominal center frequency f_0 = 24.5 kHz, a gain K=2, and a quality factor Q=4. The design values of the elements are given by

$$R_1 = \frac{2Q}{C \; \omega_0 \; K} \tag{6.6.1a}$$

$$R_2 = \frac{2 \; Q}{C \; \omega_0 \{-1 + [(K-1)^2 + 8Q^2]^{1/2}\}} \tag{6.6.1b}$$

$$R_3 = \frac{1}{C^2 \; \omega_0^2} \left[\frac{1}{R_1} + \frac{1}{R_2} \right] \tag{6.6.1c}$$

$$R_4 = R_5 = 2R_3 \tag{6.6.1d}$$

$$C_1 = C_2 = C = 5 \text{ nF} \tag{6.6.1e}$$

It is apparent from (6.6.1) that, by changing the value of C, other designs that give identical responses are possible. The element values of the actual circuit, however, were within 5% of the design values in (6.6.1).
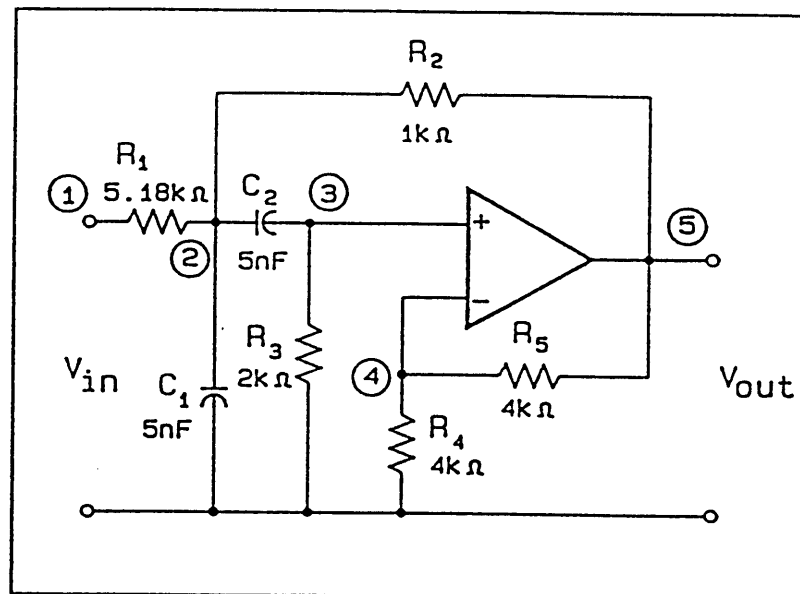
Fig. 6.6.1 Model for bandpass filter with center frequency of 24.5 kHz.

6.6.1 Linear Response Prediction

As can be seen in Table 6.6.1, only three components must be identified in order to predict the complete output (node 5) response (referring to the discussion in Section 5.4). Fig. 6.6.2 presents the results of a linear prediction of the step response, based on measurements made at node 5, at three time points selected by QR factorization. In this figure, the solid curve is the measured step response, and the dashed curve (barely distinguishable because of coincidence with the solid curve) is the response predicted by solving (5.4.1). In this case, the design values, p_d, were used for the calculation of the sensitivity matrix, and the linear model was quite satisfactory.

6.6.2 Iterative Process

To determine the effectiveness of the proposed approach for cases in which the assumed values deviate substantially form the actual values, the sensitivity matrix was recomputed based on the assumed values shown in Table 6.6.2. In this case, the assumed values deviate from the actual values by as much as 100%, and result in the large step response differences shown in Fig. 6.6.3. Because of the large differences, the linear model is inadequate, as indicated by the poor prediction results shown in Fig. 6.6.4. However by applying the iterative procedure discussed previously, excellent predictions can still be made. This is illustrated in Fig. 6.6.5, with the prediction results obtained after four iterations. In this example, a weighting factor, w (2.3.2), of 0.5 was used.

Table 6.6.1 Test Nodes and Ambiguity Groups

number of test nodes	test nodes	rank	selected elements
1	5	3	R_3, R_2, $[R_1, C_1]^*$
	3	3	R_3, R_2, $[R_1, C_1]^*$
	2	4	R_3, R_2, $[R_1, C_1]^*, [R_4, R_5]^*$
2	3,5	4	R_3, R_2, $C_1, [R_4, R_5]^*$
	2,5	5	R_3, R_2, $R_1, [C_1, C_2]^*, [R_4, R_5]^*$
3	2,3,5	5	R_3, R_2, $R_1, [C_1, C_2]^*, [R_4, R_5]^*$
4	2,3,4,5	5	R_3, R_2, $R_1, [C_1, C_2]^*, [R_4, R_5]^*$

* one of two selected depending on the initial values assumed.

Table 6.6.2 Parameter Values (kΩ, nF)

Case 1: no. of test nodes = 1 (node 5) and rank = 3

	Design values p_d	Assumed values p_0	Updated values p_u	percent changes $\dfrac{p_d - p_0}{p_0}$	percent changes $\dfrac{p_d - p_u}{p_u}$
R_1	5.18	5.5	4.815	−6	7
R_2	1.0	1.5	0.967	−33	3
R_3	2.0	1.0	1.993	100	0.4
C_1	5.0	5.2	5.2	−4	−4
C_2	5.0	5.2	5.2	−4	−4
R_4	4.0	4.0	4.0	0	0
R_5	4.0	4.0	4.0	0	0
$R_1 C_1$	25.9	28.6	25.0	−9	3

Fig. 6.6.2 Measured (solid) and predicted (dashed) step response of filter. The predicted response was based on measurements at three time points, using a single iteration with the sensitivity matrix computed from the design values, p_d.
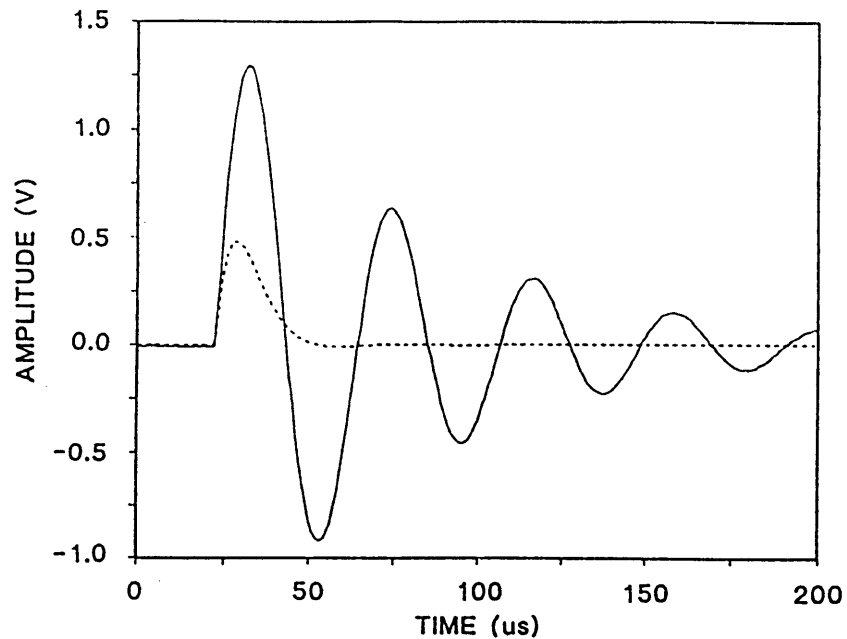
Fig. 6.6.3 Measured (solid) and computed (dashed) step response of filter. The computed response was obtained from the circuit equations where the assumed values p_u from Table 6.6.2 were used.

Fig. 6.6.4 Measured (solid) and predicted (dashed) step response of filter. The predicted response based on a single iteration, with the sensitivity matrix computed from the assumed values, p_0.
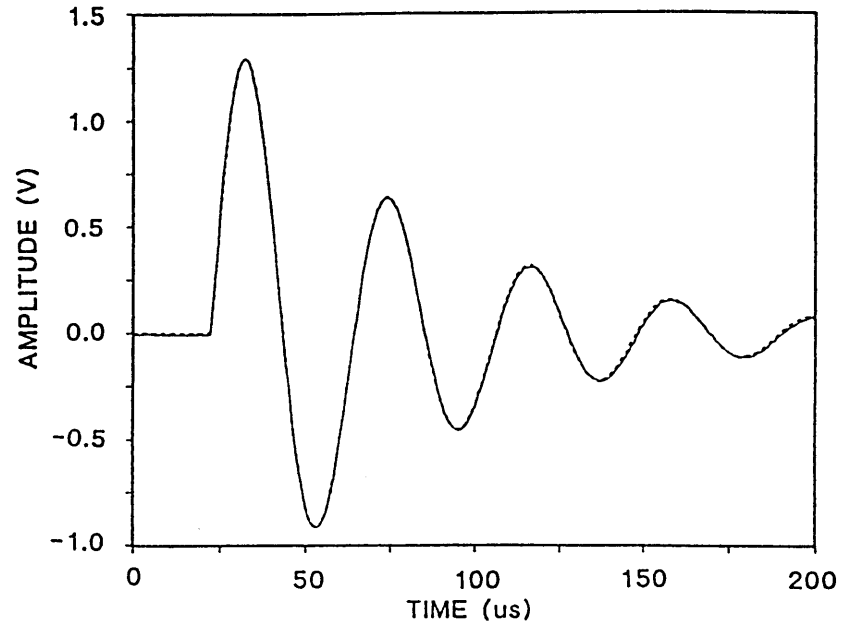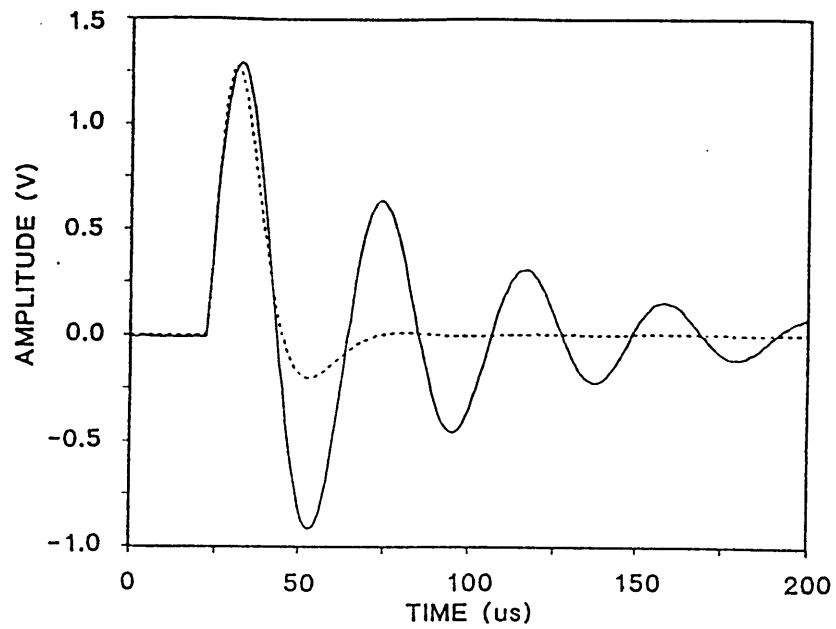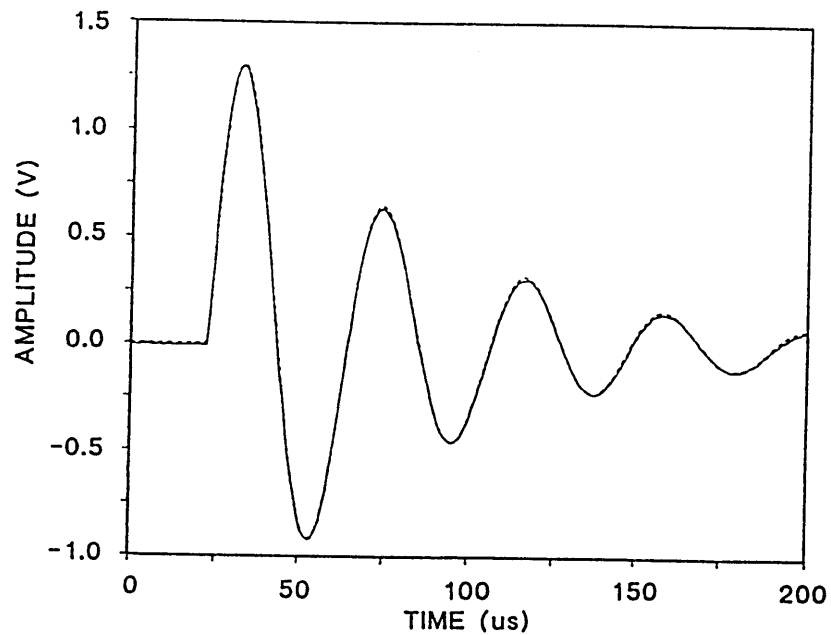

Fig. 6.6.5 Measured (solid) and predicted (dashed) step response of filter. The predicted response based on four iterations, with the sensitivity matrix computed from the updated values, p_u.

6.6.3 Nonlinear Response Prediction

For linear circuits if we know the step response, it is possible to predict the response to any other input signal. However, for nonlinear circuits, this is not generally the case. Here it becomes necessary to determine the full model parameters in order to make accurate response predictions for arbitrary input signals. Therefore, we are interested in the accuracy of the response predictions based on the new parameter estimates, as presented in Section 5.4.2.

The results from such a prediction are given in Figs. 6.6.6 and 6.6.7. Figure 6.6.6 shows an arbitrary input signal (solid) and the measured filter response (dashed). In Fig. 6.6.7 we show the measured filter response (solid) and the response predicted from the assumed model (dashed), which is based on assumed values p_0. Finally, Fig. 6.6.8 shows the predicted response to the input signal of Fig. 6.6.6, computed from the updated parameter estimates, p_u, which we have determined earlier from the step response data. The peak error in the prediction is less than 2%.

The updated parameter values that were used for the predicted response in Fig. 6.6.8 are given in Table 6.6.2. These are also the values that were used to obtain the response prediction of Fig. 6.6.5. Note that the updated values of the selected elements, R_1, R_2 and R_3, deviate significantly from the design values. This is because these elements form ambiguity groups with unselected components whose values have been arbitrarily fixed at the assumed values listed in Table 6.6.2. Any error in the value of an unselected component will be compensated for by the computed deviation for the selected component. Thus,

for example, the filter response depends on $\alpha=2Q/\omega_0 K = R_1 C_1$, rather than on R_1 and C_1 independently. In such cases where the response depends on a combination of parameters rather than on individual parameters, as indicated in Fig. 6.6.8, the predicted responses will be accurate even though the individual parameter estimates are not.

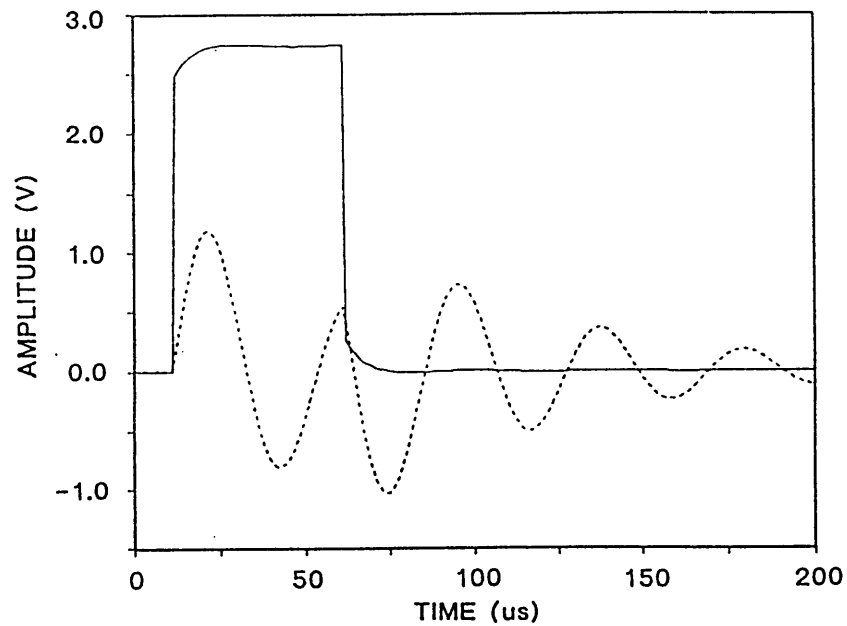Fig. 6.6.6 Measured arbitrary input signal (solid) and measured filter response (dashed)
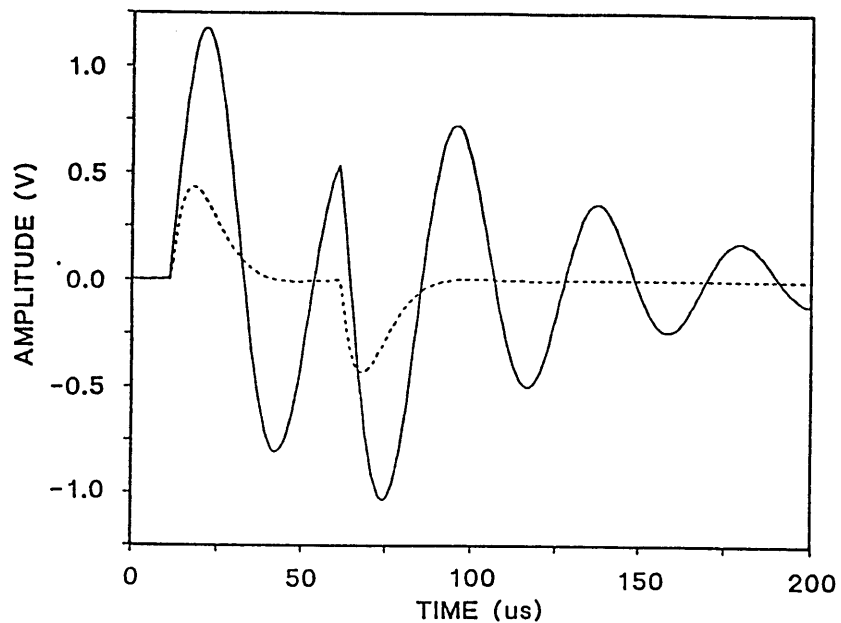
Fig. 6.6.7 Measured filter response (solid) and response computed from the assumed model (dashed), for the arbitrary input signal.
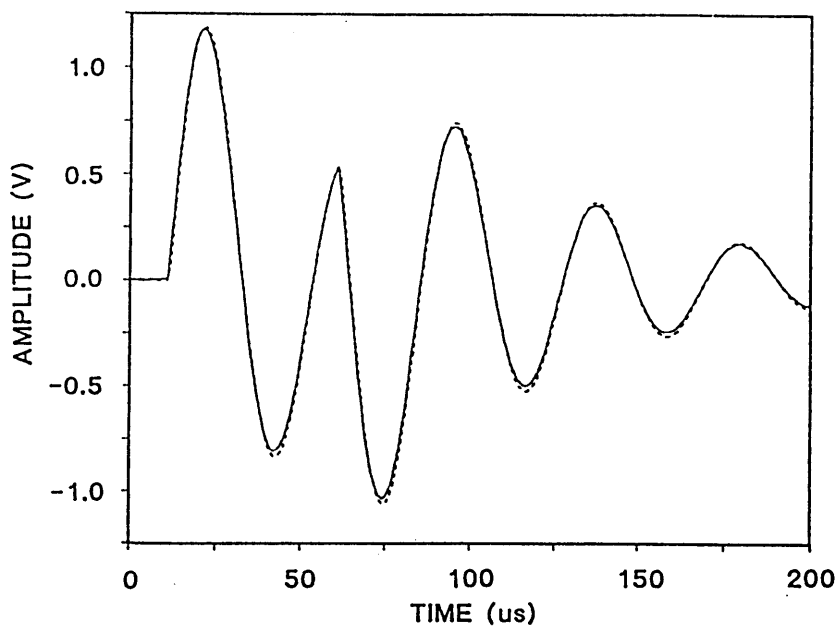
Fig. 6.6.8 Measured (solid) and predicted (dashed) responses to the input signal of Fig. 6.6.6. Prediction was based on the updated parameter estimates, p_u, determined from step response data.

6.6.4 Ambiguity Group Elimination and Parameter Evaluation

The result of the ambiguity analysis for the filter circuit is given in Table 6.6.1. It is seen, as expected, that the rank or number of observable components tends to increase as the number of test nodes increases. Nevertheless, the maximum rank is five (two pairs of ambiguous components remain), even though all test nodes are used. There is no way to distinguish between C_1 and C_2, or between R_1 and R_2, solely using voltage measurements.

However, as shown in the last column of Table 6.6.3, it is possible to increase the rank to seven (full rank) with as few as one test nodes, by making additional measurements with known components added to the circuit (refer to the discussion in Section 5.6). In this case, two resistors R_a and R_b, having nominal values of 4 kΩ and 1 kΩ respectively, were added in succession. R_a was added in parallel with R_5 between nodes 4 and 5, and R_b was added in parallel with C_1 between nodes 2 and the common node as shown Fig. 6.6.9. The perturbed sensitivity matrices, S_a and S_b, are calculated by computing sensitivities of the new circuits with respect to the seven original components. A composite sensitivity matrix S_{oab}, is then formed by combining the original and perturbed matrices so that $S_{oab} = [S', S'_a, S'_b]'$. The testability analysis showed that the circuit testability is significantly higher when using two rather than one test nodes, while further increasing of the number of nodes to four resulted in only marginally better testability.

Results obtained using this approach are listed in Table 6.6.4. In this case, measurements were made at test nodes 2 and 5, on both the original and

perturbed circuits. As seen in the fifth column, the assumed values p_0 of the components deviated by as much as 18% from the design values. After eight iterations, the updated estimates (p_u) listed in column four were obtained. The updated values deviate from the design values by only about 2% (see column six), which is within design tolerances. In Fig. 6.6.10, the step response using the updated values is plotted. The solid curve is the measured response, and the dashed curve is the step response calculated from system equations of the circuit based on the updated values p_u.
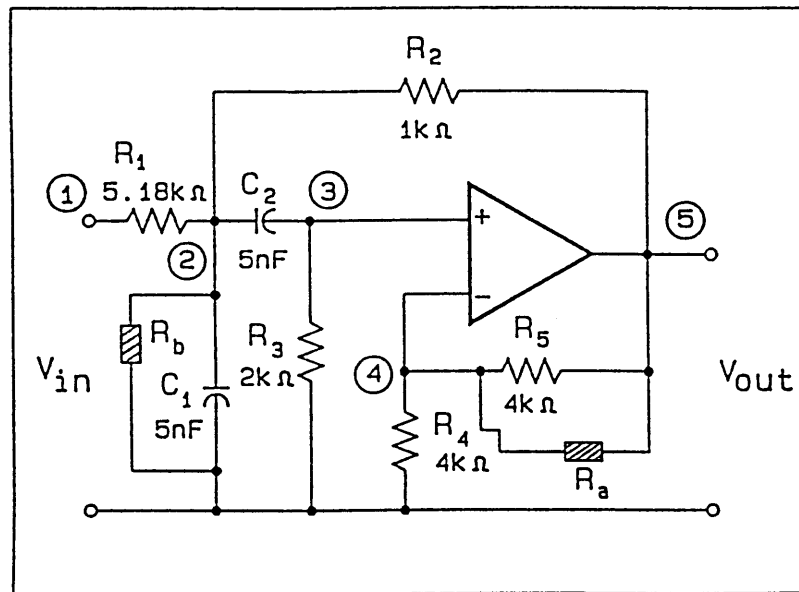
Fig.6.6.9 Perturbed bandpass filter with additional components R_a and R_b.

$$R_a = 4 \text{ k}\Omega \text{ and } R_b = 1 \text{ k}\Omega$$

Table 6.6.3 Comparison of the rank of the original sensitivity matrix S_o and rank of the composite sensitivity matrix S_{oab} using R_a and R_b.

number of test nodes	test nodes	rank(S_o)	rank(S_{oab})
1	5	3	7
	3	3	7
	2	4	6*
2	3,5	4	7
	2,5	5	7
3	2,3,5	5	7
4	2,3,4,5	5	7

Table 6.6.4 Parameter Values (kΩ, nF)

Case 2: Add R_a and R_b, no. of test nodes = 2 (node 2 and 5)
rank = 7 and no. of iterations = 8

	Design values P_d	Assumed values P_0	Updated values P_u	percent changes $\dfrac{P_d - P_0}{P_0}$	percent changes $\dfrac{P_d - P_u}{P_u}$
R_1	5.18	5.0	5.136	3.6	0.86
C_1	5.0	5.2	5.044	-3.9	-0.87
C_2	5.0	5.25	5.089	-4.8	-2.15
R_2	1.0	1.2	1.008	-17	-0.79
R_3	2.0	1.8	2.039	11	-1.91
R_4	4.0	3.5	4.033	14	-0.82
R_5	4.0	3.4	4.029	18	-0.72
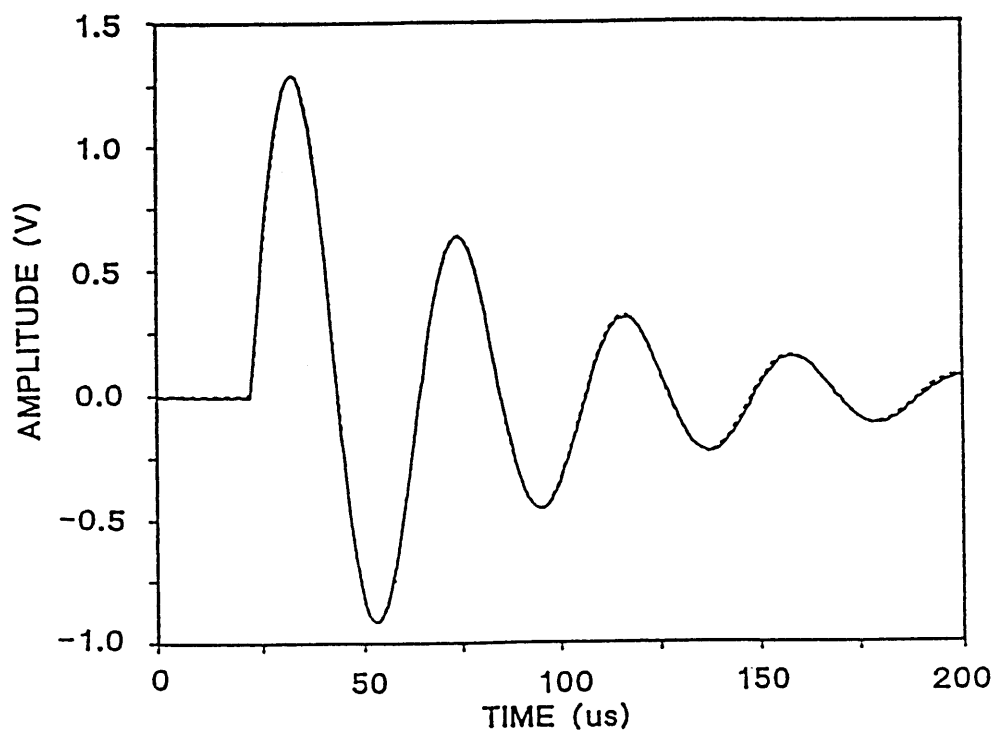
Fig. 6.6.10 Measured step response (solid) and predicted step response (dashed)

from measurements made on the original circuit and the perturbed circuit.

7. CONCLUSION

This dissertation is devoted to the development of computer aided testing (CAT) of analog and mixed—mode (analog and digital) systems. The decomposition approach to the testing of large scale circuit is developed and testing strategies related to the practical aspects are proposed.

7.1 Advantages of the Developed Methods

In the decomposition approach, the circuit being tested is decomposed into a number of small subnetworks. Measurements are taken at interconnection points of different subnetworks, resulting in a test matrix with a sparse block structure. Because of this sparsity, analysis of the test results is much easier. Test point selection and element evaluation are performed in parallel, reducing computation time and enhancing the test performance. In order to fully understand the advantages of such an approach, we have compared it with a sensitivity matrix method used in nonlinear analog testing.

The two major goals of our developed testing method are 1) to improve circuit simulation and 2) to identify parameters efficiently and accurately.

The first goal is satisfied by breaking interconnected systems into a set of smaller subsystems. Each of the subsystems can be analyzed separately in order to reduce overall analysis time and memory requirements. Different analysis methods can be used depending on the type of subcircuit analyzed. For example, a linear subcircuit can be analyzed using the Fourier transform, or

some other frequency domain method, which takes advantage of the circuit linearity. A subcircuit containing only resistive elements can use an algebraic equation solver since the differential equations will not be needed. Other types of subcircuits such as those with distributed parameters or subcircuits with ideal switches can use specialized analysis methods.

The second goal is satisfied by applying the principle of partition to the test stage. The test matrix of the test equations is of a block structure which yields solutions to the parameter identification problem locally. As a result, computer time and memory storage needs are reduced. Another important advantage of the block structure of the test matrix is that it limits the effects of changes in the system to local areas. Only the parameters inside the subnetworks adjacent to a particular test node will affect test equations at this node.

Advantages of the decomposition approach developed in this dissertation over the sensitivity approach include the following:

1) Errors in the subcircuit modeling do not affect evaluation of remote parameters.

2) In the exact method of the decomposition approach, measured voltages are used to simulate the internal voltages. Errors caused by numerical integration and nonlinear iterations are reduced when the measured voltages are highly accurate.

3) When a circuit has ideal switches (like a digital–to–analog converter), the circuit topology changes as the switches turn on or off. The decomposition approach can handle these topology changes with much less effort than the

sensitivity approach. This difference can be justified as follows. If a circuit has n switches, all of which can be either opened or closed, then 2^n different topologies have to be considered in the sensitivity matrix approach. However, in the decomposition approach, changes of switch values affect only local test equations, therefore fewer cases have to be considered.

4)   Different subnetworks can be simulated and tested using different circuit representation levels, such as the discrete element level, gate level, functional level *etc.*. Some subnetworks may be tested on the functional or macromodel level for functional testing, while other may be tested on the element level for element identification.

In the exact method, the test matrix is derived after measurements are taken. This requires more post–test processing. However, we can alleviate this problem by measuring only one sample circuit in order to derive the test matrix for other circuits of the same design. Test selection and testability analysis can then be performed on this test matrix. In this way, the post–test processing is made manageable.

This dissertation proposes test strategies for fault diagnosis of large analog circuits. Taking the practical aspects into consideration, the developed method is modified so that it is implemented in the real world. The practical aspects include determination of the test method and test environment, selection of test points, analysis of testability, prediction of the circuit's response, effect of measurement errors, elimination of ambiguity groups and estimation of time skew. Techniques related to these practical aspects are developed. The real test

was implemented at the National Institute of Standards and Technology. The experiment results verified the effectiveness of the developed techniques.

7.2 Impact of the Performed Research

Modern fabrication facilities allow analog and mixed mode electronic circuits to be built with much higher complexity than ever before. However, research interest in large scale integration analog circuits has been modest compared to the huge demand for VLSI digital circuits. This demand stemmed from the tremendous increase in popularity and applications of digital computers. This situation will soon change dramatically with the development of neural networks, whose applications could revolutionize areas such as speech and pattern recognition and information retrieval.

The new testing techniques developed in this dissertation can be used to test such large scale integration analog circuits. The research already developed had a significant impact on analog and mixed mode circuit testing and design. During the testing, voltage measurements play an active role in circuit simulation and diagnosis processes. We are able to test large systems without breaking the connections and can implement all calculations at the subsystem level. In design, the testing strategies provide design engineers with useful information so that they can make selected test points accessible.

The test method developed here can be used for testing custom integrated circuits (IC) such as analog/digital converters, filters, voltage regulators or operating amplifiers. It also can be applied to test VLSI neural networks or

complicated mixed mode circuits that combine analog and digital functions. The method is very useful at the system design, fabrication, maintenance, testing and repair stages.

Direction for future work includes improvements in the numerical integration and optimization routines, and extensions to accommodate mixed–signal devices and nonlinear elements.

REFERENCES

R. J. Allen, "Failure prediction employing continuous monitoring techniques," *IEEE Trans. Aerosp. Support Conf.* Procedures, vol. AS–1, pp. 924–930, 1963.

P. Antognetti and G. Massobrio, *Semiconductor Device Modeling with SPICE*, McGraw–Hill Book Company, New, York, 1988.

J. W. Bandler and A. E. Salama, "Fault diagnosis of analog circuits," *Proc. IEEE*, vol. 73, no. 8, pp. 1279–1325, 1985.

J. W. Bandler and Q. J. Zhang, "Large change sensitivity analysis in linear system using generalized Householder formulae", *Int. J. Circuit Theory and Appl.*, vol. 14, pp. 89–101, 1986.

J. W. Bandler and Q. J. Zhang, "Optimization techniques for modeling, diagnosis, and tuning", in *Analog Methods for Computer–Aided Analysis and Diagnosis*, (Editor, T. Ozawa), Marcel Dekker, New York, pp. 381–416, 1988.

R. M. Biernacki and J. A. Starzyk, "Sufficient test conditions for parameter identification of analog circuits based on voltage measurements," *Proc. European Conf.Circuit Theory and Design*, vol. 2, pp. 233–241, 1980.

R. S. Berkowitz, "Conditions for network–element–value solvability." IRE Trans. Circuit Theory, vol. CT–9, pp 24–29, 1962.

R. N. Bracewell, *The Fourier Transform and its Applications*, McGraw–Hill Book Company, New York, 1978.

F. D. Brown, N.F. McAllister, and R. P. Perry, "An application of inverse probability to fault isolation", *IRE Trans. Mil. Electron.*, vol. MIL–6, pp. 260–267, 1962.

G. Casinovi and A. Sangiovanni–Vincentelli, "A new aggregation technique for the solution of large systems of algebraic equations," *IEEE Trans. Computer–Aided Des.*, vol. CAD–7, pp. 976–986, 1988.

M. Catelani, G. Iuculano, A. Liberatore, S. Manetti and M. Marini, "Improvements to numerical testability evaluation", *IEEE Trans. Instru. Meas.*, vol. IM–36, no. 4, pp. 902–907, 1987.

C. W. Cha, "Multiple fault diagnosis in combinational networks", *Proc. 16th Design Automation Conf.*, pp. 149–155, 1979.

W.K. Chia, *et al.*, "Stability and convergence property of Relaxation methods for hierarchical simulation of VLSI circuits," *Proc. IEEE Int. Symp. on Circuits Syst.*, Montred, Canada, pp. 848–851, 1984.

L. O. Chua and P. M. Lin, *Computer Aided Analysis of Electronics Circuits*, Prentice Hall, Englewood Cliffs, New Jersey, 1975.

H. Cox and J. Rajski, "A method of fault analysis for test generation and fault diagnosis", *IEEE Trans. Computer–Aided Des.*, vol. CAD–7, pp. 813–833, 1988.

W. R. Curtice, "Nonlinear analysis of GaAs MESFET amplifiers, mixers, and distributed amplifiers using the harmonic balance technique", *IEEE Trans. on Microwave Theory and Techniques*, vol. MTT–35, no. 4, pp. 441–447, 1987.

H. Dai and T. M. Souders, "Time domain testing strategies and fault diagnosis of nonlinear analog circuits", to be presented at *IEEE Instrum. Meas. Test Conf.*, Washington, D.C., April, 1989.

S. W. Director, *Circuit Theory – A Computational Approach*, John Wiley & Sons, New York, 1975.

S. W. Director and R. A. Rohrer, "The generalized adjoint network and network sensitivities", *IEEE Trans. on Circuit Theory*, vol. CT–16, no. 3, pp. 318–323, 1969.

J. J. Dongarra, et. al., *LINPACK User's Guide, Society for Industrial and Applied Mathematics*, Philadelphia, 1979.

E. Flecha and R. DeCarlo, "Time domain tableau approach to the fault diagnosis of analog nonlinear circuits," *Proc. IEEE Int. Symp. Circuits and Systems* (Newport Beach, CA), pp. 828–830, 1984.

S. Franco, *Design with Operating Amplifiers and Analog Integrated Circuits*, McGraw–Hill Book Company, New York, 1988.

S. Freeman, "Optimum fault isolation by statistical inference," *IEEE Trans. Circuits Syst.*, vol. CAS–26, pp. 505–512, 1979.

C. W. Gear, *Numerical Initial Value Problems in Ordinary Differential Equations*, Prentice–Hall, Englewood Cliffs, NJ, 1971.

A. George and J. W. Liu, *Computer Solution of Large Sparse Positive Define Systems*, Prentice–Hall, Englewood Cliffs, New Jersey, 1981.

R. Goering, "Circuit simulator tackles electrical and mechnical components", *Computer Design*, November. 1986.

G. H. Golub, V. Klema, and G. W. Stewart, "Rank degeneracy and least squares problems," *Tech. Rep. TR–456, Computer Science Dept.*, Stanford University, CA, 1976.

H. P. Graf, L.D. Jackel, and W. E. Hubbard, "VLSI implementation of a neural network model", *IEEE Computer*, pp. 41–49, March, 1988.

G. D. Hachtel, R. K. Brayton, and F. G. Gustavson, "The sparse tableau approach to network analysis and design," *IEEE Trans. Circuit Theory*, vol. CT–18, pp. 101–112, January. 1971.

H. H. Happ, *Diakoptics and Networks*, Academic Press, New York, 1971.

A. A. Hatzopoulos, and J. M. Kontoleon, "Efficient fault diagnosis in analogue circuits using a branch decomposition approach," *IEE Proc.*, vol. 134, Pt. G, no. 4, pp. 149–157, 1987.

C. W. Ho, A. E. Ruehli, and P. A. Brennan, "The modified nodal approach to network analysis," *IEEE Trans. Circuits Syst.*, vol. CAS–22, pp. 504–509, June 1975.

W. Hochwald and J. D. Bastian, "A dc approach for analog fault dictionary determination," *IEEE Trans. Circuits Syst.*, vol. CAS–26, pp. 523–529, 1979.

Q. Huang and R. W. Liu, "Fault diagnosis of piece–wise linear system," *Proc. IEEE Int. Symp. Circuits and Systems* (Philadelphia, PA), pp. 418–421, 1987.

Z. F. Huang, C. S. Lin and R. W. Liu, "Node–fault diagnosis and a design of testability," *IEEE Trans. Circuits and Syst.*, vol. CAS–30, pp. 257–265, 1983.

J. Hutchinson, Ch. Koch, J. Luo, and C. Mead, "Computing motion using analog and binary resistive networks", *IEEE Computer*, pp. 52–63, March, 1988.

G. Iuculano, A. Liberatore, S. Manetti, and M. Marini, "Multifrequency measurements of testability with application to large linear analog systems", *IEEE Trans. Circuits Syst.*, vol. CAS–33, pp. 644–648, 1986.

D. Kahaner, C. Moler and S. Nash, *Numerical Methods and Software*, Prentice Hall, Englewood Cliffs, New Jersey, 1988.

K. S. Kundert and A. Sangiovanni–Vincentelli, "Simulation of nonlinear circuits in the frequency domain," *IEEE Trans. Computer–Aided Des.*, vol. CAD–5, pp. 521–535, 1986.

K. S. Kundert, G. B. Sorkin, and A. Sangiovanni–Vincentelli, "Applying harmonic balance to almost–periodic circuits", *IEEE Trans. Microwave Theory and Techniques*, vol. 36, no. 2, pp. 366–378, 1988.

S. J. Leon, *Linear Algebra With Applications*, MacMillan Publishing Co., New York, 1980.

C. S. Lin, Z. F. Huang and R. W. Liu, "Topological conditions for single branch–fault," *IEEE Trans. Circuits and Syst.*, vol. CAS–30, pp. 376–381, 1983.

P. M. Lin and Y. S. Elcherif, "Computational approach to fault dictionary", in *Analog Methods for Computer–Aided Analysis and Diagnosis*, (Editor, T. Ozawa), Marcel Dekker, New York, pp. 325–363, 1988.

H. Maeda, Y. Ohta, S. Kodama and S. Takeda, "Fault diagnosis of non–linear systems: graphical approach to detectability, distinguishability and diagnosis algorithm," *Int. J. Circuit Theory Appl.* vol. 14, pp. 195–209, 1986.

M. Mahoney, *Tutorial: DSP–Based Testing of Analog and Mixed–signal Circuits*, IEEE Computer Society Press, Washington, D.C., 1987.

M. J. Maron, *Numerical Analysis – A Practical Approach*, MacMillan Publishing, New York, 1982.

C. Mead, *Analog VLSI and Neural Systems*, Addison–Wesley, New York, 1989.

D. D. Weiner and J. F. Spina, *Sinusoidal Analysis and Modeling of Weakly*

Nonlinear Circuits – with Application Interference Effects, Van Nostrand Reinhold Company, New York, 1980

A. Miczo, *Digital Logic Testing and Simulation*, Harper & Row, New York, 1986.

A. G. Milnes, *Semiconductor Devices and Integrated Electronics*, Van Nostrand Reinhold Co., New York, 1980.

M. E. Mohari–Bolhassan and T. N. Trick, "A new iterative algorithm for the solution of large scale systems," Proc. 28th Midwest Symposium on Circuits and Systems, Louisville, KY, pp. 75–77, 1985.

M. E. Mohari–Bolhassan, D. Smart and T. N. Trick, "A new robust relaxation technique for VLSI circuit simulation," Proc. Int. Conference on Computer–Aided–Design, (Santa Clara, CA), pp. 26–28, 1985

L. W. Nagel, "SPICE 2: A computer program to simulate semiconductor circuits", University of California at Berkeley, ERL–M520, May, 1975.

M. S. Nakhla and J. Vlach, "A piecewise harmonic balance technique for determination of periodic response of nonlinear systems", *IEEE Trans. on Circuits and Syst.*, vol. CAS–23, no. 2, pp. 85–91, 1976.

N. Navid and A. N. Willson, Jr., "Fault diagnosis for resistive analog circuits," *Proc. IEEE Int. Symp. Circuits and Systems* (Tokyo, Japan), pp. 882–885, 1979.

W. Nye, D. Riley, A. Sangiovanni–Vincentelli, and A. L. Tits, "DELIGHT.SPICE: An optimization – based system for the design of integrated circuits," *IEEE Trans. Computer–Aided Des.*, vol. CAD–7, pp. 501–519, 1988

J. M. Ortega and W.C. Rheinboldt, *Iterative Solution of Nonlinear Equations in Several Variables*, Academic Press, New York, 1970.

T. Ozawa, "Decomposition approaches to fault location", in *Analog Methods for Computer–Aided Analysis and Diagnosis*, (Editor, T. Ozawa), Marcel Dekker, Inc., New York, pp. 365–380, 1988.

L. Rapisarda and R. DeCarlo, "Analog multifrequency fault diagnosis", *IEEE Trans. Circuits Syst.*, vol. CAS–30, no. 4, pp. 223–233, 1983.

D. Reisig and R. DeCarlo, "A method of analog–digital multiple fault diagnosis," *Int. J. Circuit Theory Appl.*, vol. 15, pp. 1–22, 1987.

G. W. Rhyne, M. B. Steer and B. D. Bates, "Frequency–domain nonlinear circuit analysis using generalized power series", *IEEE Trans. on Microwave Theory and Techniques*, vol. 36, no. 2, pp. 379–387, 1988.

V. Rizzoli, A. Neri, "State of the art and present trends in nonlinear microwave CAD techniques", *IEEE Trans. on Microwave Theory and Techniques*, vol. 36, no. 2, pp. 343–365, 1988.

S. M. Rubin, *Computer Aids for VLSI Design*, Addison – Wesley, 1987.

J. Rutkowski and A. Macura, "Multiple fault location in AC circuits," *IEE Proc.*, vol. 133, Pt. G, no. 6, pp. 279–284, 1986.

_____, "Fault location for nonlinear resistive circuits," *Electron. Lett.*, vol. 20, pp. 401–403, 1984.

R. Saeks, A. Sangiovanni–Vincentelli, and V. Visvanathan, "Diagnosability of nonlinear circuits and systems–Part II: Dynamical systems," *IEEE Trans. Circuits Syst.*, vol. CAS–28, pp. 1103–1108, 1981.

A. E. Salama, J. Starzyk, and J. W. Bandler, "A unified decomposition approach for fault location in large analog circuits," *Proc. European Conf. Circuit Theory and Design* (Stuttgart, West Germany), pp. 125–127, 1983.

_____, "A unified decomposition approach for fault location in large analog circuits," IEEE Trans. Circuits Syst., vol. CAS–31, pp. 609–622, 1984.

A. Sangiovanni–Vincentelli, L. K. Chen and L. O. Chua, "An efficient heuristic cluster algorithm for tearing large–scale networks," *IEEE Trans Circuits Syst.*, vol. CAS–24, no. 12, pp. 709–717, 1977.

H. H. Schreiber, "Fault dictionary based upon stimulus design," *IEEE Trans. Circuits Syst.*, vol. CAS–26, pp. 529–537, 1979.

N. Sen and R. Saeks, "A measure of testability and its application to test points selection – Theory," *Proc. 20th Midwest Symp. Circuits and Systems* (Lubbock, TX), pp. 576–583, 1977.

N. Sen and R. Saeks, "Fault diagnosis for linear systems via multifrequency measurements", *IEEE Trans. Circuits Syst.*, vol. CAS–26, pp. 457–465, 1979.

S. Seshu and R. Waxman, "Fault isolation in conventional linear systems – A feasibility study," *IEEE Trans. Reliab.*, vol. R–15, pp. 11–16, 1966.

N. Singh, *An Artificial Intelligence Approach to Test Generation,* Kluwer Academic Publishers, Boston, 1987.

S. Skelboe, "Computation of the periodic steady–state response of nonlinear networks by extrapolation methods", *IEEE Trans. on Circuits and Systems*, vol. CAS–27, pp. 161–175, March 1980.

T. M. Souders and G. N. Stenbakkken, "Modeling and test point selection for data converter testing", *Proc. of IEEE AUTOTESTCON Conf.* (Long Island, NY), pp. 813–817, 1985.

T, M. Souders and D. R. Flach, "Accurate frequency response determinations from discrete step response data", *IEEE Trans. Instrum. Meas.*, vol. IM–36, no. 2, pp. 433–439, 1987.

R. Spence and J. P. Burgess, Circuit Analysis by Computer from Algorithm to Package, Prentice–Hall Inc., Englewood Cliffs, New Jersey, 1986.

J. A. Starzyk, "Development of testing strategies for large nonlinear circuits," A

A final report submitted to the National Bureau of Standards, United States Department of Commerce, ECE Research Report #030, Ohio University, 1987.

J. A. Starzyk, "Signal–flow–graph analysis by decomposition method", *IEE Proc.*, vol. 127, Pt.G, no. 2, pp. 81–86, 1980.

J. A. Starzyk, "Development of testing strategies for large nonlinear circuits," A A final report submitted to the National Bureau of Standards, United States Department of Commerce, ECE Research Report #031, Ohio University, 1988.

J. A. Starzyk and J. W. Bandler, "Location of fault regions in analog circuits," Simulation Optimization Systems Research Laboratory, McMaster University, Hamilton, Ont., Canada, Rep. SOS–81–17–R, 1981.

J. A. Starzyk and J. W. Bandler, "Nodal approach to multiple–fault location in analog circuits," *Proc. IEEE Int. Symp. Circuits and Systems* (Rome, Italy), pp. 1136–1139, 1982.

J. A. Starzyk and H. Dai, "Multifrequency measurement of testability in analog circuits", *Proc. IEEE Int. Symp. Circuits and Systems* (Philadelphia, PA), pp. 884–887, 1987.

J. A. Starzyk and H. Dai, "Fault diagnosis and calibration of large analog circuits," *Proc. IEEE Int. Symp. Circuits and Systems* (Helsinki, Finland), pp. 941–944, 1988.

J. A. Starzyk and H. Dai, "Sensitivity based testing of nonlinear circuits," *Proc. IEEE Int. Symp. Circuits and Systems* (Helsinki, Finland), pp. 1159–1162, 1988.

J. A. Starzyk and H. Dai, "Time domain testing of large nonlinear circuits", to be presented at European Conference on Circuit Theory and Design (London, United Kingdom), September, 1989.

J. A. Starzyk and M. El–Gamal, "Fault location by nodal equations", in *Analog Methods for Computer–Aided Analysis and Diagnosis*, (Editor, T. Ozawa), Marcel Dekker, New York, pp. 265–297, 1988.

J. A. Starzyk and M. El–Gamal, "Diagnosability of analog circuits – a graph theoretical approach," *Proc. IEEE Int. Symp. Circuits and Systems*, (Helsinki, Finland), p. 945–948, 1988.

J. A. Starzyk and M. El–Gamal, "Fault diagnosis of nonlinear resistive circuits", *Proc. Midwest Symp. on Circuits and Systems* (St. Luis, MO), pp. , 1988.

J. A. Starzyk and M. El–Gamal, "Parameter identification of nonlinear resistive Circuits," to be presented at European Conference on Circuit Theory and Design (London, United Kingdom), September, 1989.

J. A. Starzyk and A. Konczykowska, "Flowgraph analysis of large electronic networks", *IEEE Trans. on Circuits and Syst.*, vol. CAS–33, no. 3, pp. 302–315, 1986.

J. A. Starzyk and E. Sliwa, "Hierarchic decomposition method for the

topological analysis of electronic networks", *Int. J. Circuit Theory Appl.*, vol. 8, pp. 407–417, 1980.

J. A. Starzyk and E. Sliwa, "Upward topological analysis of large circuits using directed graph representation", *IEEE Trans. Circuits Syst.*, vol. CAS–31, no. 4, pp. 410–414, 1984.

M. B. Steer and P. J. Khan, "An algebraic formula for the complex output of a system with multi–frequency excitation", *Proc. IEEE*, vol 71, pp. 177–179, January 1983.

G. N. Stenbakken, T. M. Souders, J. A. Lechner, and P. T. Boggs, "Efficient calibration strategies foe linear time invariant systems", *Proc. of IEEE AUTOTESTCON Conf.* (Long Island, NY), pp. 361–366, 1985.

G. N. Stenbakken and T. M. Souders, "Test point selection and testability measures via QR factorization of linear models," *IEEE Trans. Instrum. Meas.*, vol. IM–36, no. 2, June pp. 406–410, 1987.

G. N. Stenbakken, T. M. Souders and G. W. Stewart, "Ambiguity groups and testability", to be published in *IEEE Trans. Instrum. Meas.*

L. J. Stotts, "Introduction to implantable biomedical IC design", *IEEE Circuit and Devices*, pp. 12–18, January, 1989.

M. N. Swamy and L. M. Roytman, "Pseudo–multifrequency approach to fault diagnosis in DC network", *Proc. IEEE Int. Symp. Circuits and Systems* (Montreal, Canada), pp. 672–674, 1984.

G. C. Temes, "Efficient methods of fault simulation," *Proc. 20th Midwest Symp. Circuits and Systems* (Lubbock, TX), pp. 191–194, 1977.

T. N. Trick, F. R. Colon, and S. P. Fan, "Computation of capacitor voltage and inductor current sensitivities with respect to initial conditions for the steady state analysis of nonlinear periodic circuits", *IEEE Trans. on Circuits and Syst.*, vol. CAS–22, pp.391–396, May 1975.

F. F. Tsui, *LSI/VLSI Testability Design*, McGraw Hill, New York, 1986.

K. C. Varghese, J. H. Williams, and D. R. Towill, "Computer–aided feature selection for enhanced analogue system fault location," *Pattern Recogn.*, vol. 10, pp. 265–280, 1978.

V. Visvanathan and A. Sangiovanni–Vincentelli, "Diagnosability of nonlinear circuits and systems – part I: The dc case," *IEEE Trans. Circuits Syst.*, vol. CAS–28, pp. 1093–1102, 1981.

V. Visvanathan and A. Sangiovanni–Vincentelli, "A computational approach for the diagnosability of dynamical circuits," *IEEE Trans. Computer–Aided Des.*, vol. CAD–3, pp. 165–171, 1984.

J. Vlach and K. Singhal, *Computer Methods for Circuit Analysis and Design*, Van Nostrand Reinhold, 1983.

M. Vlach, "LU decomposition and forward–backward substitution of recursive bordered block diagonal matrices," *IEE Proc.*, vol. 132, Pt. G, no. 1, pp. 24–31, 1985.

K. D. Wagner and T. W. Williams, "Design for testability of mixed signal integrated circuits", *Proc. Int. Testing Conference* (Washington, DC), pp. 823–828, 1988.

C. L. Wey, "Design of testability for analogue fault diagnosis," *Int. J. Circuit Theory Appl.*, vol. 15, pp. 123–142, 1987.

C. L. Wey, "Parallel processing for analogue fault diagnosis", *Int. J. Circuit Theory Appl.*, vol. 15, pp. 303–316, 1988.

C. L. Wey and R. Saeks, "On the Implementation of an analog ATPG: the nonlinear case", *IEEE Trans. on Instrum. Meas.*, vol. 37, no. 2, pp. 252–258, June 1988.

J. K. White and A. Sangiovanni–Vincentelli, *Relaxation Techniques for the Simulation of VLSI Circuits*, Kluwer Academic Publishers, Boston, 1987.

W. K. Wong, "Simulation of nonlinear microwave circuits using harmonic balance method", M.S. Thesis, Ohio University, 1988.

C. C. Wu, "Test point selection methods for the self–testing based analogue fault diagnosis system," *IEE Proc.*, vol. 132, Pt. G, no. 5, pp. 172–183, 1985.

C. C. Wu, K. Nakajima, C. L. Wey and R. Saeks, "Analog fault diagnosis with failure bounds," *IEEE Trans. Circuits Syst.* vol. CAS–26, pp. 277–284, 1982.

C. C. Wu and Y. Y. Wu, "Computer generation of topological equations and pseudocircuits for the self testing analogue fault diagnosis algorithm," *IEE Proc.*, vol. 133, Pt. G, no. 6, pp. 273–278, 1986.

C. C. Wu, "Test point selection methods for the self–testing based analogue fault diagnosis system," *IEE Proc.*, vol. 132, Pt. G, no. 5, pp. 172–183, 1985.

F. F. Wu, "Solution of large scale networks by tearing," *IEEE Trans. on Circuits and Syst.*, vol. CAS–23, no. 12, 1976.

P. Yang, "An investigation of ordering, tearing, and latency algorithms for the time–domain simulation of large circuits," Report R–891, University of Illinois at Urbana–Champaign, 1980.

M. E. Zaghloul and D. Gobovic, "Single–fault diagnosis of nonlinear resistive networks", *IEE Proc.*, vol. 134, Pt. G, No. 1, 1987.

R. Zou, "Fault analysis of nonlinear circuits from node voltage measurements," Proc. *IEEE Int. Symp. Circuits and Systems* (Helsinki, Finland), pp. 1155–1158, 1988.

Dai, Hong.   Ph.D.   June, 1989,   Electrical and Computer Engineering

Development of Decomposition Approach for Testing Large Analog Circuits.
(168. pp)

Director of Dissertation: Dr. Janusz A. Starzyk

The objective of this dissertation is to develop a new testing method for large scale circuits. This new method must be useful for functional testing and calibration of complex systems as well as identifying element characteristics and verifying macromodels or entire subsystems. It must also be able to diagnose faults and evaluate elements efficiently and reliably, while meeting the requirements of the automatic test system.

In order to realize this objective, a decomposition approach for testing large scale analog circuits was developed and testing strategies related to calibration, functional testing and fault diagnosis were established.
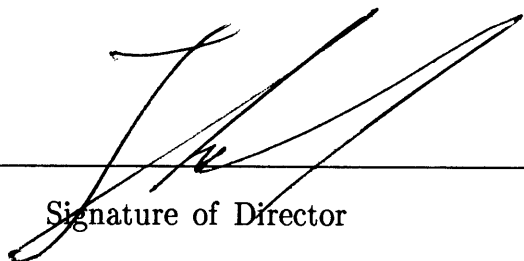
In the decomposition approach, the interconnected system was decomposed into a number of small subnetworks. To achieve this decomposition without breaking interconnections, voltage measurements were taken at the partition points and new test equations were formulated at these nodes. In this way the effects of the measurement errors were reduced to a local area, and computations were performed in each subcircuit. Subcircuit analysis was facilitated since the boundary conditions were determined by the measurement voltages. Thus, the speed and accuracy of the diagnosis process were improved. In order to fully understand the advantages of such an approach, we compared it with the sensitivity approach.

This dissertation proposed test strategies for fault diagnosis of large analog circuits. Taking the practical aspects into consideration, the developed method was modified so that it could be implemented in the real world. The practical aspects include determination of the test method and test environment, selection of test points, analysis of testability, prediction of the circuit's response, effect of measurement errors, elimination of ambiguity groups and estimation of time skew. The real test was implemented at the National Institute of Standards and Technology where experiment results verified effectiveness of the developed techniques.

The dissertation was organized as follows. First the general test methods and test procedure for element identification techniques were given. Then the sensitivity approaches, in DC, time and frequency domains was discussed, respectively. This research stemmed from the need to implement the sensitivity approach in a practical testing situation and to include it as software tools in circuit simulators. The discussion on the sensitivity approach served as an introduction to the decomposition approach. then the decomposition approach for testing large scale circuits was presented. The test equations were derived and the test procedures for DC testing, time domain testing and frequency domain testing were given. It was shown that the test matrix obtained by the decomposition approach had bordered block diagonal (BBD) structure thereby allowing sparse matrix and parallel processing techniques to be used to speed up computation in circuit simulation and fault diagnosis. Test strategies related to the practical aspects were proposed. The computer simulation and experimental results were given and the results obtained by the sensitivity approach and decomposition approach were compared.

The test method developed here can be used for testing custom integrated circuits (IC) such as analog/digital converters, filters, voltage regulators or operating amplifiers. It also can be applied to test VLSI neural networks or complicated mixed mode circuits that combine analog and digital functions. This method has a significant impact on system design, fabrication, maintenance, testing and repair stages. Voltage measurements taken during the testing play an active role in circuit simulation and diagnosis processes. Large systems can be tested without breaking the connections and all calculations can be implemented all calculations at the subsystem level. In design, the testing strategies provide design engineers with useful information so that they can make selected test points accessible.

Approved _____

Signature of Director